Master thesis

Absolute calibration of reference divider at 1 kV

Patrik Herud

August 2017

Erster Gutachter: Prof. Dr. C. Weinheimer

Zweiter Gutachter: Prof. Dr. A. Kappes

Institut für Kernphysik

Contents

List of Figures

Plagiatserklärung der / des Studierenden

Hiermit versichere ich, dass die vorliegende Arbeit über *Absolute calibration of reference divider at 1 kV* selbstständig verfasst worden ist, dass keine anderen Quellen und Hilfsmittel als die angegebenen benutzt worden sind und dass die Stellen der Arbeit, die anderen Werken auch elektronischen Medien dem Wortlaut oder Sinn nach entnommenen wurden, auf jeden Fall unter Angabe der Quelle als Entlehnung kenntlich gemacht worden sind.

_____

(Datum, Unterschrift)

Ich erkläre mich mit einem Abgleich der Arbeit mit anderen Texten zwecks Auffindung von bereinstimmungen sowie mit einer zu diesem Zweck vorzunehmenden Speicherung der Arbeit in eine Datenbank einverstanden.

_____

(Datum, Unterschrift)

1. Introduction

The standard model of particle physics describes all known particles and interactions, except for gravitational interactions, in the universe, which can be divided into matter particles and exchange particles.
The exchange particles are in charge of the exchange of forces in the three main interaction types, the electromagnetic interaction, the weak interaction and the strong interaction. The exchange particles are all bosons, with a full-numbered spin, and each exchange particle is only in charge of one interaction type. The eight gluons g are in charge of the strong interaction, the $W^{\pm}$ and Z^0 particles are in charge of the weak interaction and the γ particle is in charge of the electromagnetic interaction. In addition to these twelve elementary particles a thirteenth particle was introduced to the standard model, which is in charge of the mass production of the particles, the Higgs-Boson, which was discovered in 2012 with the LHC at CERN institute[1].

The matter particles form all visible matter in the universe and are divided into three generations. Each generation consists of two quarks and two leptons, which are all fermions with half-numbered spin. Additionally each quark and lepton has their anti particle. The three lepton generations are the electron e, muon μ and tauon τ, which have their complementary particles, the electron neutrino ν_e, the muon neutrino ν_μ and the tauon neutrino ν_τ. In the standard model of particle physics all neutrinos are massless.

Neutrino oscillation measurements proved, that neutrinos have a mass, but until now only upper limits for the neutrino mass were measured. The neutrino mass is an important variable for the cosmology, because by taking the neutrino mass into consideration, the proportion of neutrinos on hot dark matter can be determined. Therefore the KATRIN experiment is searching for the neutrino mass, or at least a new upper limit of 0.2 eV in a model independent way.

To measure the neutrino mass in this range, a high accuracy in every part of the experiment is necessary for the KATRIN experiment. The systematic uncertainty of the KATRIN experiment was analyzed within the KATRIN design report [Kat04]. With simulations the maximal allowed uncertainty for the high voltage sector was estimated as 3 ppm, which is at a high voltage of $U = -18.6\,\mathrm{kV}$ an uncertainty of 60 mV. To achieve this accuracy the high voltage dividers K35 [Thu07] and K65 [Bau10] were built. To guarantee this accuracy, these high voltage divider have to be calibrated regularly. This can be done by using Fluke 752A commercial reference dividers. These dividers have a high precision in the range up to 1 kV, which is also used at the mon-

[1] The Large Hadron Collider at the Conseil Europen pour la Recherche Nuclaire, which is the European organization for nuclear research, which is located in Geneva, Switzerland, is a particle accelerator

itor spectrometer [Erh14] and the condensed krypton source [Dyb18] at the KATRIN experiment.
In this thesis a new absolute calibration method for these reference divider was studied, especially as a preparation for the absolute calibration method of the K65 and K35, which will be discussed in [Res18].

The **second chapter** of the thesis gives a theoretical overview of the neutrino physics and especially neutrino oscillation and neutrino mass measurements. The **third chapter** describes the KATRIN setup in general, with the main focus on the high voltage system of the KATRIN experiment including the custom made high voltage dividers. The **fourth chapter** explains the calibration methods for these high voltage dividers and the new absolute calibration method for the high voltage dividers and the reference dividers. The **fifth chapter** gives a brief overview of the used reference dividers and the measurement equipment used for the calibration measurements. In the **sixth chapter**, the results of the calibration measurements are shown and the **last chapter** gives a conclusion and an outlook for further measurements.

2. Neutrino physics

In this chapter gives an introduction to neutrino mass physics and a model independent method used to measure their mases. At first the history from the postulation to the discovery of the three standard model neutrinos is briefly explained. Afterwards the observation of neutrino oscillation and a possibility for neutrino mass measurements on the example of the KATRIN experiment is explained.

2.1. The postulation and discovery of the neutrino

When a nucleon decays via β^--decay an electron e^- and an electron antineutrino $\overline{\nu}_e$ are emitted. The nucleon and the electron can be observed after the decay, but neutrinos are very difficult to observe. Before the discovery of the neutrino it was assumed, that the β-decay is a two-body-decay, which is not consistent with the continuous electron e^- spectrum, due to energy and motion conservation. Wolfgang Pauli postulated in 1930 a "neutron" which has spin 1/2, does not travel with the speed of light and with a mass, which can not be larger than 1 % of the proton mass m_p [Pau30]. The postulated "neutron" was later named neutrino, and first discovered in 1956 with the Cowan-Reines neutrino experiment via the inverse β-decay [CR56]. An electron antineutrino $\overline{\nu}_e$ interacts with a proton p and produces a neutron n and a positron e^+

$$\overline{\nu}_e + p \rightarrow n + e^+. \tag{2.1}$$

The positron e^+ annihilates with an electron e^- and produces two gamma-rays γ. The gamma-rays and the neutron can be detected. The coincidence of both events gives an evidence for the antineutrino.

The muon neutrino ν_μ was first discovered by Leon M. Lederman, Melvin Schwartz and Jack Steinberger in 1962. Muon neutrinos ν_μ were produced with the decays of pions $\pi^\pm$ at the Brookhaven National Laboratory [Led62]. The last standard model neutrino, the tau neutrino ν_τ was first discovered with the DONUT experiment at Fermi-lab in 2001. The tau neutrino was discovered with different decay channels of the tau τ [DON01].

2.2. Neutrino oscillation

Pauli postulated the neutrino mass to be in the same order of magnitude as the electron mass, but definitely lower than $0.01\, m_p$. Nevertheless the neutrinos were introduced into the standard model of particle physics as massless particles. Neutrino oscillation measurements, such as Superkamiokande and SNO [Nob15], proof, that

the neutrinos oscillate in their flavor, therefore the neutrinos can not be massless particles. For that discovery, the physics Nobel prize 2015 was awarded to T. Kajita and A. McDonald.

2.2.1. Evidence for neutrino oscillation

Cosmic rays, which mainly consists of protons, interact hadronically in the outer atmosphere of the earth. In this processes pions π and kaons K are created. Those particles decay into muons $\mu^{\pm}$ and muon (anti-)neutrinos $\overline{\nu}_{\mu}$. The muons $\mu^{\pm}$ also decay into muon (anti-)neutrinos $\overline{\nu}_{\mu}$, electron (anti-)neutrinos $\overline{\nu}_{\mathrm{e}}$ and electrons e^{-}. If all muons decay, the expected ratio of muon neutrinos ν_{μ} and electron neutrinos ν_{e} is $\frac{\nu_{\mu}}{\nu_{\mathrm{e}}} \geq 2$:

$$\left.\begin{array}{lllllllll} \pi^{+} & \rightarrow & \mu^{+} & + & \nu_{\mu} & & & & \\ & & \hookrightarrow & \mathrm{e}^{+} & + & \nu_{\mathrm{e}} & + & \overline{\nu}_{\mu} & \\ \pi^{-} & \rightarrow & \mu^{-} & + & \overline{\nu}_{\mu} & & & & \\ & & \hookrightarrow & \mathrm{e}^{-} & + & \overline{\nu}_{\mathrm{e}} & + & \nu_{\mu} & \end{array}\right\} \quad \frac{\overline{\nu}_{\mu}}{\overline{\nu}_{\mathrm{e}}} \quad \text{or} \quad \frac{\nu_{\mu}}{\nu_{\mathrm{e}}} \geq 2 \tag{2.2}$$

The Superkamiokande detector [Sup17], which consists of a large water tank with photomultipliers at each wall, can detect neutrinos. Neutrinos, which are produced in the atmosphere of the earth, enter the detector. Inside of the detector the neutrinos react with the particles and create their corresponding leptons. The charged leptons generate Čerenkov radiation, which spreads in cones behind the fast moving particles. The light cones can be observed as rings in the photomultipliers and from the sharpness of the rings it can be determined, whether it is an electron or a muon. In the experiment the neutrinos are divided into up-going neutrinos, which are produced on the other side of the earth and therefore traveled a distance of about 13.000 km and down-going neutrinos, which are produced above of the detector and therefore only traveled about 10 km. The experiment has shown, that the number of up-going neutrinos was lower than expected (see fig. 2.1). That happens, because muon (anti-)neutrinos $\overline{\nu}_{\mu}$ oscillate into tau (anti-)neutrinos $\overline{\nu}_{\tau}$, which can not be measured by the detector.

2.2.2. Neutrino flavor and mass oscillation

The neutrino flavors $|\nu_{\alpha}\rangle (\alpha = \mathrm{e}, \mu, \tau)$ are connected with the neutrino mass eigenstates $|\nu_{i}\rangle (i = 1, 2, 3)$ by the unitary 3×3 mixing matrix $U_{\alpha,i}$.

$$|\nu_{\alpha}\rangle = \sum_{i=1}^{3} U_{\alpha,i} |\nu_{i}\rangle. \tag{2.3}$$

$U_{\alpha,i}$ is called Pontecorvo-Maki-Nakagawa-Saki (PMNS) matrix. For the calculation of the neutrino oscillation the time evolution of the neutrino flavors is necessary. The neutrino flavors are not eigenstates of the time evolution operator. For this purpose the neutrino mass eigenstates can be used, whose eigenstates propagate as plane

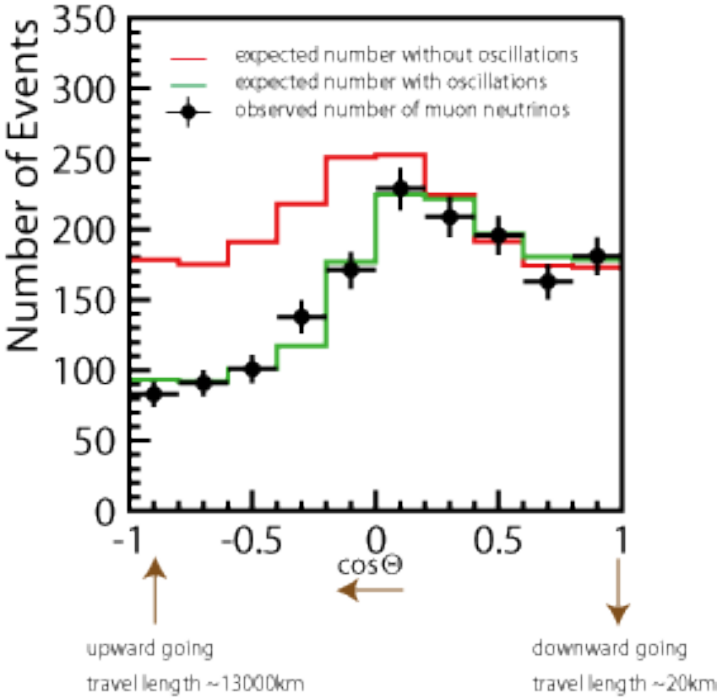

Figure 2.1.: Measurements of Superkamiokande show an evidence for neutrino oscillation. There is a distinct deficit of up-going neutrinos, which is explainable by $\nu_\mu \to \nu_\tau$ oscillation [Sup17].

waves

$$\begin{aligned} |\nu_i(x,t)\rangle &= e^{-iE_i t}|\nu_i(x,0)\rangle \\ |\nu_i(x,0)\rangle &= e^{ip_i x}|\nu_i\rangle. \end{aligned} \tag{2.4}$$

The neutrinos move relativistically, which means $p_i \gg m_i$ and $E \approx p_i$, which leads to

$$E_i = \sqrt{p_i^2 + m_i^2} \approx p_i + \frac{m_i^2}{2p_i} \approx E + \frac{m_i^2}{2E}. \tag{2.5}$$

The velocity v_ν is approximately equal to the speed of light c, the position x then can be written as

$$x = c \cdot t =: L, \tag{2.6}$$

where L is the traveled distance in a given time t. The propagation of the Neutrino masses can be described as:

$$|\nu_i(x,t)\rangle = \exp\left(-i\frac{m_i^2}{2}\frac{L}{E}\right)|\nu_i\rangle. \tag{2.7}$$

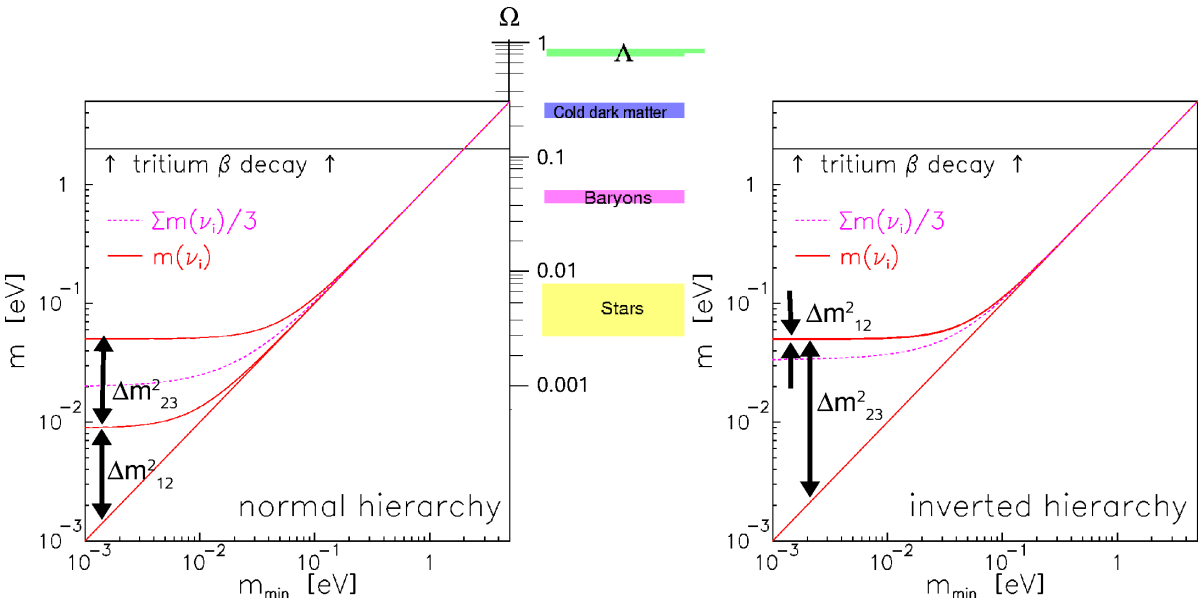

Figure 2.2.: The solid lines describe the three neutrino masses $m(\nu_i)$ for the two cases of the hierarchy (normal or inverted) as a function of the minimum neutrino mass $m_{\min}$. The dotted line is the average neutrino mass $\sum m(\nu_i)/3$ as a function of the minimum neutrino mass $m_{\min}$. The solid black line is the upper limit from the tritium β-decay experiments of Mainz and Troitsk on $m(\nu_e) < 2\,\text{eV}$ [OW08].

The probability, that a neutrino ν_α changes the flavor to ν_β can be estimated with

$$\begin{aligned} P(\nu_\alpha \to \nu_\beta) &= \left|\langle \nu_\beta(x,t)|\nu_\alpha\rangle\right|^2 = \left|\sum_i U_{\alpha,i} U^*_{\beta,i} e^{i m_i^2 \frac{L}{2E}}\right|^2. \\ P(\nu_\alpha \to \nu_\beta) &= \sin 2\theta^2 \sin \tfrac{\Delta m L}{4E}^2. \end{aligned} \tag{2.8}$$

2.3. Neutrino mass information from ν oscillation Experiments

From equation 2.8 experiments like Superkamiokande can only measure squared mass differences:

$$\begin{aligned} |\Delta m^2_{32}| &= |m^2(\nu_3) - m^2(\nu_2)| \approx 2.5 \cdot 10^{-3}\,\text{eV}^2 \\ \Delta m^2_{21} &= m^2(\nu_2) - m^2(\nu_1) \approx 8 \cdot 10^{-5}\,\text{eV}^2. \end{aligned} \tag{2.9}$$

In the second equation the algebraic sign is known from the MSW (Michejew-Smirnow-Wolfenstein) ([Wol78], [MS86]) effect on solar neutrinos. This gives two possible kinds of mass ordering for the neutrinos. One with normal hierarchy $m(\nu_1) < m(\nu_2) < m(\nu_3)$ and the other one with an inverted hierarchy $m(\nu_3) < m(\nu_1) < m(\nu_2)$ (see fig. 2.2).

The Mainz and Troitsk tritium β-decay experiment gave an upper limit for the neutrino mass:

$$m(\nu_e) := \sqrt{\sum |U^2_{ei}| m^2(\nu_i)} < 2\,\text{eV} [\text{Kra05}], [\text{Lob03}]. \tag{2.10}$$

The next section describes the method of neutrino mass determination, as it was used at the Mainz and Troitsk neutrino mass experiment, and as it is used at the KATRIN experiment.

2.4. Neutrino mass determination with the β-decay spectrum

The KATRIN experiment, as well as the Mainz and Troitsk neutrino mass experiments aims to measure the neutrino mass via the precise measurement of the endpoint β-decay spectrum of tritium. This method is entirely based on relativistic kinematics, which makes the determination of the mass model independent. In the endpoint region of the β-decay, the total energy E_{tot} of the neutrino is equal to the neutrino mass $m(\nu_{\mathrm{e}})$. Therefore the endpoint of the electron energy spectrum is directly connected with the effective neutrino mass (shown in figure 2.3)

$$m^2(\nu_{\mathrm{e}}) = \sum_i |U_{\mathrm{e},i}|^2 \, m(\nu_i)^2. \tag{2.11}$$

Due to low statistics at the endpoint region and background, the endpoint energy of the electron can not be determined directly, therefore it is necessary to measure the spectrum in a range of energies lower and higher than the endpoint energy. With the much higher mass of the tritium atom in relation to the electron, recoil energies can be neglected, when using Fermis golden rule, which gives a β-spectrum [OW08]

$$\frac{\mathrm{d}\dot{N}}{\mathrm{d}E} = R(E) \cdot \sqrt{(E_0 - E) - m^2(\nu_{\mathrm{e}})} \cdot \theta(E_0 - E - m^2(\nu_{\mathrm{e}})), \tag{2.12}$$

with,

$$R(E) = \frac{G_F^2}{2\pi^3} \cos^2(\theta_C) \, |M|^2 \, F(Z+1, E) p(E - m_{\mathrm{e}})(E_0 - E). \tag{2.13}$$

Where E is the energy of the electron, E_0 is the endpoint energy of the β-spectrum, G_F is the Fermi constant, θ_C is the Cabibbo angle, M the nuclear matrix element, Z the atomic number of the daughter nucleus and m_{e} the electron mass. The neutrino mass leads to a shift of the β-spectrum to a lower endpoint. Additionally it changes the shape of the β-spectrum.

KATRIN uses the tritium decay, because of the low endpoint energy around 18575 eV, which gives a high number of decay electrons in the endpoint region. Additionally the tritium atom contains one proton and two neutrons, which gives a minimized atomic structure, which is useful, because the atomic corrections are comparably simple. Also the low nucleon charge reduces inelastic scattering of the produced electrons in the source. The last important advantage is the small half life time of 12.3 years, which allows for strong sources with high statistics.

The most recent upper limit for the neutrino mass was given from the Mainz and Troitsk neutrino mass measurement as $m(\nu_{\mathrm{e}}) = 2\,\mathrm{eV}$. The aim of the KATRIN experiment, which is explained in the following chapter, is to measure the neutrino mass, or at least reduce this limit by a factor of 10.

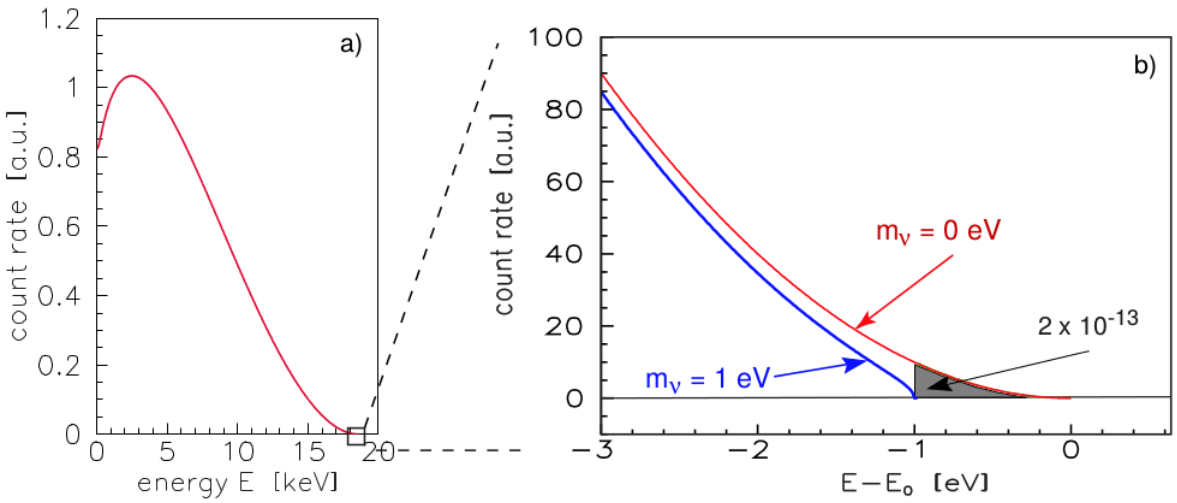

Figure 2.3.: On the left side a full tritium β-decay spectrum (a) is shown with a count rate in dependence of the energy E. On the right side, the endpoint region of the β-decay is shown with two different curves for a neutrino mass $m(\nu_e) = 1\,\text{eV}$ (blue) and $m(\nu_e) = 0\,\text{eV}$ (red) [Kat04].

3. The KATRIN experiment

The **KA**rlsruhe-**TRI**tium-**N**eutrino experiment (see fig. 3.1) is an experiment to determine the effective mass of electron antineutrinos $\overline{\nu}_e$ by measuring the endpoint spectrum of the tritium-β-decay (see chapter). With its setup the experiment has the possibility to improve the previous results of the Mainz and Troitsk neutrino mass experiments, which delivered an upper limit of 2 eV for the electron neutrino mass [Kra05], [Lob03]. The KATRIN experiment can measure the neutrino mass with a sensitivity of $m(\overline{\nu}_e) = 0.2\,\text{eV}$ at 90 % C.L. which corresponds to a discovery potential of $m(\overline{\nu}_e) = 0.35\,\text{eV}$ with 5σ. A big advantage of the KATRIN experiment is the kinematic investigation of the β-spectrum, which is model independent for neutrino mass measurements. The following sections describe the setup of the KATRIN experiment [Kat04].

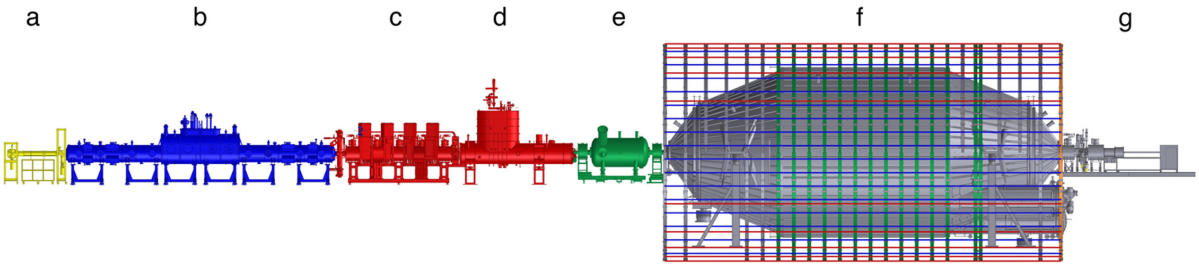

Figure 3.1.: The setup of the KATRIN experiment. The rear section (a) monitors the source activity of the windowless gaseous tritium source (WGTS). In the WGTS (b) the tritium decays into a helium-atom ^{3}He, an electron e^- and an electron antineutrino $\overline{\nu}_e$. The electron is guided into the transport section including the differential (c) and the cryogenic (d) pumping section, where tritium and helium molecules are pumped out. After the transport section, the electrons are guided into the spectrometer section with the pre- (e) and main (f) spectrometer, which both work as a MAC-E Filter (see section 3.4.1). At the end of the beamline, the electrons are counted with the focal plane detector (g) [Ams15].

3.1. Windowless Gaseous Tritium Source (WGTS)

The **W**indowless **G**aseous **T**ritium **S**ource (see fig. 3.2) is a 10 m long cylindrical tube with a diameter of 90 mm. In the center of the tube, the tritium gas is injected with a rate of $5 \cdot 10^{19}$ tritium molecules per second, which gives a throughput of 40 g tritium per day. The tritium gas has a purity of 95 % and is cooled down to $T = 27\,\text{K}$. The systematic uncertainty of the WGTS is connected with a column density of $\rho = 5 \cdot 10^{17}\,\frac{\text{molecules}}{\text{cm}^2}$, which has to be known with a precision of 0.1 % [Kat04]. Therefore the temperature inside the WGTS has to be monitored with a stability of 30 mK. The

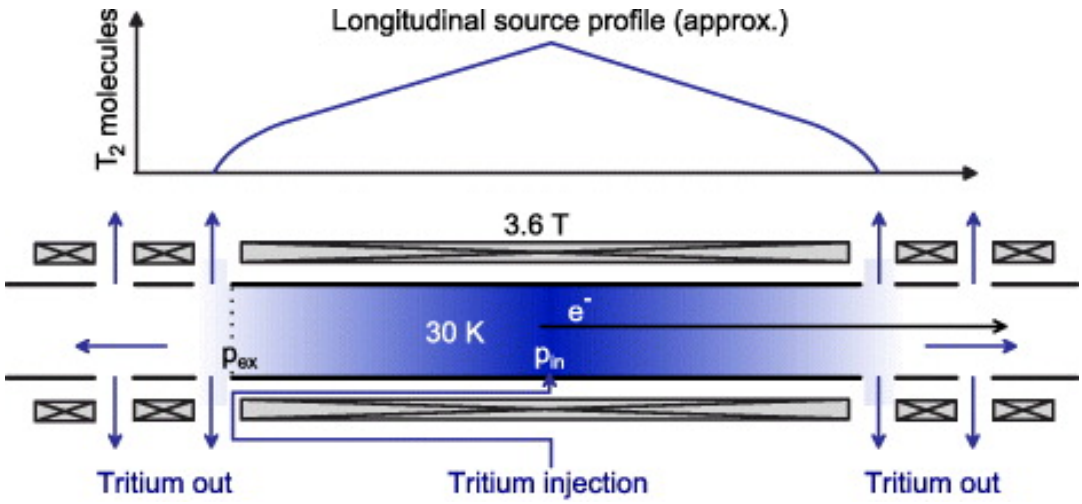

Figure 3.2.: Schematic view of the WGTS setup. At the bottom, the WGTS is shown in a simplified schematic view. The tube of the WGTS has four holes at each end, where the tritium gets pumped out. In the center tritium is injected. Around the tube solenoid magnets are placed, to guide the electrons produced by the β-decay of the tritium. At the top, the tritium concentration is shown over the length of the WGTS [Bab12].

tritium is continuously injected into the tube and flows freely through the tube it is pumped away at both ends with turbo molecular pumps. The produced electrons are adiabatically guided to both ends of the system with a magnetic field of 3.6 T.

3.2. Rear section

At the rear section a photoelectron source is installed for calibration measurements. The photoelectron source produces electrons, which are guided through the whole beamline and can be used to determine the column density inside the WGTS and the response function for the whole system. The other purpose of the rear section is the monitoring of the source activity by detection of incoming electrons from the WGTS which are guided directly to the rear section.

3.3. Differential- and Cryogenic Pumping Section

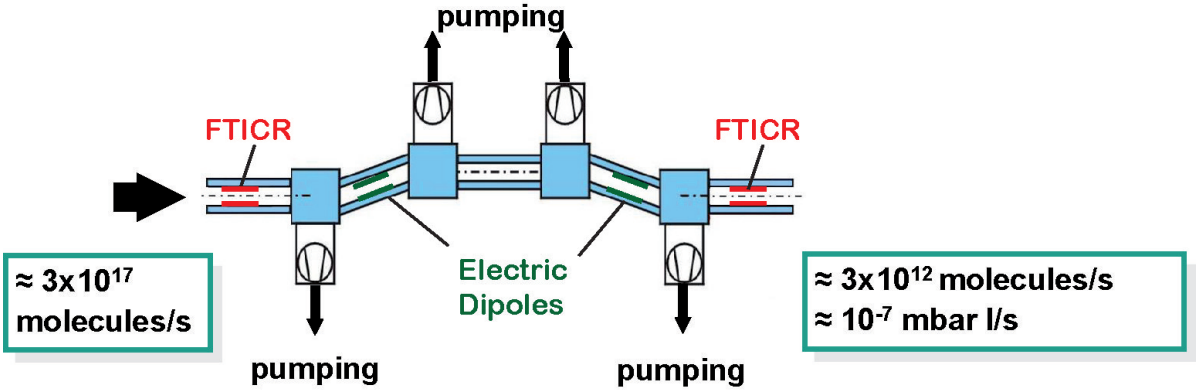

Figure 3.3.: Schematic view of the DPS setup. The electrons and a part of the tritium molecules enter the DPS on the left side. The molecule flux is about $3 \cdot 10^{17}$ molecules/s. The tube inside the DPS is tilted from the beamline to deflect the molecules. At the edge of each tilt the molecules are pumped out, but the electrons are guided adiabatically through the tilts. At the end of the DPS the molecule flux is reduced by five orders of magnitude ($\approx 3 \cdot 10^{12}$ molecules/s) [Kat17].

The **D**ifferential- and **C**ryogenic **P**umping **S**ection is used to pump out all molecules, which are inside the system in front of the WGTS. The tritium would cause a higher background in the main spectrometer, therefore the tritium flow has to be lower than $10^{-14}\ \frac{\text{mbarl}}{\text{s}}$. The DPS (see fig. 3.3) consists of five 1 m long tubes with a diameter of 75 mm. Two of the five tubes are arranged with an angle of 20 ° with respect to the beamline. The electrons are guided adiabatically through the DPS, other particles like molecules and atoms collide with the walls inside the DPS. At every connection point of the DPS a turbo molecular pump is installed to pump out the colliding molecules. The tritium flow is reduced by five orders of magnitude from $10^{-2}\ \frac{\text{mbar}\cdot\text{l}}{s}$ to $10^{-7}\ \frac{\text{mbar}\cdot\text{l}}{s}$.

The CPS (see fig. 3.4) consists of three 1 m long tubes with a diameter of 75 mm. The three tubes are also tilted with an angle of 15 ° and the electrons are guided adiabatically with a magnetic field of up to 5.75 T. The inner wall of the CPS is covered by a condensed argon frost layer. The molecules and atoms which collide with the argon layer get adsorbed and can not enter the spectrometer section.
The argon layer is saturated after 60 days of operation. After that time the valve between the CPS and the spectrometer section is closed and the beamline gets heated up to 100 K. The argon and tritium gas is pumped out by the turbo molecular pumps. After cleaning, the CPS is again cooled and Argon is freezed up.

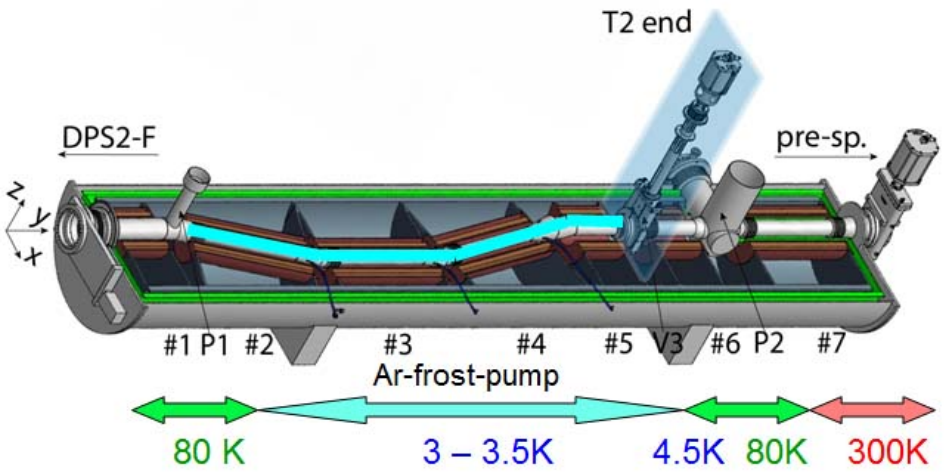

Figure 3.4.: Schematic view of the CPS. From the left side the electrons and the rest of the molecules enter the CPS from the DPS. Inside the CPS the beamline is tilted and the electrons are guided adiabatically by magnetic fields. The molecules collide with the walls of the CPS and stick to the frosted argon layer inside the tube. Therefore the tube is cooled down up to $3 - 3.5\,\mathrm{K}$. Behind the CPS the electrons are guided to the spectrometer detector section. [Kat17]

3.4. The spectrometer section

In the spectrometer section two spectrometers are installed in the beamline and a third spectrometer is placed nearby the experiment to monitor the high voltage system of the KATRIN experiment. All three spectrometers work with the principle of a **M**agnetic **A**diabatic **C**ollimation combined with an **E**lectrostatic-Filter (MAC-E-Filter).

3.4.1. Magnetic Adiabatic Collimation combined with an Electrostatic Filter

The MAC-E-Filter principle (see fig. 3.5) was first published by Beamson et al. in 1980 [Bea80] and is used as an electrostatic high pass filter for electrons. If the electrons have a kinetic energy E_{kin} higher than the electrostatic potential U

$$E_{\mathrm{kin}} > e \cdot U, \tag{3.1}$$

then the electrons pass the filter, otherwise the electrons are reflected. In this case only the kinetic energy parallel $E_{\parallel}$ to the beamline can be analyzed. Therefore the total momentum has to be in the direction of the beamline. With the momentum parallel to the beamline, the kinetic energy E_{kin} is also parallel to the beamline

$$\begin{aligned} E &= E_{\parallel} + E_{\perp} \\ \text{if : } E_{\perp} &= 0 \\ E &= E_{\parallel}. \end{aligned} \tag{3.2}$$

This can be done with the use of magnets at both ends of the spectrometer. The electrons enter the spectrometer on cyclotron trajectories around the magnetic field lines. If the change of the magnetic field over one cyclotron motion is small,

$$\left|\frac{1}{B}\frac{\partial B}{\partial t}\right| \ll \omega_{cycl} = \frac{qB}{m_\mathrm{e}}, \tag{3.3}$$

the motion is adiabatic, which means the magnetic moment μ of the electron is conserved:

$$\mu = \frac{q}{2m_\mathrm{e}}\left|\vec{L}\right| = \frac{E_\perp}{B}. \tag{3.4}$$

This means an electron, which enters the spectrometer at a high magnetic field B_i transfers most of the transversal energy $E_\perp$ into longitudinal energy $E_\parallel$, in the analyzing plane with the minimum magnetic field B_min,

$$E_{\perp,\,\mathrm{ana}} = E_{\perp,\,\mathrm{i}}\frac{B_\mathrm{min}}{B_\mathrm{i}}. \tag{3.5}$$

The energy resolution ΔE at a fixed energy E_kin can be calculated to

$$\Delta E = E_\mathrm{kin}\frac{B_\mathrm{min}}{B_\mathrm{max}}. \tag{3.6}$$

3.4.2. Pre spectrometer

The pre spectrometer (see fig. 3.6) is the first energy filter for the β-electrons in the beamline. The spectrometer is a cylindrical vessel with a length of 3.38 m and an inner diameter of 1.68 m. The spectrometer works at a voltage 300 V below the endpoint of the tritium β-decay. It reduces the β-electron flux from $10^{10}\,\frac{\mathrm{electrons}}{\mathrm{s}}$ to $10^{6}\,\frac{\mathrm{electrons}}{\mathrm{s}}$ in the normal tritium measurement mode. The retarding potential is given by the vessel potential, but can also be fine tuned with an inner electrode system.

3.4.3. Main spectrometer

The main spectrometer (see fig. 3.4.3) is the second energy filter for the β-electrons. The magnetic field strength at the entrance of the spectrometer is $B_\mathrm{max} = 6\,\mathrm{T}$, the magnetic field strength in the analyzing plane is $B_\mathrm{min} = 3\cdot 10^{-4}\,\mathrm{T}$. That leads to an energy resolution ΔE of

$$\begin{aligned} \Delta E &= E_{\mathrm{start,\,max}}\tfrac{B_\mathrm{min}}{B_\mathrm{max}} \\ &= 18.6\,\mathrm{keV}\cdot\tfrac{3\cdot 10^{-4}\,\mathrm{T}}{6\,\mathrm{T}} \\ \Delta E &= 0.93\,\mathrm{eV}. \end{aligned} \tag{3.7}$$

The main spectrometer has an inner diameter of 9.8 m at the analyzing plane and a total length of 23.28 m. The inner surface is $650\,\mathrm{m}^2$ and the vessel has a volume of $1400\,\mathrm{m}^3$. The retarding potential is applied to the vessel and can be fine tuned with an inner wire electrode system. The vessel can be evacuated by turbo molecular pumps and getter pumps up to 10^{-11} mbar.

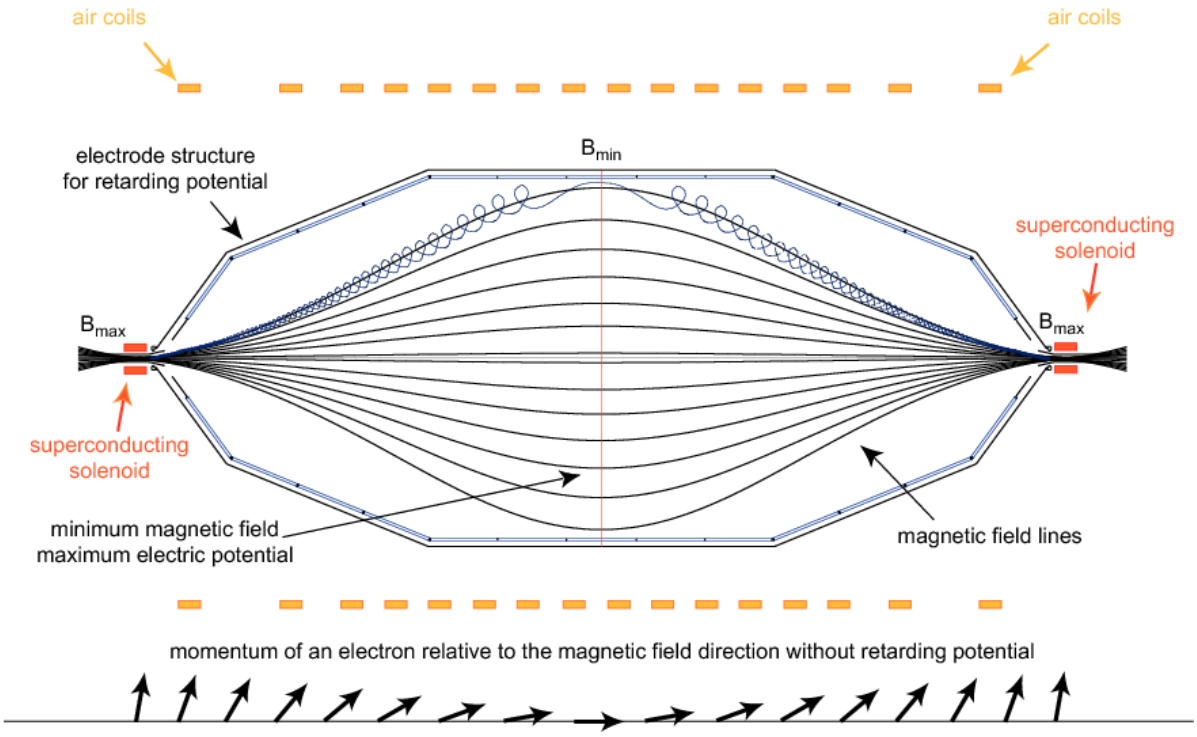

Figure 3.5.: Schematic overview of the functionality of a MAC-E Filter. Electrons enter the spectrometer on the left side through the superconducting solenoid magnet with the field B_{max}. The electrons are guided adiabatically through the spectrometer. In the center, where the B-field is lowest (B_{min}), the maximum electric potential is applied. The transversal momentum of the electrons is transformed into longitudinal momentum, which is shown at the bottom. Due to the electric potential in the center, only the electrons with a higher kinetic energy than the retarding potential can surpass the spectrometer [Bec14].

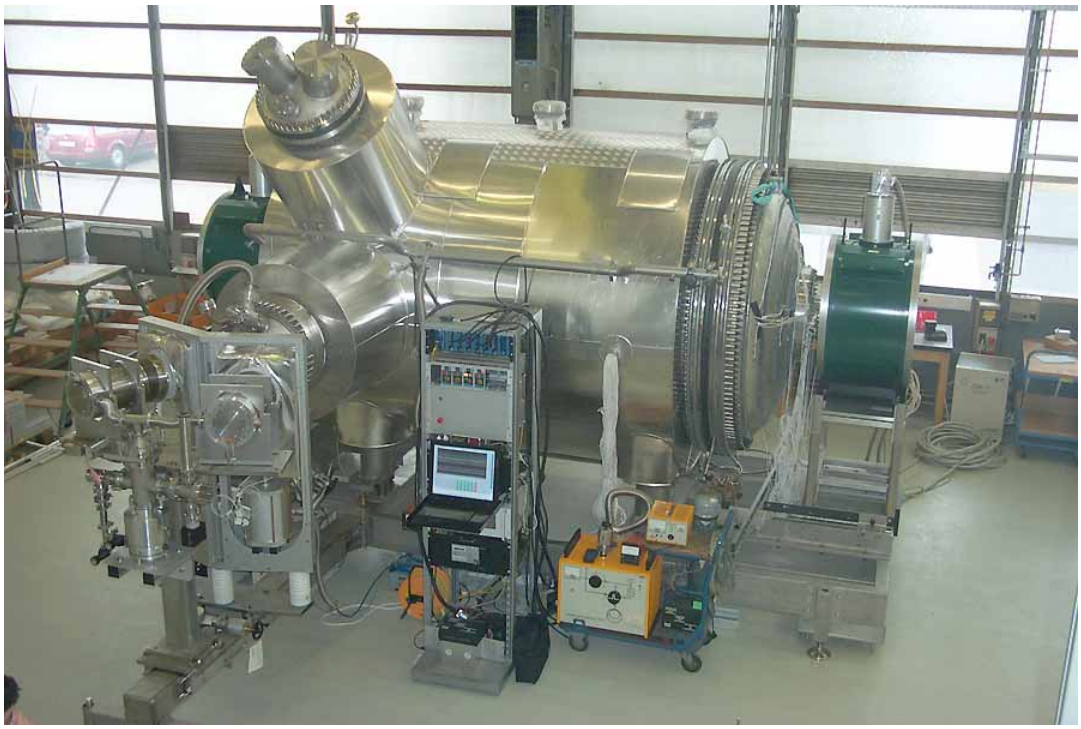

Figure 3.6.: The pre spectrometer of the KATRIN experiment consists of a cylindrical vessel (gray) with a simplified inner electrode system inside. At both ends of the vessel solenoid magnets are installed (green) to create a magnetic field, so that the spectrometer works as a MAC-E filter. [Kat04]

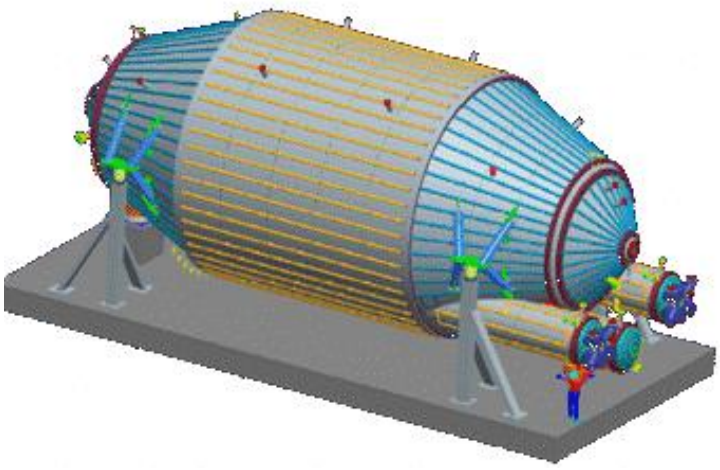

Figure 3.7.: The main spectrometer consists of a cylindrical vessel with cones at both ends and has a length of 23.28 m. It is held by four pillars (gray), two at each side. At the detector side three getter pumps are installed to evacuate the spectrometer. [Kat17]

3.4.4. Monitor spectrometer

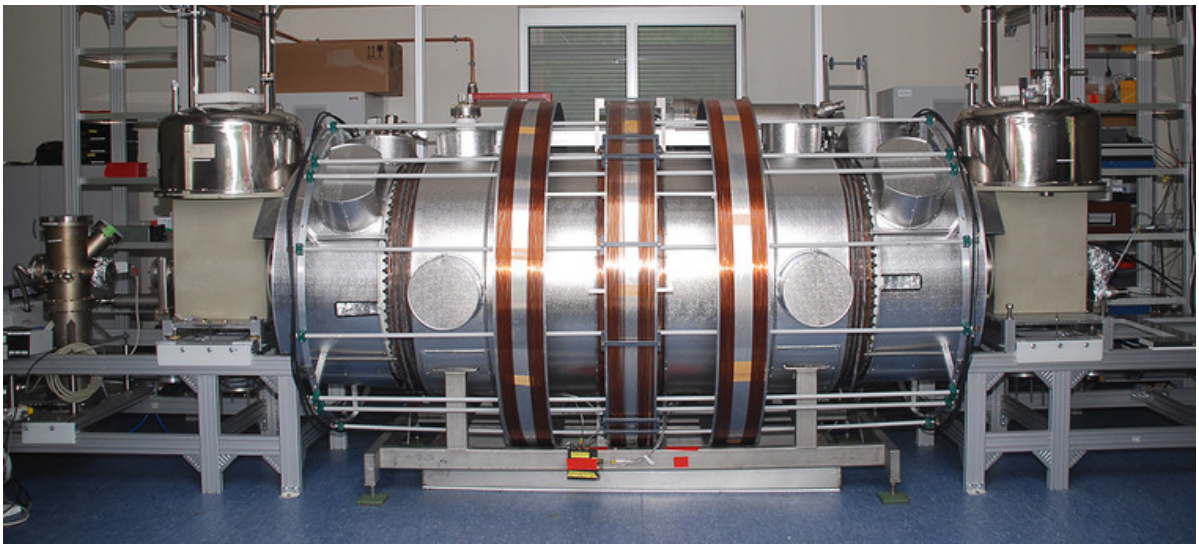

Figure 3.8.: The monitor spectrometer is the former Mainz spectrometer. It consists of a cylindrical vessel with two magnets at each side (gray squares with silver hemispheres on top). [Kat17]

The third spectrometer is the monitor spectrometer (see fig. 3.8), which is the former spectrometer of the Mainz neutrino mass experiment. The main task of the spectrometer is the monitoring of the high voltage for the main spectrometer, which is possible due to a direct electrical connection of both spectrometers. The monitor spectrometer has an implanted ^{83m}Kr source, which produces conversion electrons with an energy of 17.8 keV, which is about 0.8 keV lower than the endpoint of the tritium β-decay, which is 18.6 keV. To monitor the high voltage of the main spectrometer with the monitor spectrometer, the implanted source has to be set onto an offset potential of 800 V. This shift has also to be monitored, which can be done with a Fluke 752A reference voltage divider, which is further explained in section 5.1.

3.5. Focal plane detector

At the end of the beamline the electrons which surpass the main spectrometer are detected with the focal plane detector. The main task of the detector is to count the arriving electrons. The detector consists of 148 silicon PIN pixel diodes with an area of 44 mm^2 each. The pixels are divided into 12 rings with 12 pixels each, plus 4 center pixels (see fig. 3.9). This arrangement gives the opportunity of later corrections to account for radial electrical and magnetic inhomogeneities in the analyzing plane.

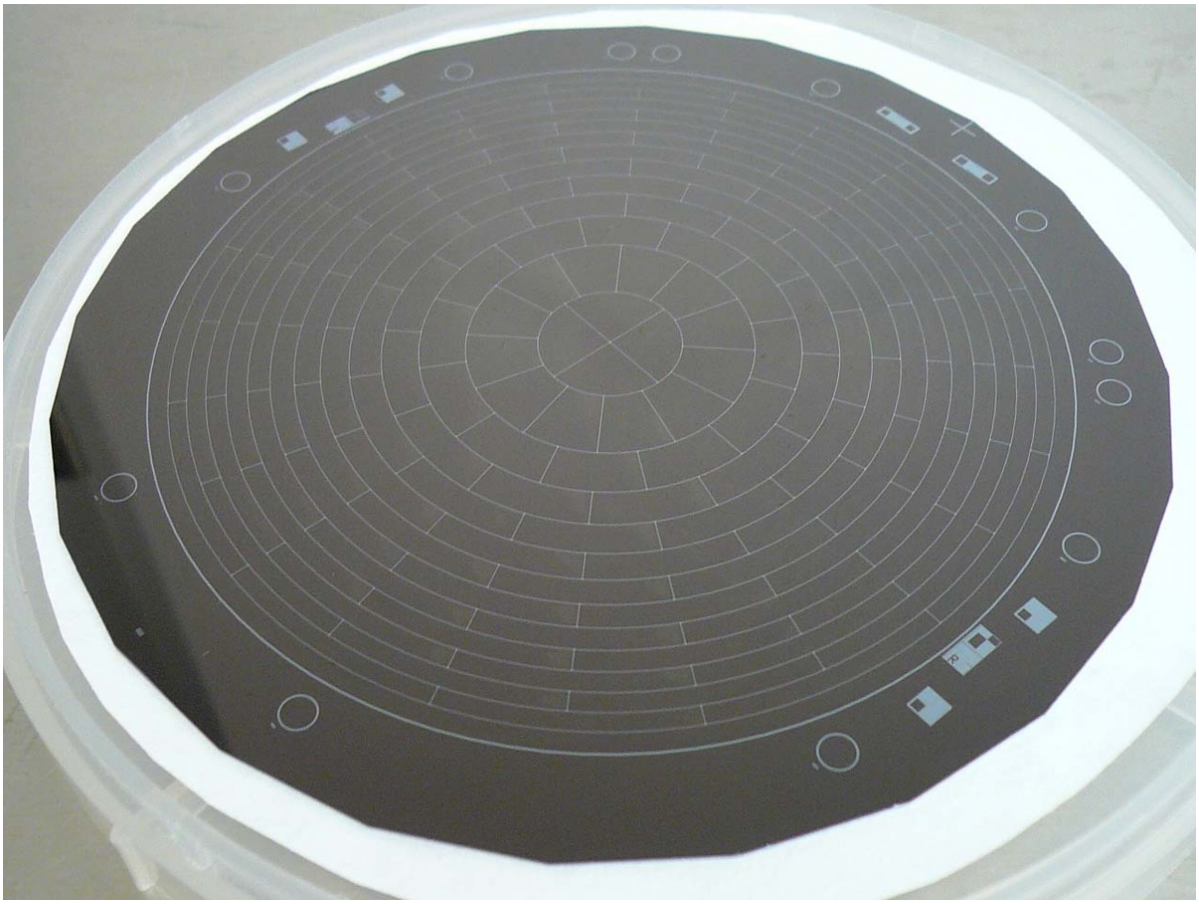

Figure 3.9.: Picture of the pixel distribution of the focal plane detector. In the center 4 pixels are arranged. Around the center 12 rings with 12 pixels each with an area of 44 mm^2 are arranged, to give the opportunity to correct for radial electric and magnetic inhomogeneities in the analyzing plane.

3.6. High voltage system of the main spectrometer

The high voltage system of the main spectrometer of the KATRIN experiment is a crucial part of the experiment. The main task of the HV-system is to provide the retarding potential for all three spectrometers. The main spectrometer works (as described in section 3.4.1) as a high pass filter for electrons. To achieve the resolution of 0.2 eV the uncertainties of the retarding potential have to be smaller than 3 ppm, which is about 60 mV at a retarding potential of -18.6 kV. Therefore two high precision high voltage dividers (K35 ([Thu07]) and K65 ([Bau10])) were built in Münster. These voltage dividers scale down the high voltages to a voltage range of 10 V, which can be measured ultra precise to the sub ppm level with commercial high precision digital voltmeters. Further Independent methods to control the stability and the voltage of the retarding potential are the condensed, gaseous and implanted krypton sources.

The condensed krypton source, which is installed at the CPS, and the implanted krypton source, which is used at the monitor spectrometer, are important tools to

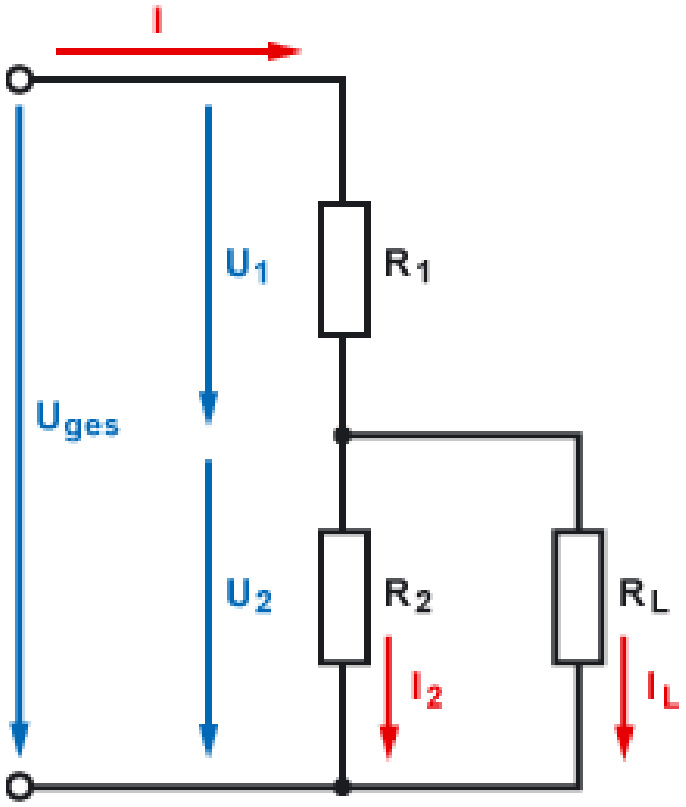

Figure 3.10.: Schematic view of a voltage divider. The input voltage U_{ges} is divided by the resistors R_1 and R_2 into U_1 and U_2 [Ele17].

measure and control the retarding potential of the main spectrometer. Both krypton sources deliver monoenergetic conversion electrons from the decay of ^{83m}Kr. With the condensed krypton source, the high voltage system can be calibrated between various tritium measurements. At the monitor spectrometer, the same high voltage as at the main spectrometer is connected. Therefore the high voltage can be monitored during tritium measurements.

The precise measurement of the voltage of $U = -18.6\,\text{kV}$ is only possible with one of the high voltage dividers K35 and K65. Both dividers were built in cooperation with the **P**hysikalisch-**T**echnische **B**undesanstalt. These dividers scale down the retarding potential of $-18.6\,\text{kV}$ in the voltage range of $-10\,\text{V}$, in which the high precision digital volt meter are calibrated with Fluke 732A 10 V reference sources, which are stable to the ppm level over years and are regularly calibrated at PTB. Voltage dividers are characterized by their scale factors M, which are defined as the ratio of the input Voltage U_{in} over the output voltage U_{out},

$$M = \frac{U_{\text{in}}}{U_{\text{out}}} = \frac{R_{\text{tot}}}{R_{\text{tap}}}, \tag{3.8}$$

where R_{tot} is the total resistance of the voltage divider and R_{tap} is the resistance

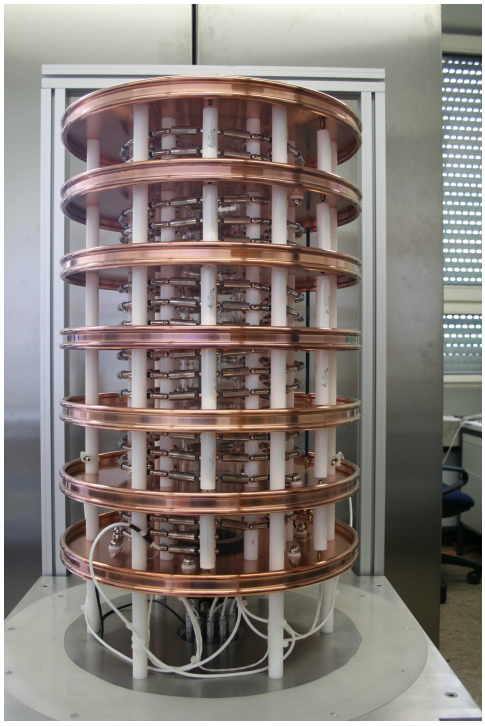

Figure 3.11.: This is the K65 high voltage divider, which was build in Münster. Between each of the first six copper electrodes 33 resistors are installed, to divide the high voltage into a lower voltage. Between the last both copper electrodes the tap plane is installed, were 14 different resistors scale the voltage to different scale factors. (Picture taken by S. Bauer)

of the voltage tap. In the figure 3.6.1 $U_{\text{in}} = U_{\text{ges}}$, $U_{\text{out}} = U_2$, $R_{\text{tap}} = R_2$ and $R_{\text{tot}} = R_1 + R_2$. The custom made high voltage dividers showed a stability of their scale factors, of 3 ppm in calibration measurements over the last years.

3.6.1. The KATRIN High voltage divider

Both high voltage dividers K35 and K65 were built with the same construction principle in Münster. This section describes the setup of the K65, further information on the K35 can be found in [Thu07].

The divider consists of two divider chains, which are located between seven copper plates (see fig. 3.6.1). In between of the plates, the two chains are independent from each other. The primary divider chain gives the scale factors of the high voltage divider. It consists of 165 Vishay VHA518-11 resistors with 880 kΩ each, which are aligned in a helix shape between the plates. The resistors are connected in series in the upper five planes with 33 resistors each.

In the last plane, the tap plane, 14 resistors are aligned in pairs of two or four resistors, to create different voltage taps with a scale factor of approximately 1:100, 1:500, 1:2000 and 1:4000 (see fig. 3.12).

The control divider chain consists of one 36 MΩ resistor and a 7 nF capacity between every copper electrode (see fig. 3.6.1). With these resistors the voltage drop between two copper electrodes is in the same order of magnitude as the voltage drop of the primary divider chain. This leads to a homogeneous electrical field between two copper electrodes. The built-in capacitors work as a high pass filter and protect the high voltage divider from high frequent high voltage transients.

Every resistor has a specific temperature coefficient of resistance (TCR), which means

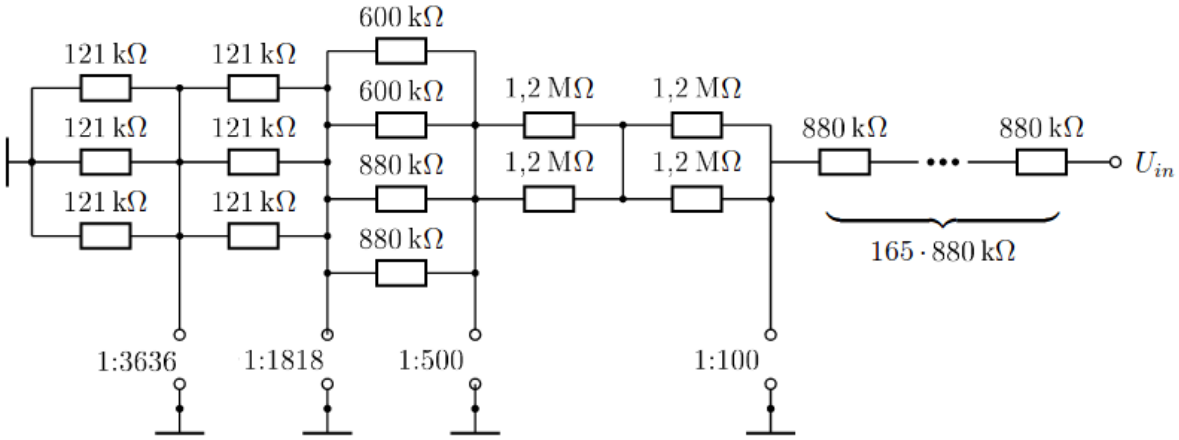

Figure 3.12.: Schematic view of the primary divider chain of the K65. On the right side is the high voltage input. Afterwards the 165 880 kΩ resistors are connected. After these resistors the 100:1 tap is installed. Behind the 100:1 tap different combination of resistors in parallel are installed to get a 500:1, 1818:1 and 3636:1 scale factor [Bau10].

Figure 3.13.: Schematic view of the primary and the control divider chain of the K65. At the top the high voltage is connected to the system. The right arm represents the primary divider chain with 33 880 kΩ resistors each. In the middle the resistor of the control divider chain is placed, which is a single 36 MΩ resistor. On the left side a 7 nF capacity is installed. The first five planes represent the normal divider planes, the plane at the bottom is the tap plane with resistors with smaller resistances in the primary and the control divider chain [Bau10].

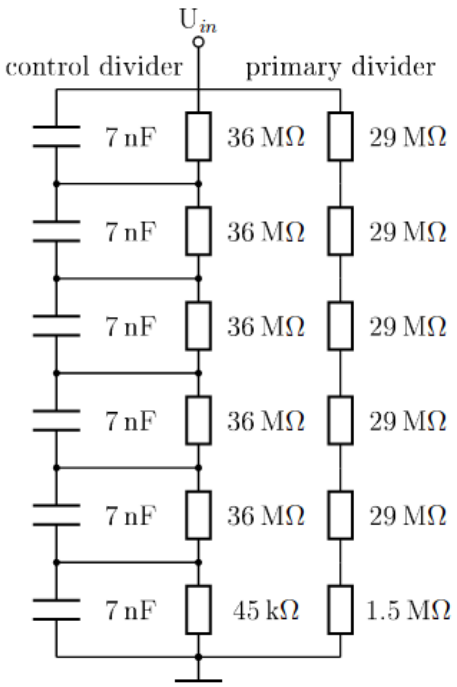

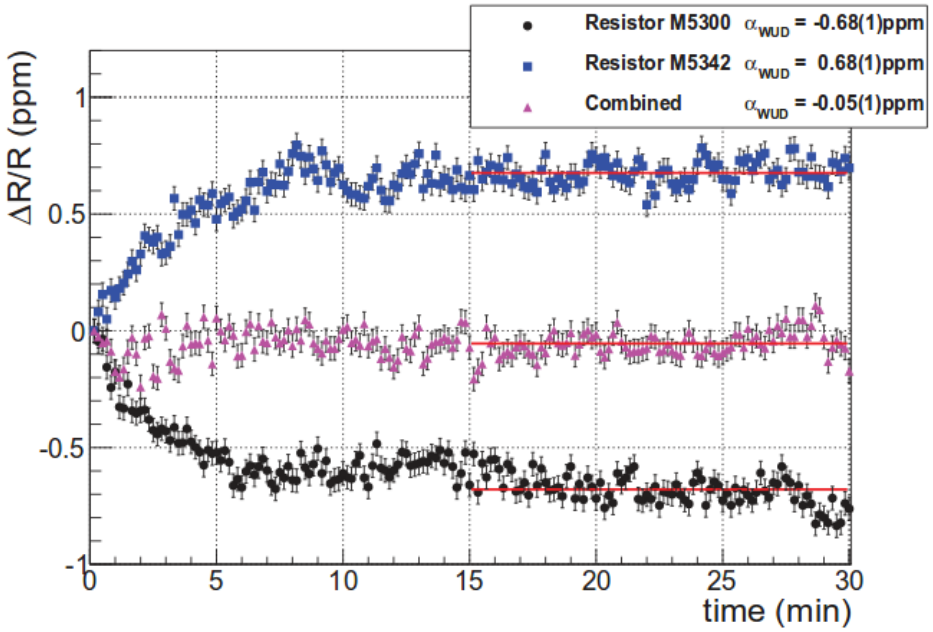

Figure 3.14.: The warm-up behavior of two resistors (M5300 and M5342) for the K65 high voltage divider. The blue squares is a resistor with a positive TCR and the black circles is a resistor with a negative TCR show the resistance change for both resistors with a voltage of $U = 255.2\,\mathrm{V}$. The purple triangles show the combined heating behavior for both resistors connected in series with a voltage of $U = 510.4\,\mathrm{V}$. The heating behavior is compensated within the measurement [Bau13].

the resistance changes with a change of the temperature or with a connected high voltage, due to Joule heating. Therefore the temperature coefficient of every resistor has been measured to be able to compensate the effects described in the following. Resistors with positive and negative TCRs and equal absolute TCR values are paired such that the temperature/voltage dependency is minimized (see fig. 3.14). Furthermore the inside of the high voltage divider is temperature monitored with Pt100 temperature sensors and stabilized to $(25.00 \pm 0.01)\,\mathrm{K}$.

Additionally to the high voltage dividers, Fluke 752A reference voltage dividers for voltages of up to 1 kV are used at different points of the KATRIN experiment, e.g. for the calibration measurement of the high voltage dividers, explained in chapter 4. Additionally the condensed krypton source [Dyb18] and the implanted krypton source at the monitor spectrometer [Erh14] are used to calibrate and monitor the high voltage system. Therefore an offset voltage of 800 V is applied to the source, which has to be monitored as well. This offset voltage is monitored and measured with the Fluke 752A reference dividers. The reference dividers are described in detail in section 5.1. In total four reference voltage dividers are used for measurements in the high voltage subgroup in this institute. The voltage dividers are named A, B, C and D.

4. Absolute calibration of voltage divider

The idea of a precision voltage measurement is the traceability to a Josephson standard reference, which is provided by metrology institutes like the PTB [Jos62]. High precision digital voltmeters like Fluke 8508A [Flu06] can be calibrated with a commercial Fluke 732A 10 V standard reference, which is calibrated regularly at PTB with a Josephson standard reference. Due to possible non-linearity effects in the measurement ranges, the optimized range for a high precision voltage measurement is the range in which it is calibrated, e.g. 12 V-20 V range for all KATRIN high precision digital voltmeter. Higher voltages can only be measured with a limited accuracy, e.g. with high voltage voltmeters a voltage of 18.6 kV can only be measured with an accuracy of 5 % [Rem10]. Therefore high precision voltage dividers are required to measure high voltages.
In general voltage dividers are characterized by their scale factor M, which is defined by the ratio of the input voltage U_{in} over the output voltage U_{out} as shown in section 3.6. During the calibration of a voltage divider the input and output voltage are measured, and the ratio gives the scale factor. Unlike the output voltage the input voltage can only be measured with a insufficient accuracy.
In the following chapter, the former used calibration method of the K35 and K65 are shortly explained. Subsequently a new absolute calibration method is explained, which is possible with a reference voltage divider with an accuracy, which is orders of magnitude lower than the calibrated divider. In the last section of the chapter, the absolute calibration method for commercial reference voltage divider, like the Fluke 752A reference dividers, which are also at the KATRIN experiment, is described.

4.1. The former calibration of the K35 and K65

The calibration of the K35 and the K65 is one of the most important calibration measurements at the KATRIN experiment. Only with the knowledge of the exact scale factors of the high voltage dividers the high voltage at the main spectrometer can be determined. Therefore a regular calibration of both dividers is needed. The dividers have three main scale factors of approximately 100:1, 2000:1 and 4000:1, which have to be calibrated.

4.1.1. High voltage calibration of the K35 and K65

The scale factors of high voltage dividers usually show a voltage dependency. Due to working ranges of the usual 18 kV up to 35 kV, both dividers have to be calibrated in these voltage ranges. Therefore a ppm stable voltage divider as a reference is needed, which is only available at the PTB (MT100 [Mar01]). The K35 and K65 were transported to PTB regularly to make these calibration measurements. A stable high voltage source is connected to the reference voltage divider MT100 and to the high voltage

divider K35/K65. The output of both dividers is measured and with the scale factor of the MT100 the scale factor of the K35/K65 can be calculated. The high voltage calibration is time consuming, because it is only possible at the PTB with the MT100. Additionally the transport of the high voltage divider can cause damage at the dividers. Measurement results from the last years can be found in [Res14]. The 2000:1 scale factor of the K35 high voltage divider was determined as $M_{2000}^{hvc} = 1972.4531 \pm 0.0059$ for the high voltage calibration.

4.1.2. Low voltage calibration of the K35 and K65

The low voltage calibration method is done with commercial equipment, which is only available for voltages of up to 1 kV. For the calibration a Fluke 5720A calibrator is used as ppm stable voltage source with a maximum output of 1 kV. The Fluke 752A commercial reference divider with a 100:1 scale factor and an accuracy of 0.5 ppm is used. These dividers can be self-calibrated, which is explained in detail in section 5.1.2 and can be traced back to the Josephson standard reference. For the measurement the Fluke 8508A and Agilent 3458a, 8.5 digit high precision digital voltmeters, are used.

The different scale factors are calibrated in different ways, with regard to the different ranges of the multimeters. The calibration of the 100:1 scale factor can be performed by connecting the voltage source to both dividers K35 and K65 and to the reference voltage divider. From this measurement a scale factor with an uncertainty of ± 0.6 ppm [Bau13] can be calculated. The precision is limited by the single uncertainties of the precision multimeters and the reference dividers. The setup of the 100:1 low voltage calibration is shown in figure 4.1. The schematic overview is divided into three layers: the voltage source, the voltage divider and the precision digital voltmeters. As a voltage source the Fluke 5720A calibrator was used with an output voltage of 1 kV. The voltage is connected to the high voltage divider (K35/K65) and the reference divider Fluke 752A. The divided voltage is divided and measured with the high precision digital voltmeters Fluke 8508A and Agilent 3458a. In this case, the input voltage of the K35 and K65 is determined with the commercial Fluke 752A reference divider.
The calibration of the other scale factors with this method would lead to a voltage 0.5 V for the 2000:1 scale factor and 0.25 V for the 4000:1 scale factor, which results in a loss of one order of magnitude with the precision multimeter. Therefore the voltage source is connected to the 100:1 scale factor output of the high voltage divider and the high voltage input is grounded. With this setup a sub scale factor can be measured. The input voltage for the calibration of 350 V, corresponds to an input voltage of 35 kV to the high voltage divider. The input voltage is also connected to the commercial reference divider and the sub scale factor can be calculated. To obtain the 2000:1 scale factor the sub scale factor has to me multiplied with the 100:1 scale factor. The setup for this calibration is shown in figure 4.2. The 4000:1 scale factor can be calibrated in the same way. Measurement results for the low voltage calibration can be found in [Res14]. The 2000:1 scale factor of the K35 high voltage divider for a low voltage calibration was determined as $M_{2000}^{lvc} = 1972.4612 \pm 0.0004$.

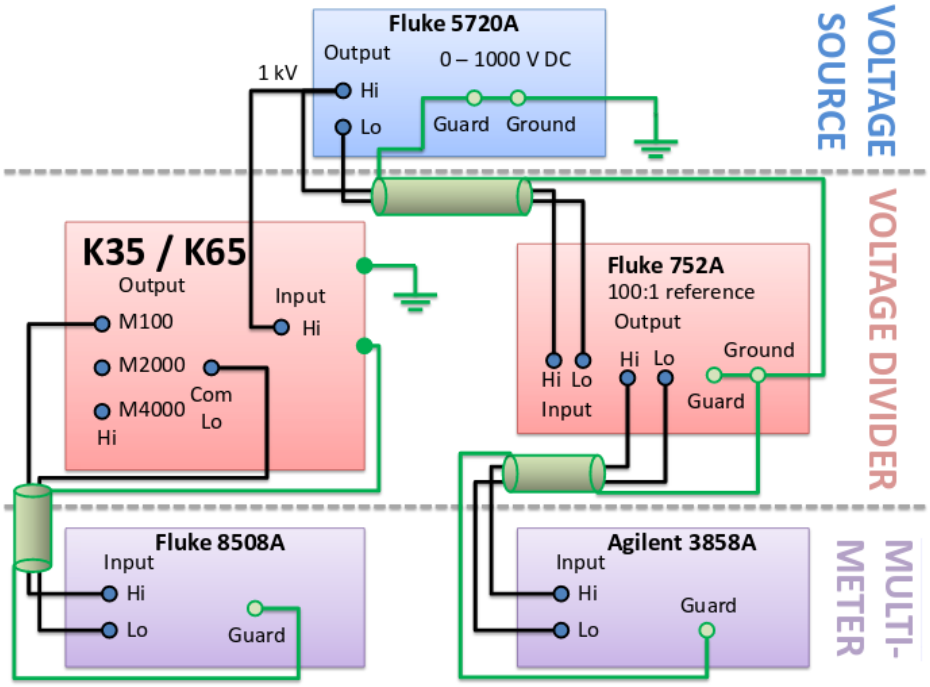

Figure 4.1.: Schematic view of the low voltage calibration of the 100:1 scale factor of the K35 and the K65.[Res14]

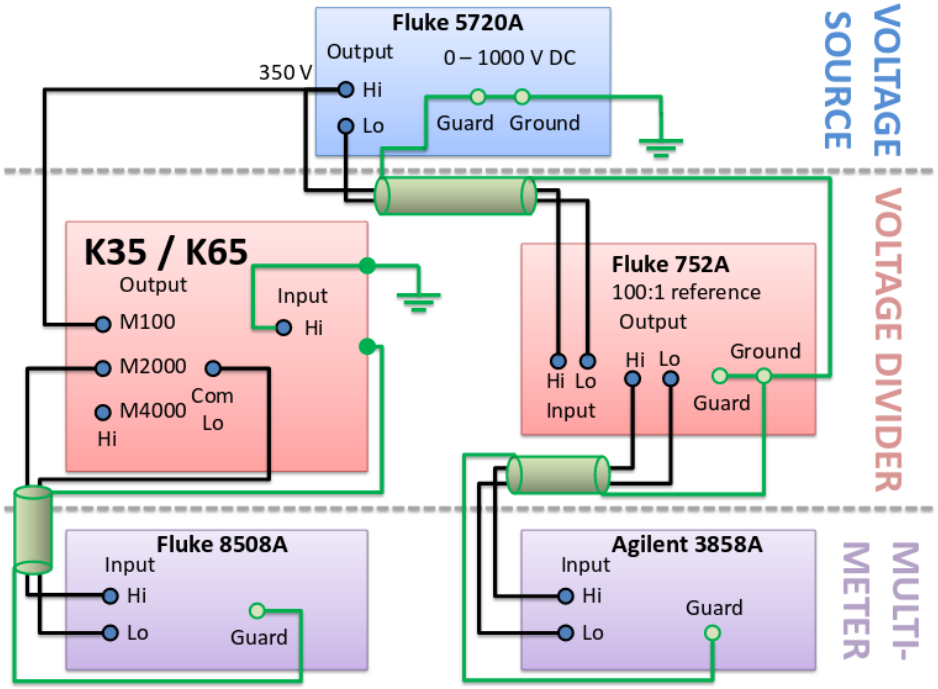

Figure 4.2.: Schematic view of the low voltage calibration of the 2000:1 scale factor of the K35 and the K65. [Res14]

4.2. Absolute calibration method for the K65 and K35

Due to the great effort needed to perform the high voltage calibration at the PTB and the problem, that the low voltage calibration only works in low voltage areas a new calibration method was invented in Münster in the past years. The basic concept of the high voltage absolute calibration is a low voltage calibration at high voltages. With this methods it is possible to calibrate a high voltage divider at high voltages with a traceability back to a Josephson standard.
A stable high voltage supply is connected to two high voltage dividers with a voltage of U_{HV} (see figure 4.3). The high voltage divider, which is calibrated has a scale factor M_{Signal}, the high voltage divider, which is used for the calibration has the scale factor M_{Base}. Both output voltages (U_{Base} and U_{Signal}) are measured with high precision digital voltmeters in a difference measurement against a voltage U_{Ref}, provided by a Fluke calibrator 5720A. With the difference measurement it is ensured that both digital voltmeters measure with the same reference potential. With a first measurement the ratio μ of the scale factors of both high voltage dividers can be calculated

$$\begin{aligned} U_{HV} &= M_{\mathrm{Base}}(U_{\mathrm{Base}} + U_{\mathrm{Ref}}) = M_{\mathrm{Signal}}(U_{\mathrm{Signal}} + U_{\mathrm{Ref}}) \\ \mu := \frac{M_{\mathrm{Base}}}{M_{\mathrm{Signal}}} &= \frac{U_{\mathrm{Signal}}+U_{\mathrm{Ref}}}{U_{\mathrm{Base}}+U_{\mathrm{Ref}}}. \end{aligned} \tag{4.1}$$

In a second measurement a voltage $U_{\mathrm{Calibration}}$ is added only to the input voltage of the high voltage divider to be calibrated (M_{Signal}). For the absolute calibration of the high voltage divider, the voltage is $U_{\mathrm{Calibration}} = 1\,\mathrm{kV}$, therefore the voltage is downscaled with a Fluke 752A commercial voltage divider ($M_{\mathrm{Calibration}} = 100$) to scale down the voltage to the most precise range. The voltage can be added with a second high voltage supply, which is set onto the high voltage potential. This can be done with the help of a high voltage measurement cage, which was built in Münster within this thesis (see figure 4.4). The high voltage cage will be further described in section 5.7. From the second measurement the scale factor can be calculated:

$$U_{\mathrm{HV}} = M_{\mathrm{Base}}(U_{\mathrm{Base}} + U_{\mathrm{Ref}}) = M_{\mathrm{Signal}}(U_{\mathrm{Signal}} + U_{\mathrm{Ref}}) - U_{\mathrm{Calibration}}. \tag{4.2}$$

With the ratio factor μ, both scale factors can be separated from each other

$$\begin{aligned} \underbrace{(M_{\mathrm{Base}} - M_{\mathrm{Signal}})}_{(\mu-1)M_{\mathrm{Signal}}} U_{\mathrm{Ref}} &+ M_{\mathrm{Base}}U_{\mathrm{Base}} + U_{\mathrm{Calibration}} = M_{\mathrm{Signal}}U_{\mathrm{Signal}} \\ M_{\mathrm{Base}}U_{\mathrm{Base}} + U_{\mathrm{Calibration}} &= M_{\mathrm{Signal}}\left[U_{\mathrm{Signal}} + (1-\mu)U_{\mathrm{Ref}}\right]. \end{aligned} \tag{4.3}$$

This results in the equation of the scale factor

$$M_{\mathrm{Signal}} = \frac{M_{\mathrm{Base}}U_{\mathrm{Base}} + U_{\mathrm{Calibration}}}{U_{\mathrm{Signal}} + (1-\mu)U_{\mathrm{Ref}}}. \tag{4.4}$$

To be able to perform both measurements immediately after each other, a relay is installed inside of the high voltage cage, which makes a short circuit over the additional 1 kV high voltage supply inside the cage. This principle was invented by C. Weinheimer and proven in 2015 by O. Rest and D. Winzen and will be published.

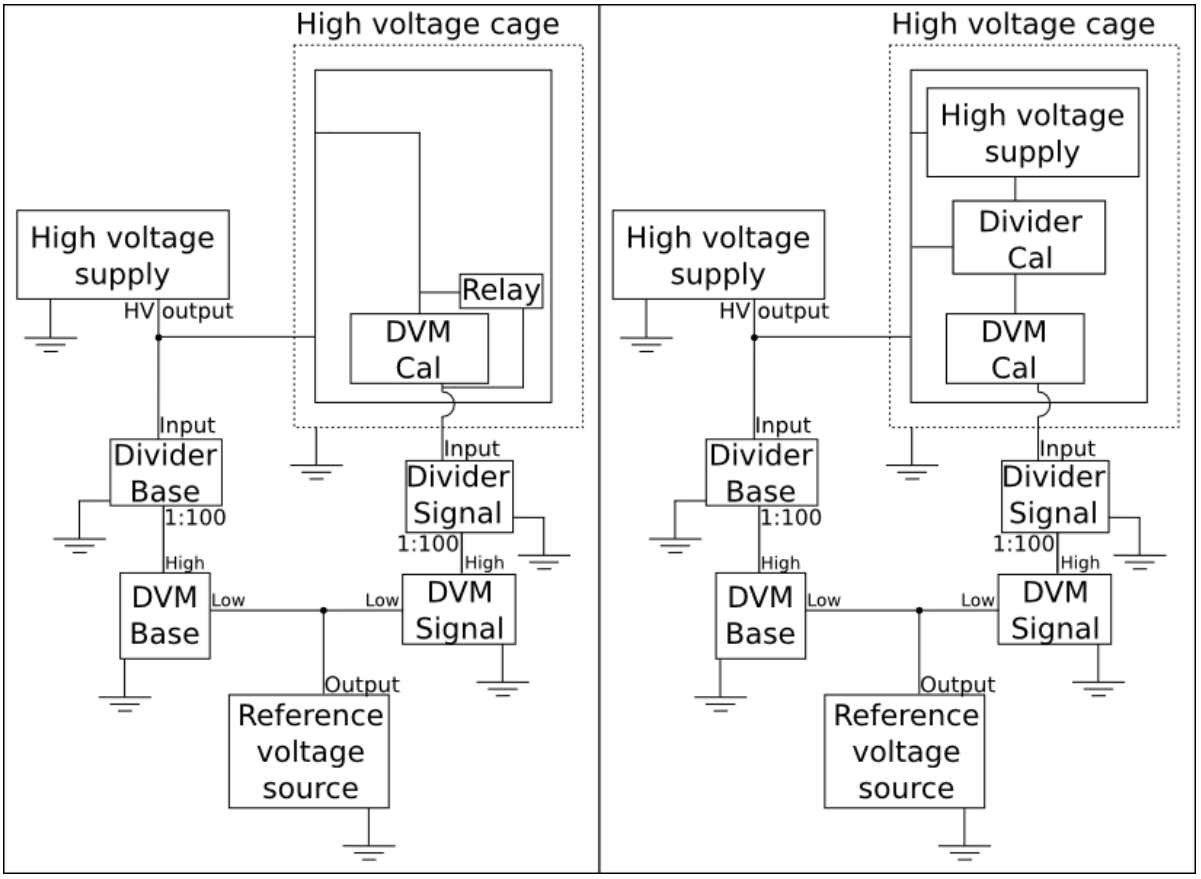

Figure 4.3.: Schematic overview of the setup for the absolute calibration measurements with the high voltage divider K65 and K35. The setup for the ratio measurement is shown on the left hand side and the calibration measurement setup on the right hand side. The first voltage supply creates a high voltage U_{HV}, which is directly measured by one of the high voltage dividers with scale factor M_{Base} and a digital voltmeter, which measures U_{Base}, and guided to the high voltage cage. Inside of the cage, in the ratio measurement, the connection over the digital voltmeter (DVM) $U_{\mathrm{Calibration}}$ and the high voltage power supply is short-circuited and goes directly out of the cage. In the calibration measurement a second voltage supply creates an additional voltage $U_{\mathrm{Calibration}} \cdot M_{\mathrm{Calibration}}$, which is scaled down by the second high voltage divider M_{Signal} and measured with $Usig$. Both high voltage divider outputs are measured with high precision digital voltmeters in a difference measurement against the Fluke calibrator U_{Ref}.

Figure 4.4.: This is the self made high voltage measurement cage. The inner cage has five shelves for the measurement equipment and stands on four insulators. Below the inner cage the isolating transformer is placed to supply the used devices inside the cage. The cage has a front and a back door to allow access to both sides of the cage. The cage was tested for high voltages of up to 35 kV.

4.3. Application of the new calibration method to 1 kV reference dividers

The calibration principle described in 4.2, should also be applicable to calibrate commercial Fluke reference voltage dividers for voltages up to 1 kV. At the KATRIN experiment multiple commercial reference dividers from the company Fluke (752A) are used at different points of the experiment as it is explained in section 3.6. Therefore it is crucial to know the exact scale factor of these commercial reference dividers.

An advantage of a calibration of these voltage dividers is the opportunity to compare the self calibration of the reference dividers, which is described in section 5.1.2 with the absolute calibration method. By comparing the new method with an established method it is possible to validate the investigated method. The absolute calibration setup for the reference divider is similar to the setup for the absolute calibration of the K35 and K65. The main difference is the different input voltages for both voltage dividers. The maximum input voltage for the Fluke reference divider is 1.1 kV, which allows to measure only with voltages in that range.

4.3.1. Ratio measurement for two voltage dividers

As in the high voltage absolute calibration described in section 4.2 the first measurement is the ratio measurement. For the ratio measurement a stable voltage source of up to 1 kV is needed to put voltage on both voltage dividers (see figure 4.5). For these measurements an MCP 14-1250 voltage supply from the company FuG [FuG14] was used. The voltage $U_{\mathrm{MCP}} = -1\,\mathrm{kV}$ is measured with one reference divider M_{Base} and the high precision digital voltmeter Fluke 8508A (U_{Base}). Additionally the voltage is connected to the high voltage cage. For the ratio measurement, the high voltage inside the cage is short circuited with the relay and connected to the second reference voltage divider outside of the cage (M_{Signal}). The second voltage divider output is measured with the high precision digital voltmeter Agilent 3458a (U_{Signal}). Both digital voltmeters measure the output voltages of the voltage dividers in a difference measurement with a Fluke 732A 10 V standard reference U_{Ref}. The first measurements showed, that a correction term U_{corr-1}, which is explained in detail in section 6.1 has to be implemented on the high voltage side of the measurement, which gives

$$U_{\mathrm{MCP}} = M_{\mathrm{Base}}(U_{\mathrm{Base}} + U_{\mathrm{Ref}}) = M_{\mathrm{Signal}}(U_{\mathrm{Signal}} + U_{\mathrm{Ref}}) + U_{corr-1}. \tag{4.5}$$

That leads to a new equation for the ratio factor μ

$$\mu := \frac{M_{\mathrm{Base}}}{M_{\mathrm{Signal}}} = \frac{U_{\mathrm{Signal}} + U_{\mathrm{Ref}} + \frac{U_{corr-1}}{M_{\mathrm{Signal}}}}{U_{\mathrm{Base}} + U_{\mathrm{Ref}}}. \tag{4.6}$$

4.3.2. Calibration Measurement

For the calibration measurement, the short-circuit is removed, and the voltage supply inside of the high voltage cage provides a voltage $U_{\mathrm{Calibration}}$. Again the measure-

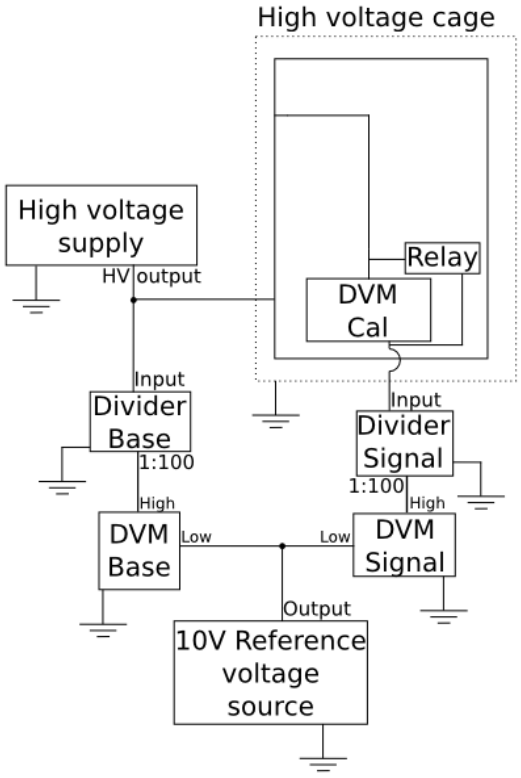

Figure 4.5.: Setup for the ratio measurement of the reference voltage divider calibration. The main difference to the absolute calibration setup (see figure 4.3) is the usage of a 10 V reference for the difference measurement with the digital voltmeter behind the voltage divider, and the lower input voltage of 1 kV.

ments showed, that a correction term U_{corr-2}, which is further explained in section 6.1 has to be included to the calculation, which gives

$$U_{MCP} = M_{\text{Base}}(U_{\text{Base}} + U_{\text{Ref}}) = M_{\text{Signal}}(U_{\text{Signal}} + U_{\text{Ref}}) - U_{\text{Calibration}} + U_{corr-2}. \quad (4.7)$$

With the ratio factor μ, both scale factors can be separated from each other

$$\begin{aligned} \underbrace{(M_{\text{Base}} - M_{\text{Signal}})}_{(\mu-1)M_{\text{Signal}}} U_{\text{Ref}} \quad &+ \quad M_{\text{Base}}U_{\text{Base}} + U_{\text{Calibration}} - U_{corr-2} = M_{\text{Signal}}U_{\text{Signal}} \\ M_{\text{Base}}U_{\text{Base}} + U_{\text{Calibration}} - U_{corr-2} \quad &= \quad M_{\text{Signal}}\left[U_{\text{Signal}} + (1-\mu)U_{\text{Ref}}\right]. \end{aligned} \quad (4.8)$$

This results in the equation of the scale factor

$$M_{\text{Signal}} = \frac{M_{\text{Base}}U_{\text{Base}} + U_{\text{Calibration}} - U_{corr-2}}{U_{\text{Signal}} + (1-\mu)U_{\text{Ref}}}. \quad (4.9)$$

The new setup of the calibration measurement for the commercial reference divider is shown in figure 4.6.

4.3.3. Uncertainty assessment

For a better understanding of the scale factor determination, the uncertainties can be estimated. The scale factor measurement depends on the reference voltage U_{Ref}, all

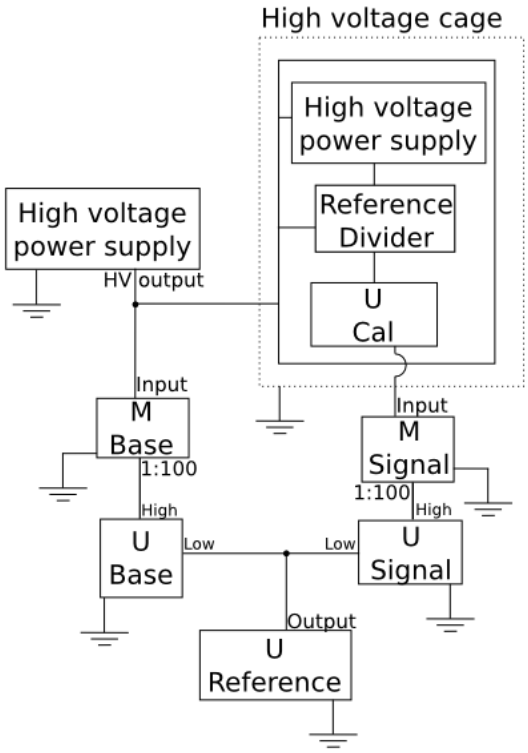

Figure 4.6.: Setup for the scale factor measurement of the reference divider calibration. The difference between the reference divider calibration and the high voltage divider calibration are again the lower voltages of 1 kV for the outer high voltage supply and 90 V for the inner voltage supply. Therefore the voltage inside the cage can be measured directly with a digital voltmeter.

three digital voltmeters U_{Signal}, U_{Base} and $U_{\text{Calibration}}$, the correction term U_{corr-2} and the scale factor M_{Base}. The scale factor is given as

$$M_{\text{Signal}} = \frac{M_{\text{Base}} U_{\text{Base}} + U_{\text{Calibration}} - U_{corr-2}}{U_{\text{Signal}} + (1-\mu) U_{\text{Ref}}} := \frac{n}{d}. \tag{4.10}$$

The relative uncertainty of the scale factor can be calculated by adding the relative uncertainties of the numerator n and the denominator d

$$\frac{\Delta M_{\text{Signal}}}{M_{\text{Signal}}} = \sqrt{\left(\frac{\Delta n}{n}\right)^2 + \left(\frac{\Delta d}{d}\right)^2}. \tag{4.11}$$

The numerator consists of the scale factor M_{Base}, the measured voltages U_{Base} and $U_{\text{Calibration}}$ and the correction term U_{corr-2}. The absolute uncertainty of U_{Base} is estimated as 1 ppm. The experimental value is in the order of $U_{\text{Base}} = \mathcal{O}(1\,\text{mV})$. The relative uncertainty of M_{Base} is estimated as 10 ppm, which is significantly higher than the manufacturer given uncertainty. Therefore the absolute uncertainty of $M_{\text{Base}} U_{\text{Base}}$ can be calculated as

$$\begin{aligned} \Delta(M_{\text{Base}} U_{\text{Base}}) &= \sqrt{\left(\tfrac{\Delta M_{\text{Base}}}{M_{\text{Base}}}\right)^2 + \left(\tfrac{\Delta U_{\text{Base}}}{U_{\text{Base}}}\right)^2} \cdot (M_{\text{Base}} U_{\text{Base}}) \\ \Delta(M_{\text{Base}} U_{\text{Base}}) &= \sqrt{(10^{-5})^2 + \left(\tfrac{10^{-6}\,\text{V}}{10^{-3}\,\text{V}}\right)^2} \cdot (0.1\,\text{V}) = 0.0001\,\text{V}. \end{aligned} \tag{4.12}$$

The absolute uncertainty of $U_{\text{Calibration}} \approx 0.0001\,\text{V}$ is estimated with the specifications for the digital voltmeter, the absolute uncertainty of the correction term is

$U_{corr-2} \approx 10^{-5}\,\mathrm{V}$ is estimated within the measurement of the correction term in section 6.1. That leads to an absolute uncertainty for the numerator

$$\Delta n = \sqrt{(\Delta(M_{\mathrm{Base}} U_{\mathrm{Base}}))^2 + (\Delta U_{\mathrm{Calibration}})^2 + (\Delta U_{corr-2})^2} \approx \sqrt{2} \cdot 10^{-4}\,\mathrm{V}. \tag{4.13}$$

The absolute value of the numerator is

$$n = M_{\mathrm{Base}} U_{\mathrm{Base}} + U_{\mathrm{Calibration}} - U_{corr-2} = 100 \cdot 0.0001\,\mathrm{V} + 100\,\mathrm{V} - 0.001\,\mathrm{V} \approx 100. \tag{4.14}$$

That results in a relative uncertainty of

$$\frac{\Delta n}{n} = \sqrt{5} \cdot 10^{-6}. \tag{4.15}$$

The denominator consists of the measured voltage U_{Signal}, the ratio factor μ and the standard voltage reference source U_{Ref}. In the measurements the ratio factor is about $\mu \approx 1$ up to the sub ppm scale. Therefore the uncertainty of the second part can be neglected. Only the relative uncertainty of U_{Signal} is important for the uncertainty of the denominator. The relative uncertainty of U_{Signal} is given as

$$\frac{\Delta d}{d} \approx \frac{\Delta U_{\mathrm{Signal}}}{U_{\mathrm{Signal}}} = 10^{-6}. \tag{4.16}$$

That gives a relative uncertainty for the scale factor as

$$\begin{aligned} \frac{\Delta M_{\mathrm{Signal}}}{M_{\mathrm{Signal}}} &= \sqrt{\left(\frac{\Delta n}{n}\right)^2 + \left(\frac{\Delta d}{d}\right)^2} \\ \frac{\Delta M_{\mathrm{Signal}}}{M_{\mathrm{Signal}}} &= \sqrt{5 \cdot 10^{-12} + 10^{-12}} \approx \sqrt{6} \cdot 10^{-6} \approx 2.5\,\mathrm{ppm}. \end{aligned} \tag{4.17}$$

The expected relative uncertainty for a measurement is therefore given as 2.5 ppm.

5. Devices for the absolute calibration measurements

The absolute calibration measurements require precise measurement equipment and an accurate data readout. Also the multimeter readouts should be synchronized, because of drift effects of the voltage supplies or reference dividers. Therefore some tests were made, to check the readout system of all three multimeters. Another important feature is the self calibration of the reference divider, which is used to check the validity of the absolute calibration. In this chapter the important measurement devices are introduced and the measurements to synchronize all three multimeters are presented.

5.1. The reference divider Fluke 752A

Three reference dividers (A, B and D) from the company Fluke (752A) (see fig. 5.1) were used and calibrated for different absolute calibration measurements. The reference voltage dividers have two scale factors 10:1 and 100:1 with a precision of 0.2 ppm for the 10:1 scale factor and 0.5 ppm for the 100:1 scale factor. The maximum input voltage for the 10:1 scale factor is 100 V, for the 100:1 scale factor 1.1 kV. In the following subsections the reference dividers are explained in their whole functionality.

5.1.1. The electrical setup

The voltage divider consists of one divider chain featuring different parts (see fig. 5.2). The first part is the driven guard divider, which is located parallel to the resistors of the 100:1 divider chain. The resistors in the 100:1 divider chain are separated into three groups, which are surrounded by metal enclosures. The driven guard divider has a resistance of 4 MΩ, which is in the same order of magnitude as the 100:1 voltage divider.
The second part is the 100:1 divider chain. This divider chain consists of 90 resistors with 40 kΩ each. That results in a total resistance of 3.6 MΩ. These resistors are divided into four subgroups, three of them are surrounded by the metal enclosures and the fourth subgroup is a potentiometer, which is used to calibrate the 100:1 voltage divider.
The third part is the 10:1 divider, which consist of nine resistors with 40 kΩ each. That 10:1 divider has a total resistance of 360 kΩ. These nine dividers are also separated into three subgroups, where the third subgroup contains the potentiometer, to calibrate the 10:1 divider.
The fourth part is the output resistor. The output resistor has a resistance of 40 kΩ. All three main divider chains are connected in series, to get the total divider ratio of 4 MΩ:40 kΩ for the 100:1 divider and 400 kΩ:40 kΩ for the 10:1 divider.
In addition a passive guard system surrounds the whole voltage divider, which is

Figure 5.1.: Front panel of the Fluke 752A reference voltage divider.

connected to the guard connector at the front panel. This is an additional passive guard system to protect the voltage divider for outer disorder.

5.1.2. The self calibration operation mode

The important feature of the reference voltage divider is the self calibration mode. In this mode, the voltage divider can be calibrated up to an accuracy of 0.2 ppm for the 10:1 divider and 0.5 ppm for the 100:1 divider. For the self calibration process a ppm stable voltage source and a precision multimeter, which has an accurate 0 V read out, are needed. For the self calibration in Münster the Fluke calibrator 7520A, which has an accuracy of ± 3.25 ppm for voltages up to ± 1100 V, is used as the voltage source and the Fluke 8508A precision multimeter, which has an accuracy of ± 0.5 ppm in voltage range up to 200 mV, is used for the measurement. The calibrator is connected to the high voltage input and the multimeter is connected to the null detector input. If the mode switch is in the calibration mode, two switches inside the voltage divider make a shortcut between the resistors, so that packages of resistors are parallel aligned (see fig. 5.3). That leads to a total resistance R_{tot} of

$$\frac{1}{R_{\text{tot}}} = \frac{1}{3R} + \frac{1}{3R} + \frac{1}{3R} = \frac{1}{R}. \tag{5.1}$$

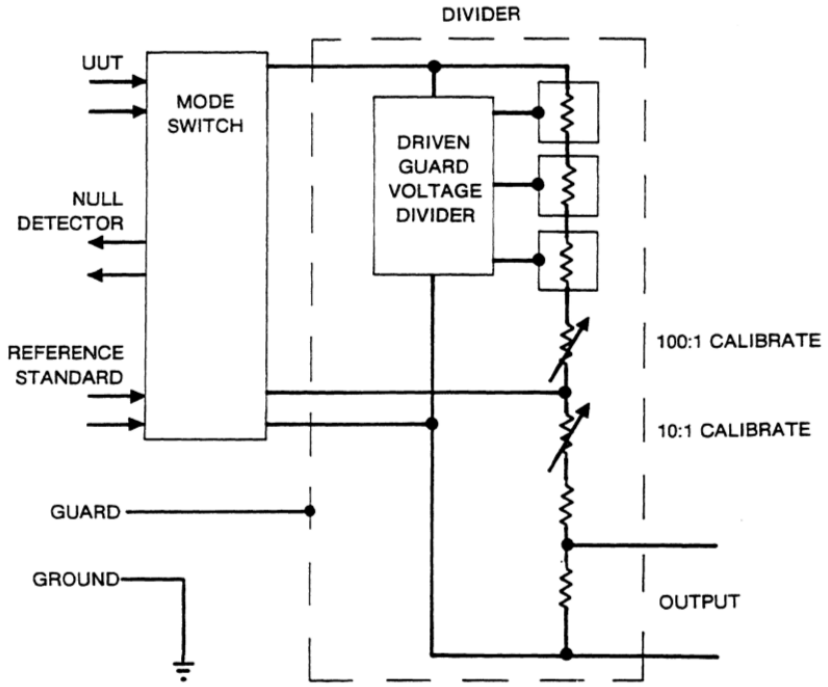

Figure 5.2.: Schematic view of the electrical setup of the Fluke 752A reference divider. The mechanical input terminals of the front panel are marked on the left hand side as UUT, which is the high voltage input, null detector, reference standard, guard and ground. The input voltage is connected with the mode switch, depending on the desired output to the top or one of the bottom cables. The main divider chain is the right string, with the shielded resistors of the 100:1 divider chain at the top and the calibration resistor for the 100:1 operation mode. After that part comes the 10:1 calibration resistor and the 10:1 divider chain. At the bottom is the output resistor and the output terminal. In parallel to the 100:1 main divider chain, the driven guard voltage divider is located, which divides the input voltage down to similar voltage drops of the divider, to realize the protection of the primary divider chain. The dashed line around all divider chains is the external guard [Flu93].

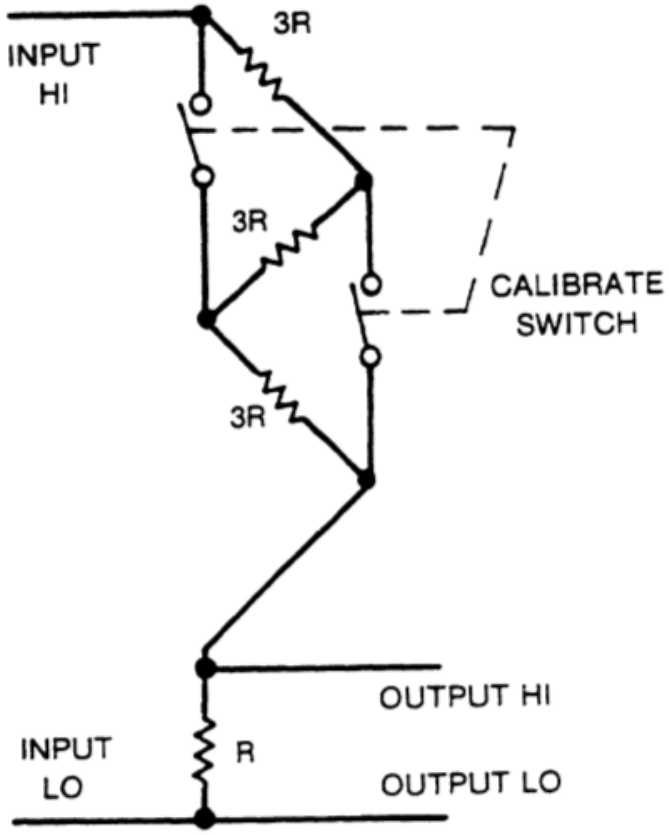

Figure 5.3.: Internal setup for calibration measurement of the Fluke 752A reference divider. If the divider is in calibration mode, the switches connect the three $3R$ resistors in parallel to create a total resistance of R [Flu93].

The tap resistance of the 10:1 divider is $R_{\text{tap}} = R$, which is the same value as R_{tot}. The connection of the multimeter in the null detector input gives the opportunity to use the calibration circuit as a Wheatstone bridge (see fig. 5.4). On the left hand side, the high voltage divider chain is located as a part of the high voltage chain and the tap resistor. On the right hand side two 120 kΩ resistors are placed for a polarity calibration. With this circuit the reference divider can be calibrated, if the resistor pairs of both sides have the same ratio.

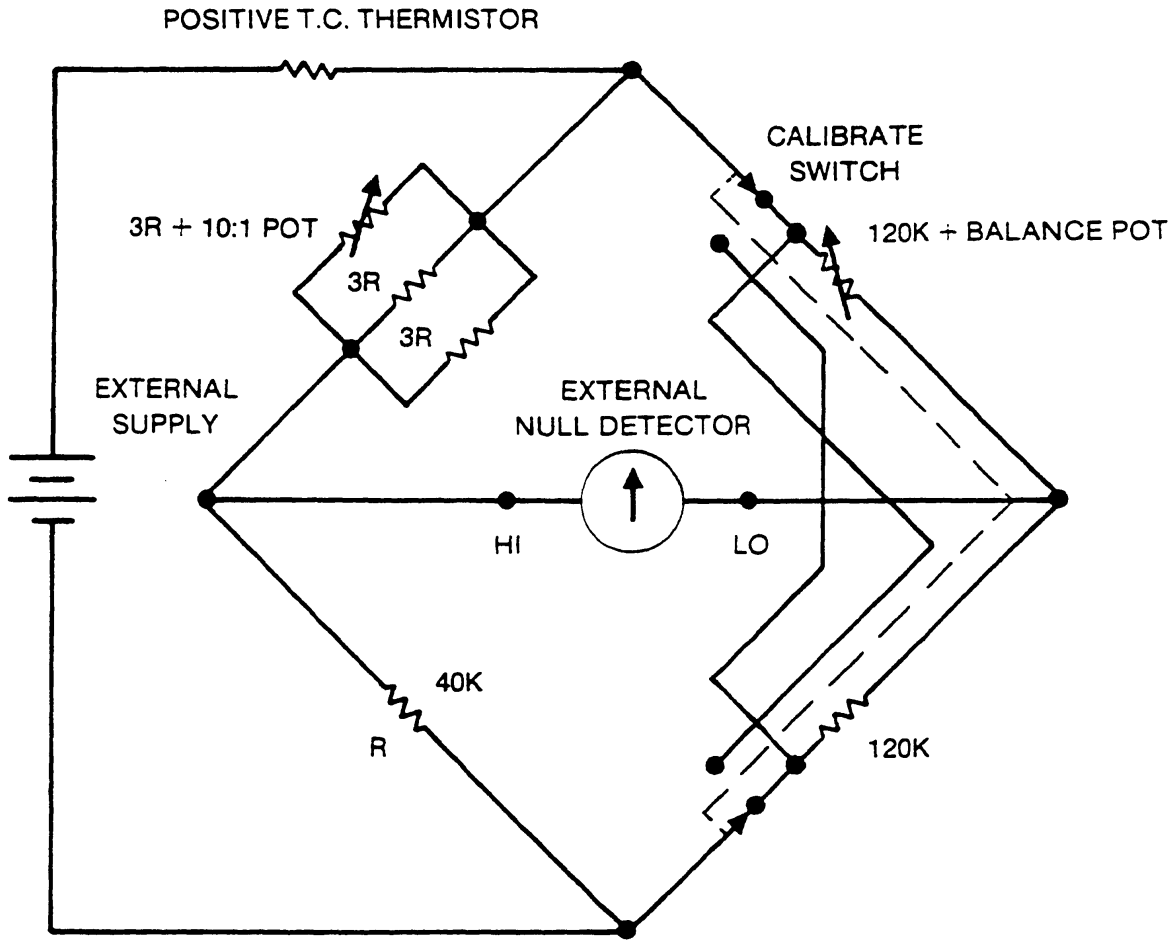

Figure 5.4.: Schematic of the Wheatstone circuit for the self calibration measurement of the reference voltage divider [Flu93].

After the 10:1 divider is calibrated, the 100:1 divider can be calibrated. That changes the electrical circuit in a way, that the resistors are now in 3 different groups, that the total resistance R_{tot} is now

$$\frac{1}{R_{\text{tot}}} = \frac{1}{30R} + \frac{1}{30R} + \frac{1}{30R} = \frac{1}{10R}. \tag{5.2}$$

The tap resistance of the 100:1 divider is $R_{\text{tap}} = 10R$, which is the same value as R_{tot}.
Within both calibrations, the scale factor is calibrated with a the potentiometers inside of the reference voltage dividers. The Fluke 8508A has to measure a maximum voltage of $0.5\,\mu$V for the 10:1 scale factor and a voltage of $1\,\mu$V for the 100:1 scale factor. If this condition is fulfilled, the scale factors are $M_{10} = 10.000000(2)$ and $M_{100} = 100.00000(5)$. The uncertainty is indicated by the manufacturer, but no time dependence for the scale factor is given. Therefore the time dependency of the self calibration is investigated within this thesis.

5.1.3. Previous calibration and stability measurements

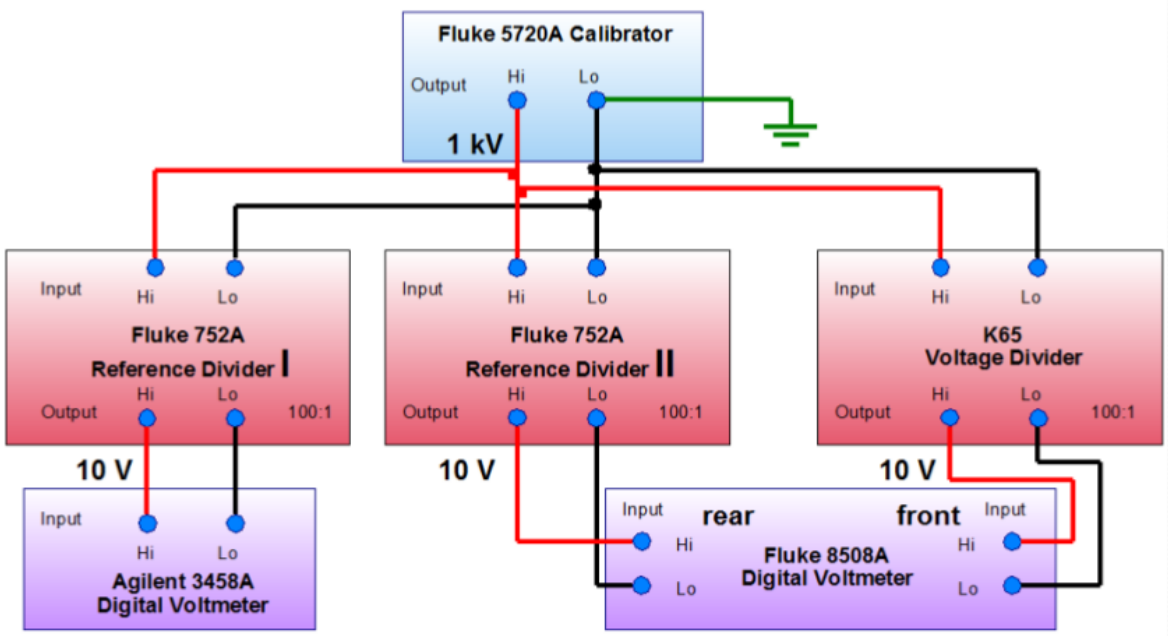

Figure 5.5.: The Fluke 5720A Calibrator (blue) provides an input voltage of 1 kV, which is downscaled with the three voltage divider (two reference dividers Fluke 752A and a high voltage divider K65, all red). The downscaled voltage is measured with the two digital voltmeters Agilent 3458a and Fluke 8508A (purple). [Fri15]

In 2015 calibration and stability measurements were conducted with the Fluke reference divider 752A. Within these measurements, the stability of the high precision voltmeter and of the reference divider were measured, additionally the voltage was monitored with the high voltage divider K65. From these measurements, the scale factors of the used reference dividers were determined (see fig. 5.5). For the measurements, the Fluke calibrator 5720A was used as the voltage source. The high voltage was connected to two reference dividers and the K65. The downscaled voltage was measured with the Agilent 3458a digital voltmeter, which measured the output voltage of one reference divider, and the Fluke 8508A digital voltmeter, which measured with the output voltages of the second reference divider and the K65. These measurements were done with different combinations of reference dividers and with calibrated and uncalibrated reference dividers. The results of the stability measurements are shown in figure 5.6.

The stability measurement shows an unexpected behavior of the Agilent 3458a digital voltmeter, which had a significantly higher drift, than the Fluke 8508A voltmeter. From the results in figure 5.6, the scale factor of the used reference divider can be calculated, which is shown in figure 5.7.

The absolute value of the calculated scale factor ranges between 1 and 4 ppm above 100 in every measurement. The scale factor should be 100.00000(5) after a calibration.

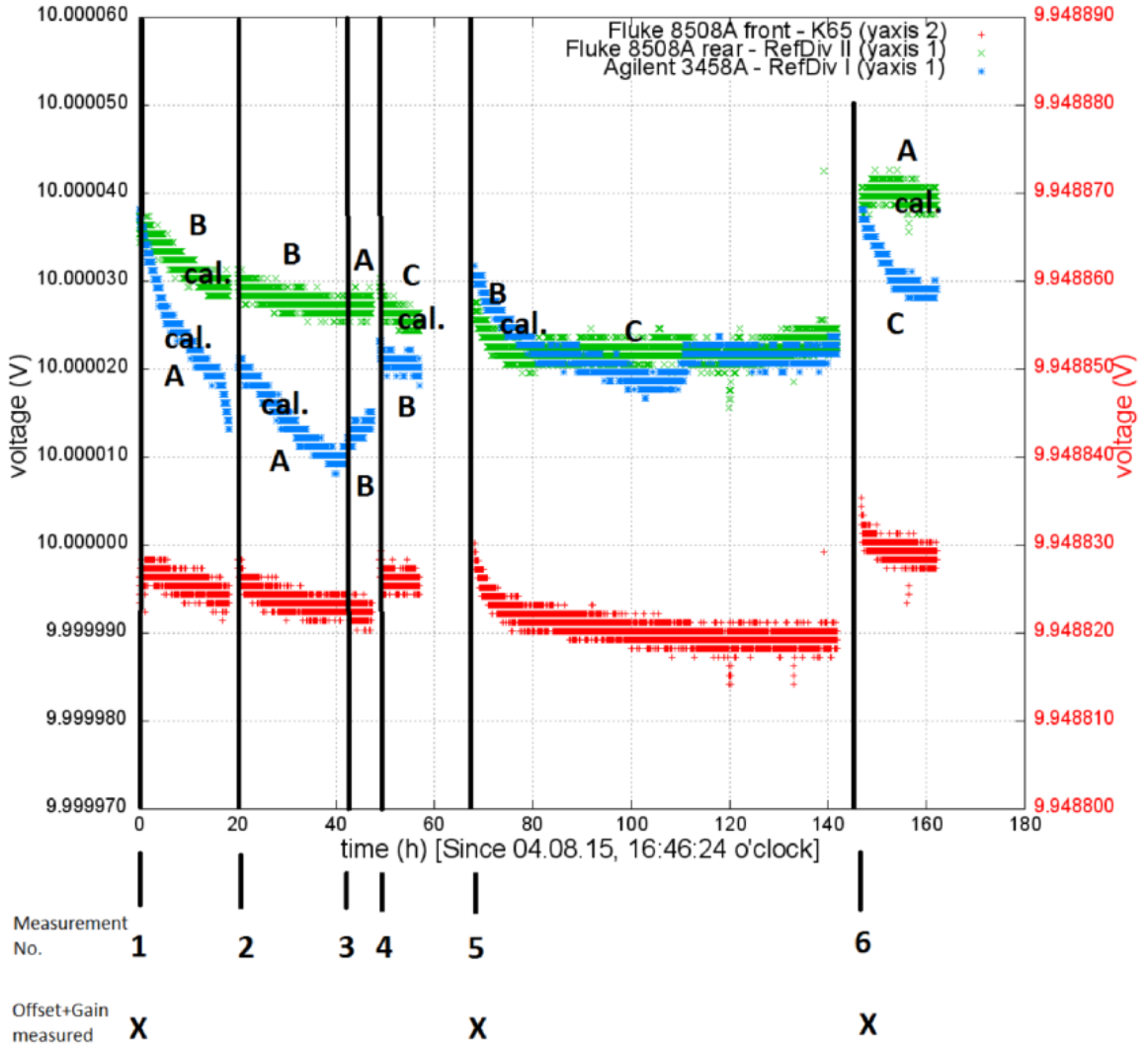

Figure 5.6.: Results of the stability measurements, conducted with the different reference dividers. The reference voltage was determined with the K65 (red data points) The output voltage of the reference dividers is shown on the left axis, the output of the K65 is shown on the right axis, because of the higher scale factor of $M_{100}^{K65} = 100.51485 \pm 0.00001$. The green data points are measured with the Fluke 8508A rear panel, which measured one reference divider, the blue data points are taken from the Agilent 3458a, which measured the other reference divider. [Fri15]

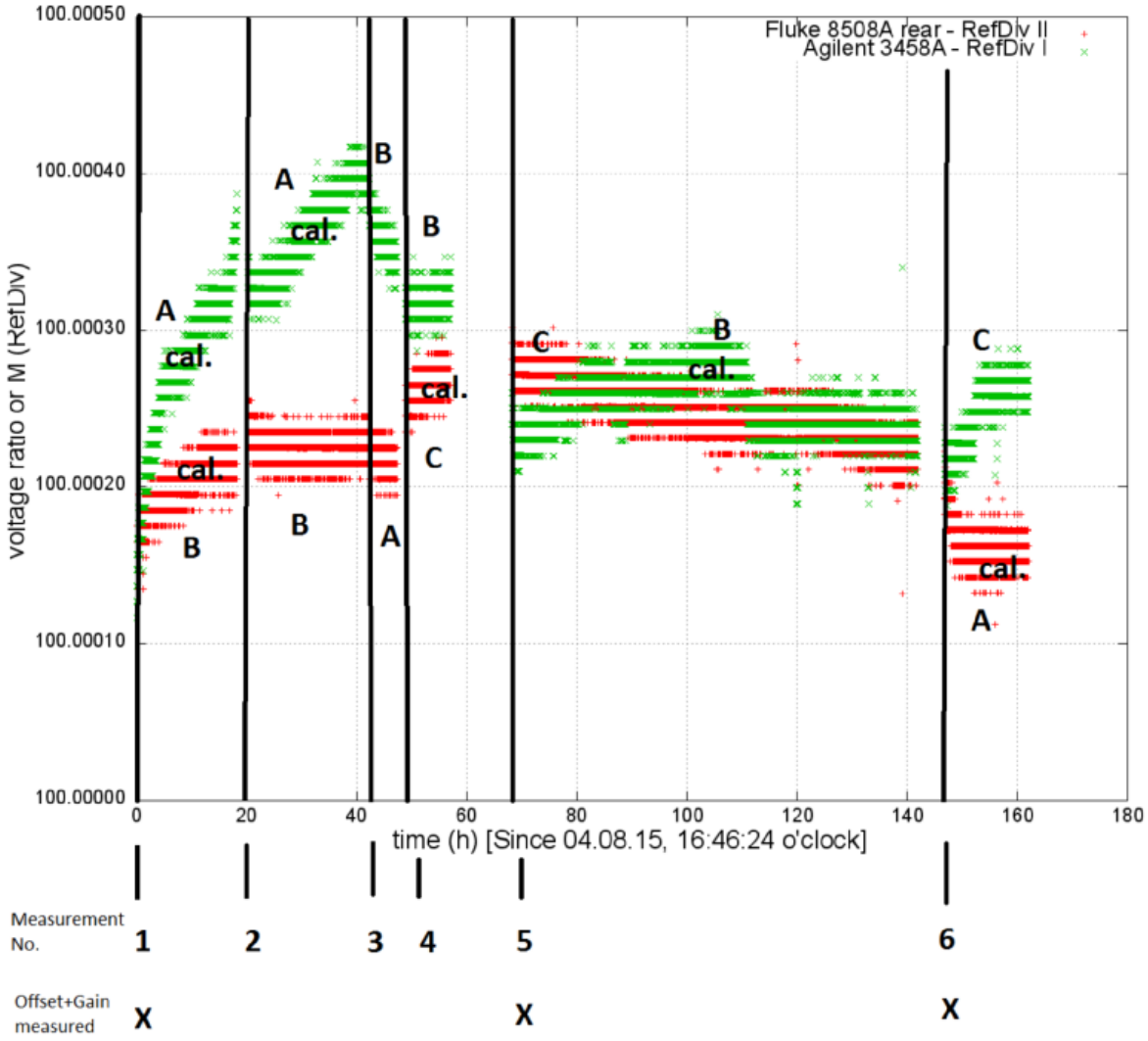

Figure 5.7.: Calculated scale factor from stability measurements shown in figure 5.6. The red data points are measured with the Fluke 8508A voltmeter, and the green data points are measured with the Agilent 3458a voltmeter. The calculated scale factors stay within in a band of about 3 ppm and the absolute value is in every case greater than 100:1. The scale factors calculated with the Agilent 3458a voltmeter show a strong drift and differ from the measured scale factor of the Fluke 8508A. [Fri15]

With this measurements the absolute scale factor of the reference divider could not be determined. The absolute scale factor strongly depends on the accuracy of the digital voltmeters. But one piece of the important information from this measurements is, that the Agilent 3458a has a strong drift at the beginning of the measurement. Every time, the Agilent 3458a and the Fluke 8508A were calibrated with the gain and offset calibration, which is explained in the next section, indicated by the calibration marker X at the bottom of the plot, both scale factors start at the same value, but after some measurement time, the measured scale factor of the Agilent 3458a drifts away from the initial scale factor.

5.2. Calibration of high precision digital voltmeters

Before the used digital voltmeters are described, the calibration procedure for a high precision digital voltmeter is shortly described. High precision digital voltmeters measure a voltage difference between a given potential and a reference potential, which is mostly given by the ground potential. The calibration of the voltmeters can drift. Therefore calibration on regular bases is essential. For the offset measurement, both inputs of the digital voltmeter have to lie on the same potential. Therefore a first offset measurement is done, in which both inputs of the voltmeter are short-circuited and measure for a defined time period (in case of this thesis the time period usually was 5 to 10 minutes). From the taken data, the mean offset U_{offset} can be estimated. With a Fluke standard reference the gain of a digital multimeter can be determined. Therefore the Fluke standard reference is connected to the digital voltmeter and again measured for a defined time period, which was again 5 to 10 minutes in this thesis. The mean value of the gain measurement is U_{meas}, from which the mean gain factor U_{gain} can be calculated:

$$U_{\text{gain}} = \frac{U_{10\,\text{V}}}{U_{\text{meas}} - U_{\text{offset}}}. \tag{5.3}$$

The $U_{10\,\text{V}}$ is the calibrated value of the 10 V standard reference source. For the measurements in Münster four reference sources can be used, which are named A, B, C and D. For the measurements in this thesis the Fluke reference voltage source D was taken with an exact value of $U_{\text{D}} = -10.000240 \pm 0.000005$. To calculate the real value U_{real} from measurements U_{meas} the equation has to be converted

$$U_{\text{real}} = (U_{\text{meas}} - U_{\text{offset}}) \cdot U_{\text{gain}}. \tag{5.4}$$

5.3. The high precision digital voltmeter Fluke 8508A

The following section describes the high precision digital voltmeter Fluke 8508A, which was used during the absolute calibration measurements to measure U_{Base} (see fig. 4.3). The voltmeter was used during the absolute calibration measurements in the 8.5 resolution fast mode and the 20 V range. The technical information come from [Flu06].

Table 5.1.: Integration time of the Fluke 8508A for the different resolutions with or without the fast mode. The NPLC are the number of power line cycles, which are at a given power frequency of $f_{\text{power}} = 50\,\text{Hz} \Rightarrow 1\,\text{PLC} = 20\,\text{ms}$. This table is taken from [Flu06].

Resolution	Fast mode on	Fast mode off
5.5	3.3 ms	1 PLC
6.5	1 PLC	16 PLC
7.5	64 PLC	4·64 PLC
8.5	4·64 PLC	16·64 PLC

Table 5.2.: This table shows the time delay of the Fluke 8508A within the external trigger mode active. The time delay depends on the resolution chosen for the measurement, and whether a filter is active of not. This table comes from [Flu06].

Resolution	Filter on	Filter off
5.5	0.8 s	0.08 s
6.5	1 s	0.1 s
7.5	5 s	1 s
8.5	10 s	5 s

5.3.1. Operation modes of the Fluke 8508A

The Fluke 8508A has different operation modes for DC voltage measurements. The voltmeter can measure with the precision of 5.5 up to 8.5 digits in fast mode or in normal mode. The different modes have different integration times for the measurement of a DC voltage (shown in table 5.1).

The voltmeter was used in the 8.5 resolution fast mode, which has an integration time of $t_{\text{int}} = 4 \cdot 64\,\text{PLC} = 5.12\,\text{s}$. With this integration time an expected measurement time of about 6 s was intended. The data recording has taken 11 s. Within voltmeter synchronization measurements (see sec. 5.5), a gap of $t_{\text{gap}} = 5.055\,s$ was found at the beginning of every measurement. This measured gap agrees well with the data in the manual, which is shown in table 5.2. The time delay is only active in the external trigger mode, and depends on whether a low-pass filter is on or off.

Another observation was done within the synchronization measurements. The actual measurement time of the Fluke 8508A was determined as $t_{\text{int-real}} = 5.975\,\text{s}$, which is $\Delta t = 0.855\,\text{s}$ higher, than the calculated measurement time.

5.4. The high precision digital voltmeter Agilent/Keysight 3458a

The following section describes the high precision digital voltmeter Agilent 3458a, which was used during the absolute calibration measurement to measure U_{Signal}, and the Keysight 3458a, which measured $U_{\text{Calibration}}$ (see fig. 4.3). The Agilent voltmeter was used during the measurements in the 10 V range with 8.5 digits and 150 NPLC,

the Keysight voltmeter was used in the 100 V range with 8.5 digits and 150 NPLC. The following informations come from [Agi12].

5.4.1. Operation modes of the Agilent/Keysight 3458a

The Agilent and Keysight 3458a high precision digital voltmeters have different possibilities of operation for DC voltage measurements. The precision of the voltmeter can be operated with a resolution from 4.5 up to 8.5 digits, with the possibility to set the NPLC manually. An overview of the different NPLC with the different precision modes is given in table 5.3.

Table 5.3.: This table shows the dependency of the integration times and the precision for the Agilent/Keysight 3458a. Additionally the number of readings per second dependent on the AZERO function is shown for the single integration times [Agi12].

		Readings/sec	
NPLC	digits	A-Zero off	A-Zero on
0.0001	4.5	83300	3440.3
0.0006	5.5	41650	2624
0.01	6.5	4415	774.7
0.1	6.5	493	204
1	7.5	50	24.5
10	8.5	5	2.5
100	8.5	0.5	0.25
1000	8.5	0.05	0.025

In the A-Zero measurement mode, the digital voltmeter performs a decoupled offset measurement between every measurement step, which is subtracted from the previous measurement. Therefore, the number of measurements for high integration times is increased by the factor of two. Furthermore, the voltmeter makes measurements in 10 NPLC sections for integration times $t > 10\,\text{NPLC}$. In between these integration sections, the voltmeter conducts the additional offset measurement. This gap between two measurement packages of $t_{\text{gap}} = 10.6\,\text{NPLC} = 0.212\,\text{s}$ was observed during the synchronization measurements, shown in the next section.

5.5. Synchronization measurements for the three digital voltmeter

Due to a measurement on the 09.06.2017 (see fig. B.1 in the appendix) with a strong drift a missing synchronization of the three voltmeter was assumed. Mainly the desynchronization of the Fluke 8508A and the Agilent 3458a was observed, because both voltmeters measure the voltages U_{Base} and U_{Signal} that affect most of the μ-determination measurements. From the observed drift of about $\mu_{\text{drift}} = 0.1\,\text{ppm}\frac{1}{10\,\text{min}}$ a desynchronization was observed due to offsets of the data points (see fig. B.2 in the appendix). The drift indicates problems with the read out of the voltmeter, which

could be examined with a defined input signal, created by a function generator (Tectronix AFG 3102 [Tec05]) with an accuracy of 1 % of a voltage setting. To investigate the synchronization problems, the function generator produces a defined sawtooth signal, which is simultaneously read out by the voltmeter. The first measurements were conducted with a 10 V amplitude, which was ramped up repeatedly with a 120 s period. The first measurement was only conducted with the Fluke 8508A and the Agilent 3458a (see figure 5.8).

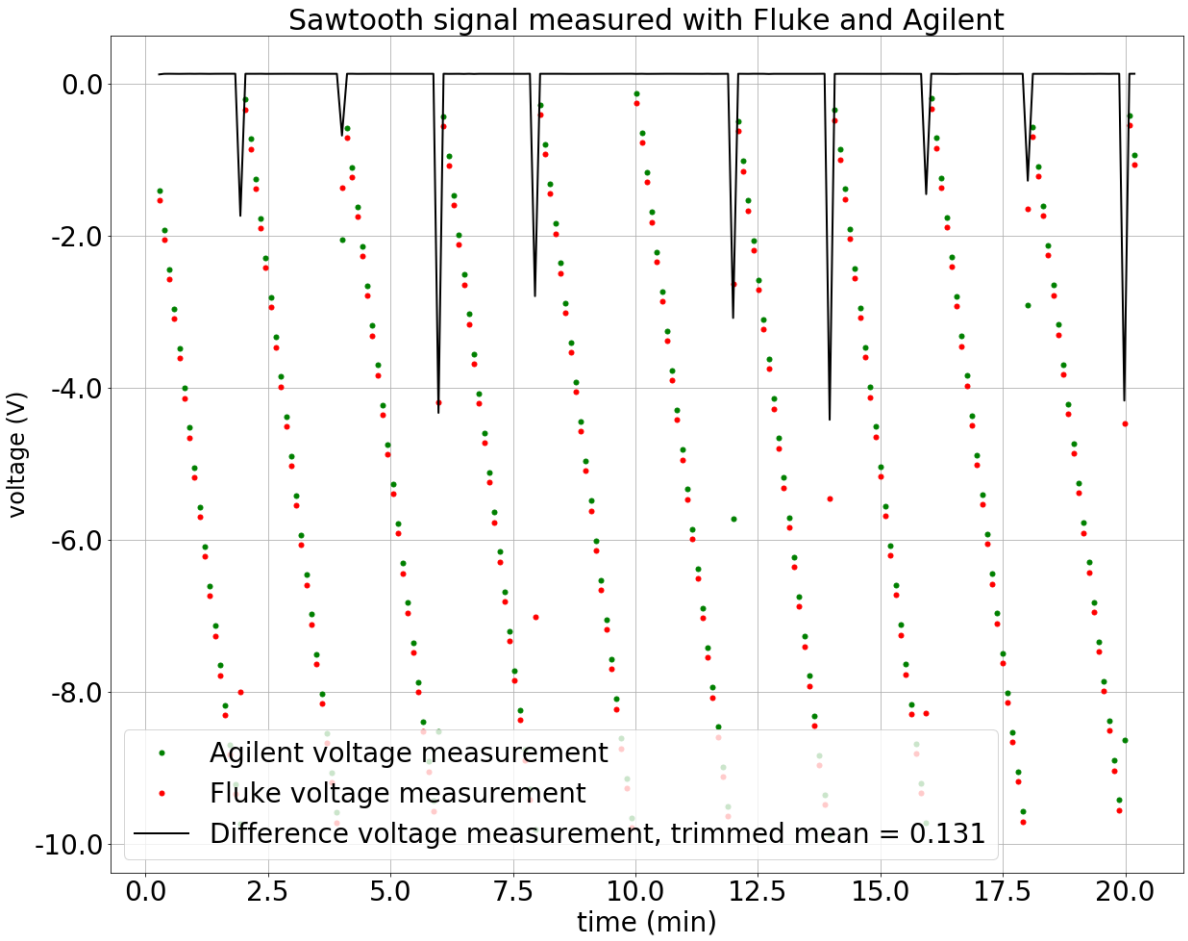

Figure 5.8.: The plot shows the measurement results from the Fluke 8508A and the Agilent 3458a of the sawtooth signal created by the Tectronix AFG 3102. The solid line is the difference of both results ($U_{\text{Agilent}} - U_{\text{Fluke}}$, which has a truncated mean of 0.131 V).

These measurements showed a problem within the data taking of the three digital voltmeters, because the AZERO of the Keysight/Agilent 3458a digital voltmeter, and the time delay of the Fluke 8508A were not considered. For the final measurement setup the NPLC of the Keysight/Agilent 3458a digital voltmeter have been adjusted to 150 NPLC and a time delay of $t_{\text{Agilent}} = 5040\,\text{ms}$ and $t_{\text{Keysight}} = 4955\,\text{ms}$, in order to account for the initial $\approx 5\,\text{s}$ delay of the Fluke digital voltmeter. The time delay of $\approx 100\,\text{ms}$ between the Agilent and Keysight digital voltmeter which is caused by to

the slow control.

5.6. Uncertainty determination of the digital voltmeters

For the analysis of the absolute calibration, it is important to determine the uncertainty for the μ determination and the scale factor determination correctly. Therefore uncertainty measurements were done with all three digital voltmeters and the Fluke calibrator 5720A. The uncertainty of a digital voltmeter depends of the uncertainty of the measurement range and the uncertainty of the voltmeter reading. The data sheets of all three digital voltmeters have different values for the uncertainties, which are shown in 5.4.

Table 5.4.: Transfer uncertainties of the high precision digital voltmeters Fluke 8508A and Keysight/Agilent 3458a according to the manufacturer. In this table, only the used measurement ranges and the corresponding uncertainties of all three digital voltmeters are shown. The uncertainty for the Fluke 8508A is the transfer uncertainty for a 20 min measurement in a $\pm 1\,^{\circ}$C temperature stable environment with a 4 hour warm up period. The uncertainties for the Agilent and Keysight 3458a is the transfer accuracy for a 10 min measurement in a $\pm 0.5\,^{\circ}$C temperature stable environment with a 4 hour warm up period. These uncertainties are given for the reproducibility of a measurement. [Flu06] [Agi12]

Voltmeter	Range (V)	uncertainty of reading (ppm)	uncertainty of range (ppm)
Fluke 8508A	20	0.12	0.1
Agilent 3458a	10	0.05	0.05
Keysight 3458a	100	0.5	0.1

The uncertainty given by the companies are the transfer accuracies. In this case the digital voltmeters are calibrated before or after each measurement with a gain and an offset measurement. Additionally the measurement time is larger than 4 min measurement time given in the manual. Therefore additional uncertainty measurements were done.

For the uncertainty measurements each digital voltmeter is connected to a ppm stable voltage source and measured over night. In this longterm measurement the scattering of the data points is analyzed in a period with low drift. For the calculation of an uncertainty of the range and of the reading, two different voltages should be measured in the given voltage range. For the Fluke 8508A and the Agilent 3458a voltages of -10 V and -5 V were chosen, the Keysight 3458a measured -10 V and -90 V. All voltages were generated with the Fluke Calibrator 5720A. The data points behave Gaussian, therefore a mean value and the standard deviation σ_{meas} can be determined for the uncertainty calculation. An example plot of the uncertainty determination is shown in 5.9.

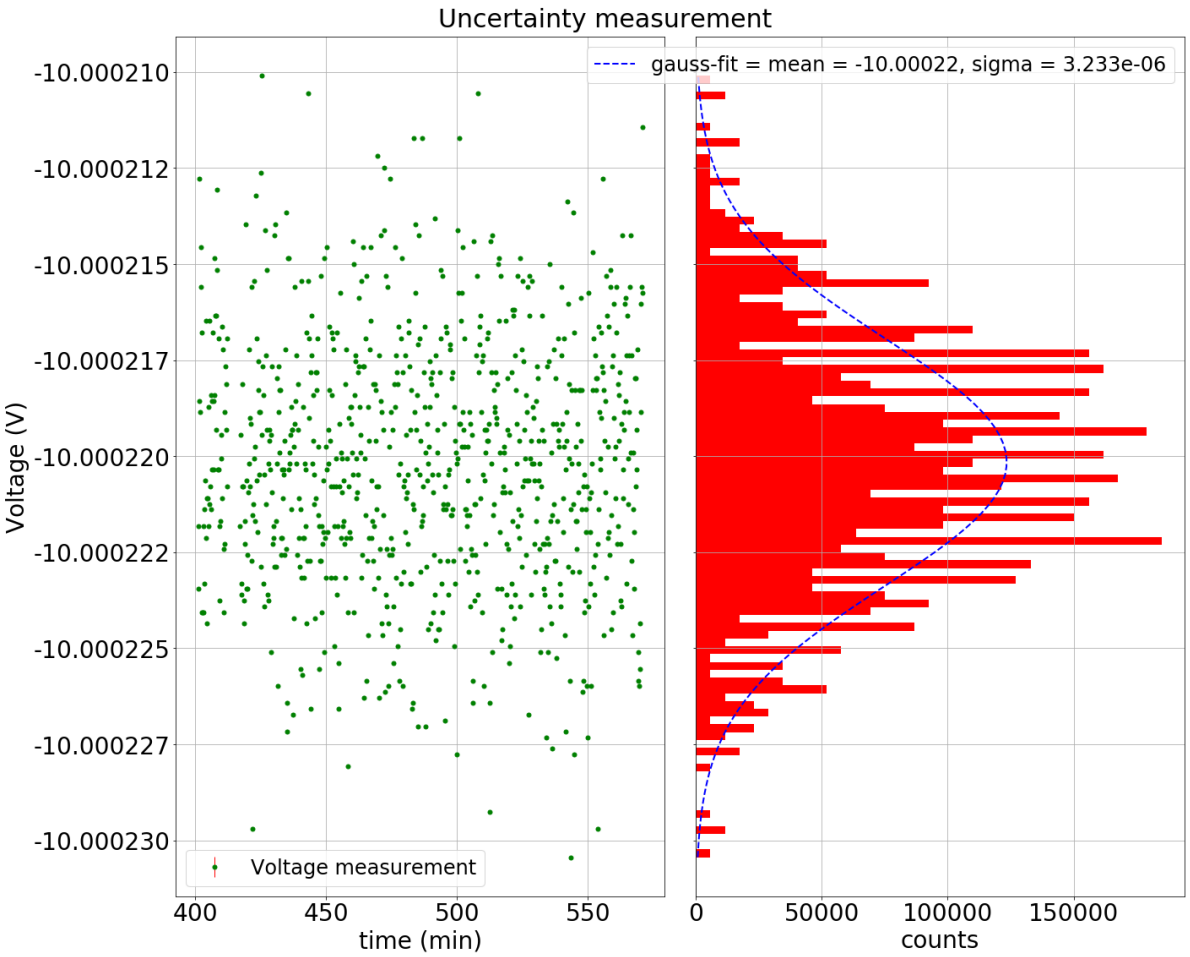

Figure 5.9.: Stable voltage measurement with a 10 V input created by the Fluke 5720A calibrator for the Keysight 3458a digital voltmeter in the 100 V range. The plot on the left shows the voltage measurement versus time, the plot on the right shows the histogram of the data points with a Gaussian fit of the data points.

With these measurements the uncertainty of the range (σ_{range}) and reading (σ_{reading}) can be calculated, because the whole uncertainty σ_{meas} consists of both uncertainties σ_{range}, σ_{read}, the measurement range $\rho = 100\,\text{V}$ and the voltmeter reading U_{meas}

$$\sigma_{\text{meas}} = \sigma_{\text{range}} \cdot \rho + \sigma_{\text{read}} \cdot U_{\text{meas}}. \tag{5.5}$$

The uncertainties are added linearly, according to the manufacturer, and not as usual in square. With all six measurements with the different voltages, σ_{range} and σ_{read} can be determined for each voltmeter. Therefore the measurement results of the higher voltage measurement (U_{high}, σ_{high}) and lower measurement (U_{low}, σ_{low}) are included as σ_{meas} and U_{meas}

$$\sigma_{\text{read}} = \frac{\sigma_{\text{low}} - \sigma_{\text{high}}}{U_{\text{low}} - U_{\text{high}}} \tag{5.6}$$

Table 5.5.: These are the measured uncertainties of the three high precision digital voltmeters Fluke 8508A and Keysight/Agilent 3458a for the used voltage ranges. Additionally the measured σ_{low} of the low (-5 V for Fluke 8508A and Agilent 3458a and -10 V for Keysight 3458a) measurement and the σ_{high} of the high (-10 V for Fluke 8508A and Agilent 3458a and -90 V for Keysight 3458a) measurement are shown.

Voltmeter	σ_{low} (V)	σ_{high} (V)	σ_{range} (ppm)	σ_{read} (ppm)
Fluke 8508A	$5.26 \cdot 10^{-7}$	$6.93 \cdot 10^{-7}$	0.018	0.033
Agilent 3458a	$3.03 \cdot 10^{-7}$	$5.18 \cdot 10^{-7}$	0.009	0.043
Keysight 3458a	$4.14 \cdot 10^{-6}$	$5.49 \cdot 10^{-6}$	0.040	0.017

and

$$\sigma_{\text{range}} = \frac{\sigma_{\text{low}} - \sigma_{\text{read}} \cdot U_{\text{low}}}{\rho}. \tag{5.7}$$

These are the uncertainties of the single digital voltmeters. The results of these measurements are shown in table 5.5.

The calculated uncertainties come from two measurements at two different voltages. In addition a linear relationship is required for the calculation of the uncertainties. In the measurement, the measured voltages are in different ranges, except for the Keysight 3458a, which measures in the second measurement a voltage of about -90 V.

Additionally to the statistical uncertainties systematic uncertainties can influence the measurement. The first systematic uncertainty comes from the Agilent 3458a digital voltmeter, which showed a time depending drift in one of the reference measurements. The drift was only seen at -10 V measurements with the Fluke 5720A calibrator and the Fluke 732A 10 V reference source. In both cases the other digital voltmeter measured the same voltage, but no time dependent drift could be observed. The data points of the Agilent 3458a are shown in figure 5.10. Compared to the Fluke 8508A (see fig. 5.11), which measured the same voltage. The Agilent drifted with the total value of about 30 μV in 70 hours. Such a strong drift can not be observed with the Fluke 8508A, only a temperature dependent drift with about 1 $\frac{\mu\text{V}}{\text{K}}$.

In a long term offset measurement no time dependent drift was visible with the Agilent 3458a (see fig. 5.12). The temperature dependence of the Fluke 8508A is not visible in the offset measurement (see fig. 5.13).

Other systematic uncertainties can come from the used cables. The connectors of the cables are not thermally protected, which can result in thermo voltages. Copper has different seebeck coefficients, which indicates thermoelectric voltages. An example of different seebeck coefficients is shown in table 5.6.

The measured voltage of the Fluke 8508A in fig. 5.11 was about 10 V, which had a temperature dependency of about 1 $\frac{\mu\text{V}}{\text{K}}$, which is inside the range of the thermoelectric voltages.

Another possible uncertainty can come from other measurement cables. In the correction factor only the high voltage cables are included (see sec. 6.1). The cables are

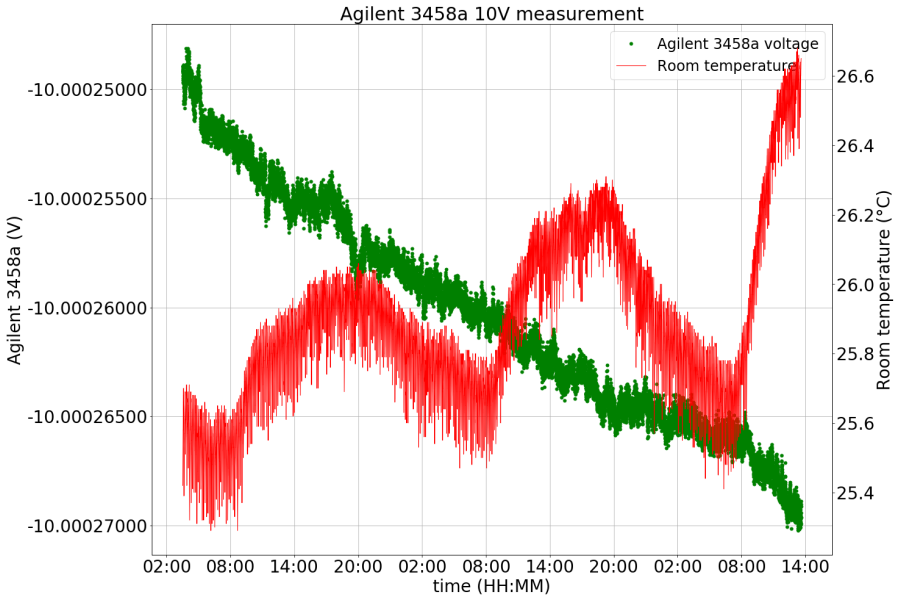

Figure 5.10.: The Agilent 3458a measured $-10\,\mathrm{V}$ of the Fluke 7520A calibrator for 70 h (green). The high precision digital voltmeter shows a strong drift of about $D_{\mathrm{Agilent}} = 10\,\frac{\mu\mathrm{V}}{d}$. Additionally the room temperature measured with a Pt100 is shown (red).

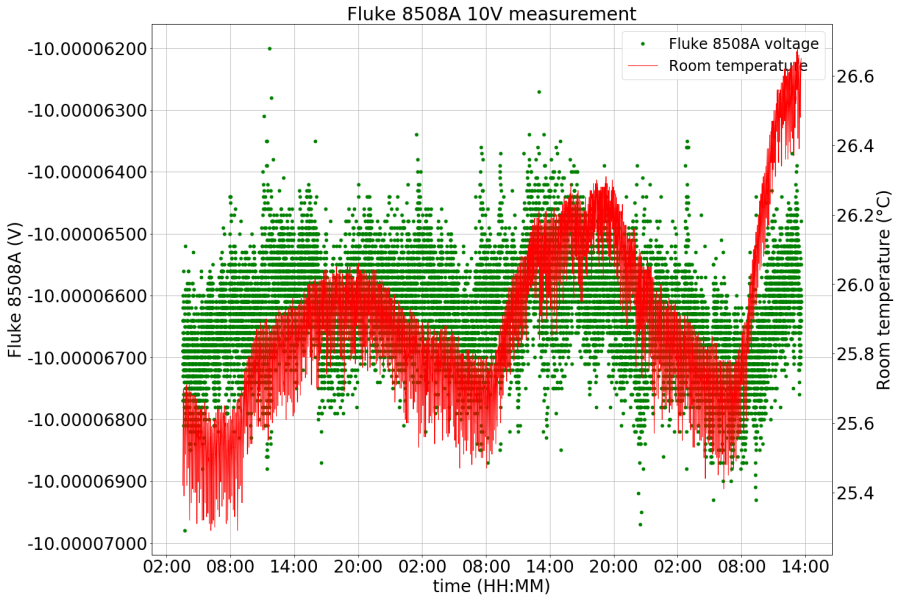

Figure 5.11.: The Fluke 8508A measured $-10\,\mathrm{V}$ created with the Fluke 7520A calibrator for 70 h (green). The high precision digital voltmeter shows a temperature dependent drift of $D_{\mathrm{Fluke}} = 1\,\frac{\mu\mathrm{V}}{\mathrm{K}}$. Additionally the room temperature measured with a Pt100 is shown (red).

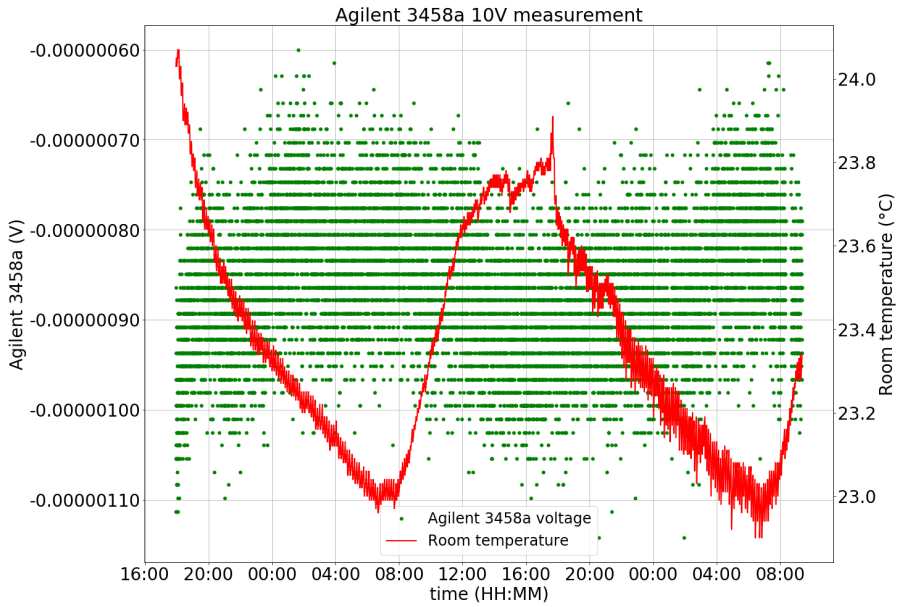

Figure 5.12.: The offset measurement of the Agilent 3458a for 40 hours (green). The high precision digital voltmeter shows a temperature dependent drift of the offset. Additionally the room temperature measured with a Pt100 is shown (red).

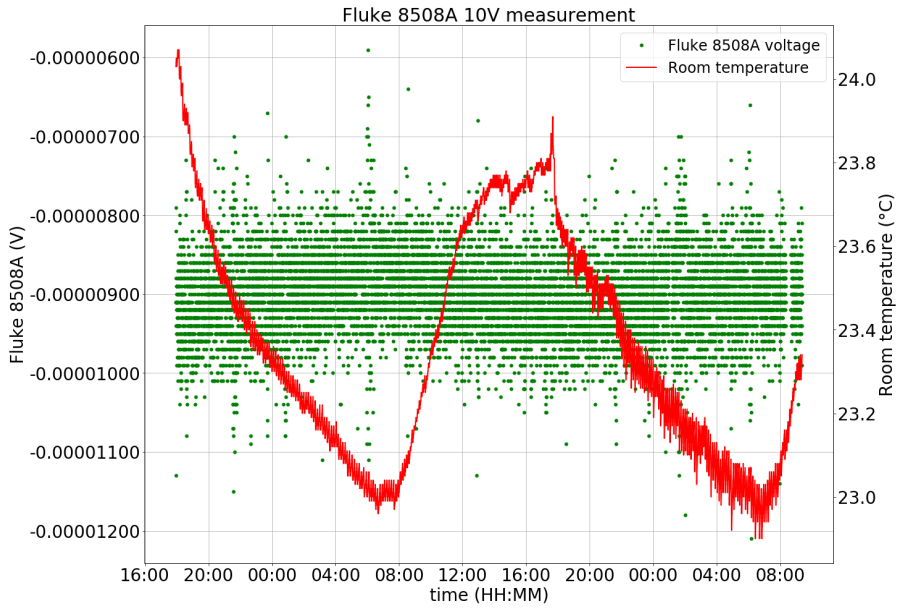

Figure 5.13.: The offset measurement of the Fluke 8508A for 40 hours (green). The high precision digital voltmeter shows no significant drift of the offset. Additionally the room temperature measured with a Pt100 is shown (red).

Table 5.6.: Seebeck coefficients for different pairs of copper and other materials [Tec16].

Paired Materials	Seebeck Coefficient ($\frac{\mu V}{K}$)
$Cu - Cu$	$\leq$0.2
$Cu - Ag$	0.3
$Cu - Au$	0.3
$Cu - Pb/Sn$	1-3
$Cu - Si$	400
$Cu - CuO$	$\approx$1000

not included as a correction up to now.
Additionally the non-linearity of the digital voltmeter can result in a systematic uncertainty. All three digital voltmeters are calibrated before each measurement with an offset measurement, where the high and low input of the voltmeter is short-circuited, and a gain measurement, where the digital voltmeters are connected to a Fluke 732A 10 V reference source. The digital voltmeters are therefore calibrated in the range of 10 V. The Keysight 3458a digital voltmeter measures voltages in the range of 90 V, where non-linearities can influence the measurement. The Agilent 3458a digital voltmeter measures a voltage in the range of 0 V and a voltage in the range of 1 V. For the 0 V measurement the gain calibration has no significant impact, therefore the calibration works. For the 1 V measurement the gain factor has a larger impact, that non-linearities can influence the measurement. The Fluke 8508A digital voltmeter measures voltages in the range of 0 V, where the gain calibration has no impact and only the offset measurement is essential. Additionally to the possible non-linearity, the calibration of the digital voltmeter is done at the beginning of a series of measurements and at the end. Therefore the manuals of the digital voltmeter give uncertainty factors for different times depending when a calibration measurement was done. The uncertainties in the given measurement ranges are given in table 5.7.

Table 5.7.: Uncertainties of the digital voltmeters in the given measurement ranges [Flu06] [Agi12].

Voltmeter	uncertainty of reading (ppm)	uncertainty of range (ppm)
Fluke 8508A	0.5	0.2
Agilent 3458a	0.5	0.05
Keysight 3458a	2.5	0.3

These uncertainties were taken to estimate the systematic uncertainty for the ratio and scale factor measurements.

5.7. Self constructed high voltage calibration cage

Within the calibration measurement a second voltage is added onto the high voltage created with the first FuG MCP 14-1250. To add the voltage, the second MCP is

set on the potential created of the first MCP. Due to measurement safety, the second MCP and the measurement equipment is locked into a self constructed high voltage measurement cage. The following section describes the measurement cage and the measurement setup inside the high voltage cage in detail.

5.7.1. The mechanical setup of the high voltage measurement cage

The high voltage cage consists of two cages, made of KANYA profiles and perforated sheets, to protect the high voltage from any outer disorders. The outer high voltage cage is 175 cm height, 85 cm width and 112 cm depth, the inner and outer cage both have s door at the front and rear side, to make access possible at the front and rear side of the inner devices. Inside the outer cage, four high voltage isolators are mounted, which hold the inner cage and provide sufficient clearance for a isolating transformer. The inner cage has four layers, which provide sufficient space for the different measurement devices. Hooks are mounted at the top of the outer cage, which allow transport by a crane. At the bottom four wheels are mounted for a possible movement of the cage.

5.7.2. The electrical setup of the high voltage measurement cage

The outer cage has to be grounded at every time. This is realized by a grounding cable, which connects the cage directly with the laboratory ground. If no measurement is done, the inner cage should be grounded as well, therefore three grounding connections are included inside the outer cage, a first grounding connection, with a ground lance to ground the cage with a protection from the high voltage. The second grounding connection is done with a crocodile clip, which allows another quick grounding connection. Another grounding connection is manually mounted every time, the measurement is done. Every other part of the outer and inner cage is connected safely with at least two grounding connections, e.g. the grounding connections of the doors (see fig, 5.14). In the inner high voltage cage, every layer is directly connected to a grounding bar. This grounding bar has a direct connection to the feeding high voltage supply, which allows to set the high voltage cage to the intended potential. Every other device used inside the high voltage cage is also directly connected to the grounding bar (see fig. 5.15). The devices inside the cage get their power via the isolating transformer, which is located at the bottom of the outer cage at the front side. The isolating transformer then supplies the inner devices with a voltage of 230 V, even if they are used at a high voltage potential.

5.7.3. The measurement chain inside the high voltage measurement cage

To control the voltage of the FuG MCP 14-1250 inside the cage and the readout of the Keysight 3458a digital voltmeter, several other devices are needed for the measurement procedure. A sketch of the measurement setup is shown in fig. 6.6. The high voltage is directly wired to the grounding bar on the inside of the cage, from where every other device inside the cage is sets to the potential of the applied high voltage.

Figure 5.14.: The doors of the high voltage cage are grounded at two points with two independent cables, one at the top, the other at the bottom. The cables connect the KANYA profiles from the doors to the rest of the cage.

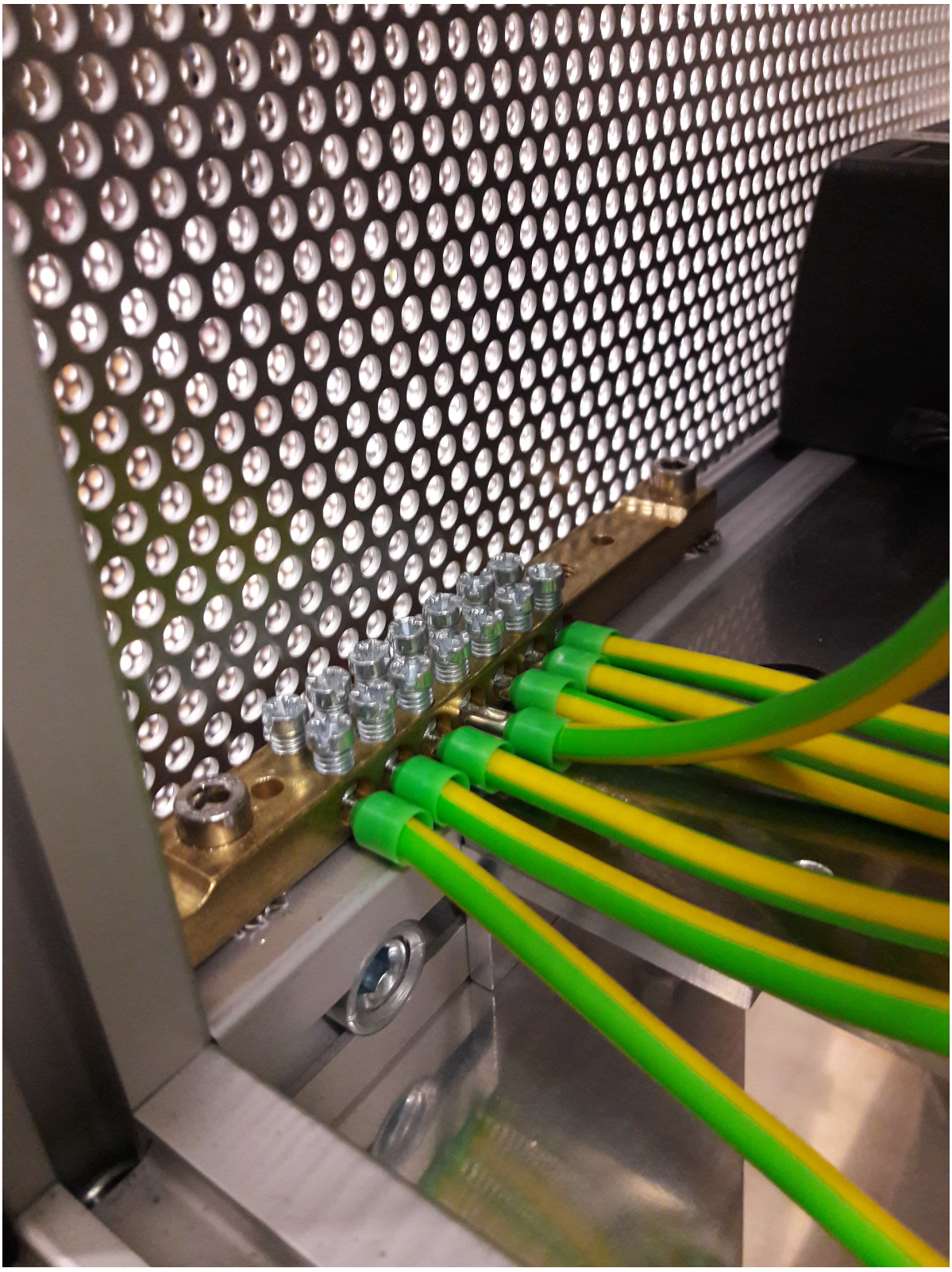

Figure 5.15.: Every device, which is needed for the measurement is directly connected via a grounding cable to the grounding bar at the bottom right.

From the grounding bar, a cable is connected to the low input of the Keysight voltmeter, to lift the low potential to the high voltage potential for a difference voltage measurement. The high input of the Keysight is connected to the high output of the FuG MCP. A third high voltage cable leads the high voltage outside of the cage to the reference voltage divider. The reed relay is directly connected with two short cables to the high and low input of the Keysight voltmeter. This relay is controlled over the remote socket in the lowest layer of the high voltage cage. The remote socket can open and close the relay for the different measurements. The Keysight voltmeter is controlled over GPIB, which is done via a Prologix GPIB Ethernet converter. All three devices, the GPIB Ethernet converter, the remote socket and the FuG MCP are controlled and read out over an Ethernet connection, which is lead out of the cage via an optical converter MOXA, which is connected to another optical converter outside the cage, with the computer.
In the μ determination measurement, the reed relay is short-circuited. With the short circuit the high voltage is directly connected to the reference voltage divider outside of the cage, and the Keysight voltmeter measures the voltage drop over the resistance of the relay. In the scale factor determination measurement, the short circuit of the relay is removed and the FuG MCP delivers a voltage of $-90\,\mathrm{V}$, which is now measured by the Keysight voltmeter.

6. Measurements

6.1. First explorative measurements by downscaling of absolute calibration measurement method to 1 kV

The first idea for the absolute calibration of the Fluke 752A reference voltage divider was to downscale the method for the high voltage divider. Therefore the setup was arranged as described in section 4.3. For the measurement both FuG MCP 14-1250 were used, the voltage outside of the cage was chosen to 1 kV, the voltage inside of the cage was primarily chosen to 10 V, to keep the same ratio of the voltages for the downscaled method. As the voltage source U_{Ref} the Fluke 10 V standard reference source D was taken. In the first measurements, reference divider B was calibrated with the help of reference divider A. The resulting plot for the ratio μ determination and the scale factor M_{Signal} measurement is shown in 6.1, 6.2.

The uncertainties for all measurements are calculated as explained in section 6.2. For the first measurements only the statistical uncertainties were calculated. The results of the first measurements gave a ratio factor $\mu = 0.999999716 \pm 0.000000004$. That means, the difference between both scale factors is 0.3 ppm. The scale factor measurement gives a scale factor of $M_{\mathrm{Signal}} = 99.99699 \pm 0.00004$, which is 30 ppm lower than the expected value of 100. That leads to the assumption, that a simple downscaling does not give proper results for 1 kV reference divider.

The first problem of the measurements was the reed relay, which is used to generate the short-circuit in the ratio measurement. The Keysight 3458A digital voltmeter measured a voltage of about 250 μV during the μ determination. The relay has a contact resistance up to $(230 \pm 23)\,\Omega$ regarding to the data sheet [Med11]. The current in the circuit can be calculated with the given specifications of the used devices [FuG14] [Flu93]. The FuG MCP creates a voltage of (1.000 ± 0.001) kV, the voltage mainly drops at the reference divider, which has a total resistance of $(2.00 \pm 0.01)\,\mathrm{M}\Omega$. That leads to a current I of

$$I = \frac{(1.000 \pm 0.001)\,\mathrm{kV}}{2.00 \pm 0.01\,\mathrm{M}\Omega} = (0.500 \pm 0.005)\,\mathrm{mA}. \tag{6.1}$$

The uncertainty is calculated with Gaussian error propagation. With this current a voltage of $(115 \pm 12)\,\mu$V was predicted to drop at the reed relay. In the first calculation the reed relay voltage was not included. Due to the first results the reed relay voltage U_{relais} has to be implemented in the ratio calculation as the first correction. Because of other problems, which are described in the following, another correction term U'_{corr-1}

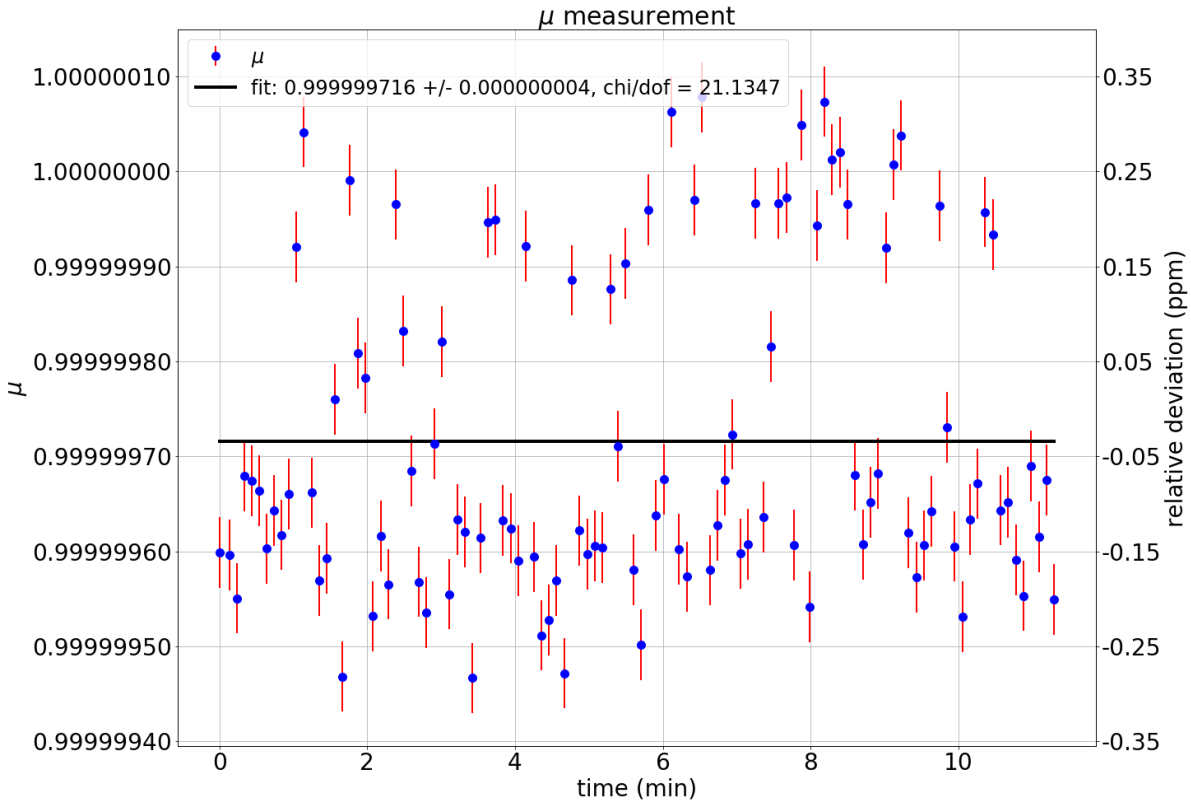

Figure 6.1.: First μ measurement done with the downscaled setup of the absolute calibration of the K65 and K35 to 1 kV reference divider. Two identical dividers were taken, which were both uncalibrated. The measured ratio factor is $\mu = 0.999999716 \pm 0.000000004$.

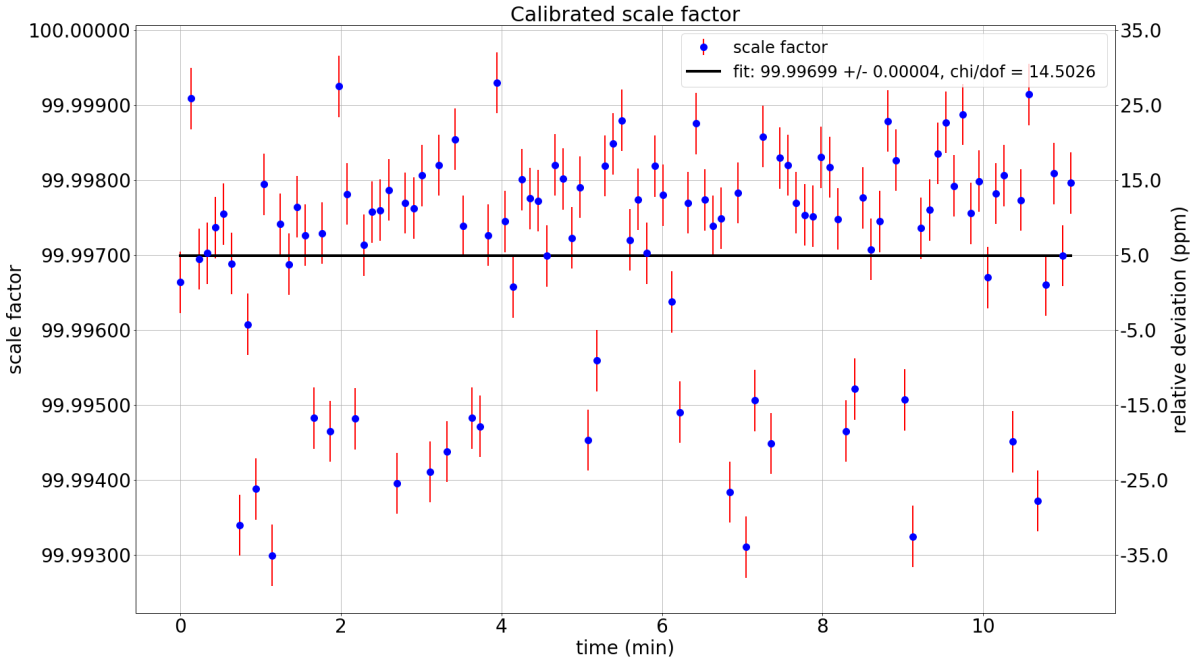

Figure 6.2.: First scale factor M_{Signal} measurement done with the downscaled setup of the absolute calibration of the K65 and K35 to 1 kV reference divider. The same 1 kV reference divider as in 6.1 was taken to calibrate reference divider B. The measured scale factor $M_{\text{Signal}} = 99.99699 \pm 0.00004$ is 31 ppm lower than 100.

is still included to the calculation

$$\frac{M_{\text{Base}}}{M_{\text{Signal}}} = \mu = \frac{U_{\text{Signal}} + U_{\text{Ref}} + \frac{U'_{corr-1} + U_{\text{relais}}}{M_{\text{Signal}}}}{U_{\text{Base}} + U_{\text{Ref}}}. \tag{6.2}$$

Additionally to the correction term U_{relais} the connectors of the relay have been soldered, to ensure a lower contact resistance. A second correction factor U'_{corr-1} has to be included due to the resistance of the high voltage cable and the high voltage cage. The used cable and the high voltage cage had a resistance of $R_{\text{cage}} = (2.39724 \pm 0.00002)\,\Omega$ measured directly with the Fluke 8508A digital voltmeter in a resistance measurement mode. With the current of $I = (0.500 \pm 0.005)\,\text{mA}$, the voltage drop U'_{corr-1} is

$$U'_{corr-1} = R_{\text{cage}} \cdot I = (2.39724 \pm 0.00002)\,\Omega \cdot (0.500 \pm 0.005)\,\text{mA} = (1.199 \pm 0.012)\,\text{mV}, \tag{6.3}$$

for the ratio measurement. The uncertainty is calculated with Gaussian error propagation. At the scale factor measurement the current is slightly different, because of the higher voltage inside the cage. For the first measurements, where 10 V is used, the current inside the cage was $I = (0.505 \pm 0.005)\,\text{mA}$, which gave a correction term U_{corr-2}:

$$U_{corr-2} = R_{\text{cage}} \cdot I = (2.39724 \pm 0.00002)\,\Omega \cdot (0.505 \pm 0.005)\,\text{mA} = (1.211 \pm 0.012)\,\text{mV}. \tag{6.4}$$

The uncertainty is calculated with Gaussian error propagation. These problems could be solved within the analysis of the measurements. The correct analysis gave results, that were fitting better with the predicted results. The μ determination is shown in 6.3, the scale factor determination is shown in 6.4.

The corrected measurements give a scale factor of $M_{\text{Signal}} = 99.99946 \pm 0.00004$, which is 5.4 ppm lower than the expected value, but the standard deviation of the points is $\sigma \approx 15.6$ ppm, which is large and the majority of the points is around 100, that indicates, that the first measurements have proven the principle of the absolute calibration, but still the measurement setup can be improved, for example, the digital voltmeters measurement were not synchronized as explained in section 5.5

Simulations showed (see fig. 6.5), that an increase of the voltage inside the cage will lower the standard deviation of the scale factor. The standard deviation decreases to 1 ppm when a voltage of about -80 V is used. The increase of the inner voltage results in an increase of $U_{\text{Calibration}}$ and U_{Signal}. Therefore in the calculation of the scale factor

$$M_{\text{Signal}} = \frac{M_{\text{Base}} U_{\text{Base}} + U_{\text{Calibration}} + U_{corr-2}}{U_{\text{Signal}} + (1-\mu) U_{\text{Ref}}}, \tag{6.5}$$

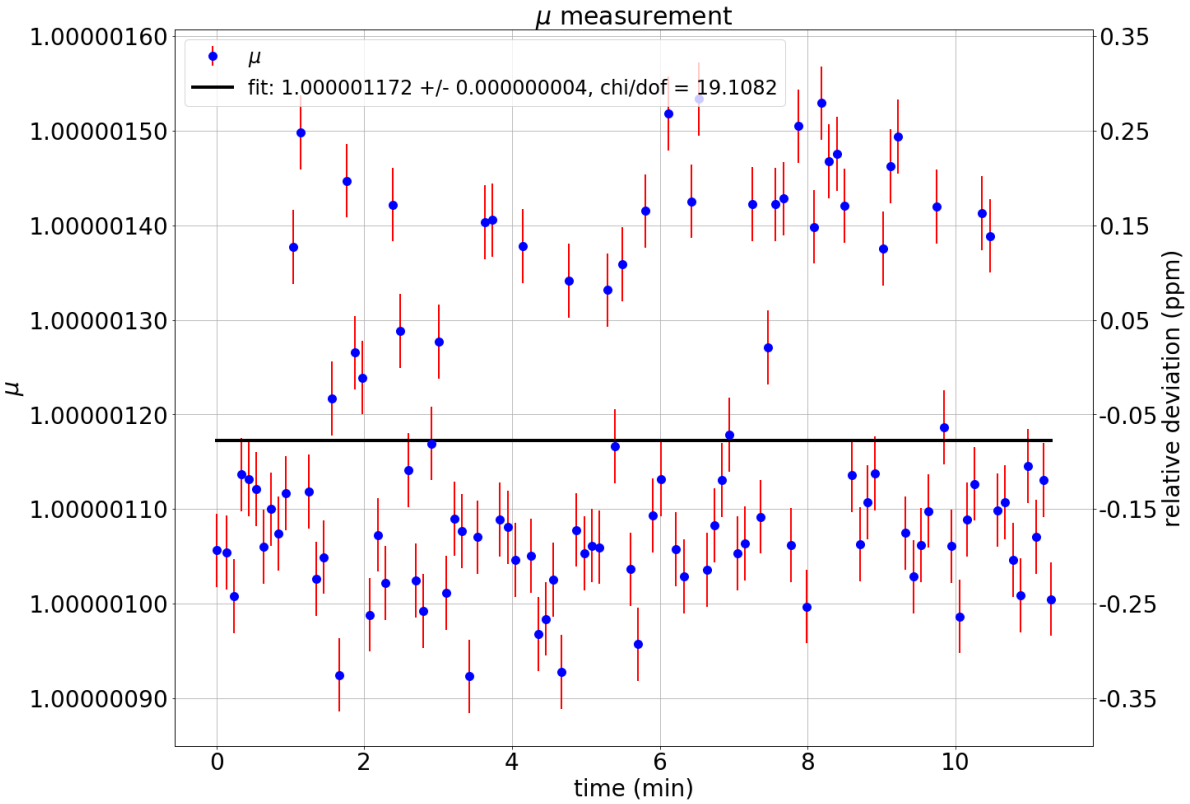

Figure 6.3.: This is the first μ measurement done with the downscaled setup of the absolute calibration, with the relay and the cable correction. Two identical dividers were taken, which were both uncalibrated. The measured ratio factor $\mu = 1.000001172 \pm 0.000000004$.

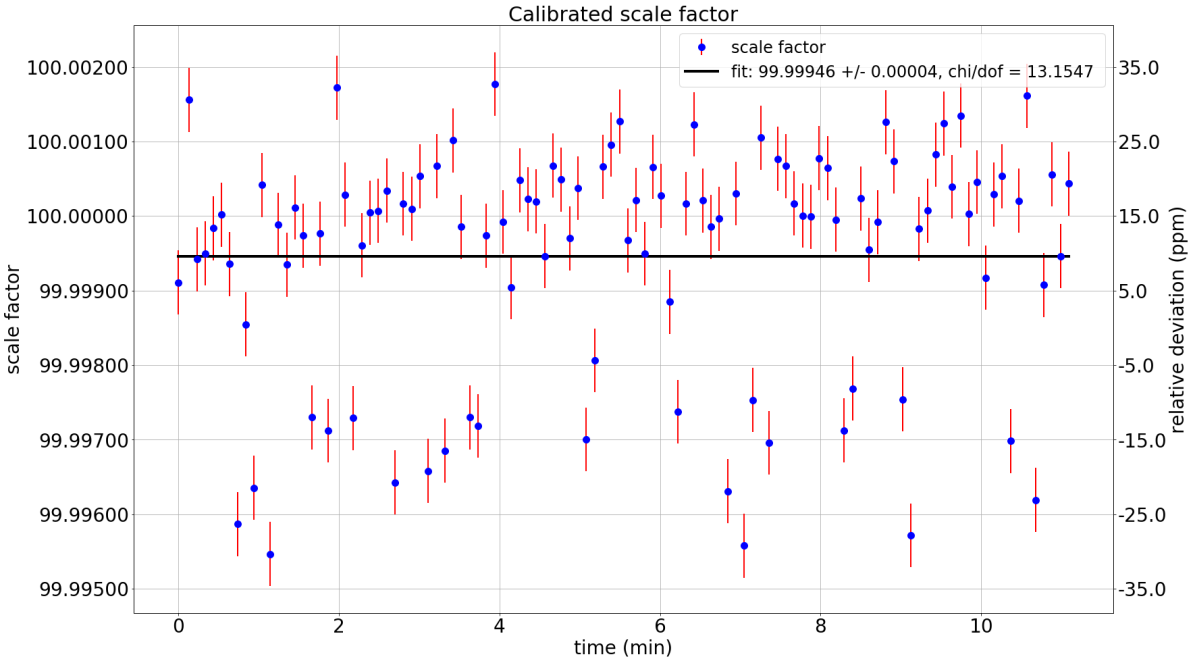

Figure 6.4.: This is the first scale factor M_{Signal} measurement done with the down-scaled setup of the absolute calibration, with the relay and the cable correction. The same 1 kV reference divider as in 6.3 were taken to calibrate reference divider B. The actual measured scale factor $M_{\text{Signal}} = 99.99946 \pm 0.00004$, which is 5.4 ppm below than 100.

the influence of both parts is larger. In a setup with -10 V, the numerator is given as

$$n = M_{\text{Base}} U_{\text{Base}} + U_{\text{Calibration}} + U_{corr-2} \approx 100 \cdot (-10^{-3})\,\text{V} - 10\,\text{V} - 10^{-3}\,\text{V} = -10.101\,\text{V}. \tag{6.6}$$

The influence of the U_{Base} is therefore about 1 % of the scale factor. The denominator is given as

$$d = U_{\text{Signal}} + (1-\mu) U_{\text{Ref}} = -0.1\,\text{V} + 2 \cdot 10^{-6} \cdot (-10)\,\text{V} = -0.10002\,\text{V}. \tag{6.7}$$

The influence of the ratio factor μ and the standard reference U_{Ref} is about 0.2 % of the scale factor. With an increase of the voltage up to -100 V, the numerator is

$$n = 100 \cdot (-10^{-3})\,\text{V} - 100\,\text{V} - 10^{-3}\,\text{V} = 100.101\,\text{V}. \tag{6.8}$$

The U_{Base} influence to the scale factor is therefore reduced by one order of magnitude. That improves the measurement results, because the U_{Base} measurement is only important for the stability of the measurement. The $U_{\text{Calibration}}$ measurement is the important measurement for the scale factor. In the denominator analogous the influence of the ratio factor μ and the standard reference U_{Ref} is reduced by one order of magnitude

$$d = -1\,\text{V} + 2 \cdot 10^{-6} \cdot (-10)\,\text{V} = -1.00002\,\text{V}. \tag{6.9}$$

Simulations showed, much higher voltages than -80 V would not result in a better standard deviation, because the accuracy of the digital voltmeter is limited. Therefore the voltage inside the cage was increased to -90 V. Additionally the maximum input voltage of the Fluke 752A reference divider is 1.1 kV.
Another problem occurred, as a strong drift of the FuG MCP 14-1250 was measured with the single digital voltmeters. With the ratio calculation, the drift should dissolve, but it was still visible within the μ determination. That lead to the assumption, that the integration time of the digital voltmeters were not synchronized. The voltmeters were synchronized, that every voltmeter measures over the same time, which lead to very small scattering of the data points (see section 5.5). Another difference between the first and the final measurements is the calibration of all three voltmeters. In the first measurements, a 10 V reference potential was connected with positive polarity to the three voltmeters. The calibrating voltage from both FuG MCP 14-1250 had a negative polarity. Therefore all three voltmeters were calibrated with the negative polarity for the final measurements. Lastly, the number of measuring cables was reduced to minimize ground loops.

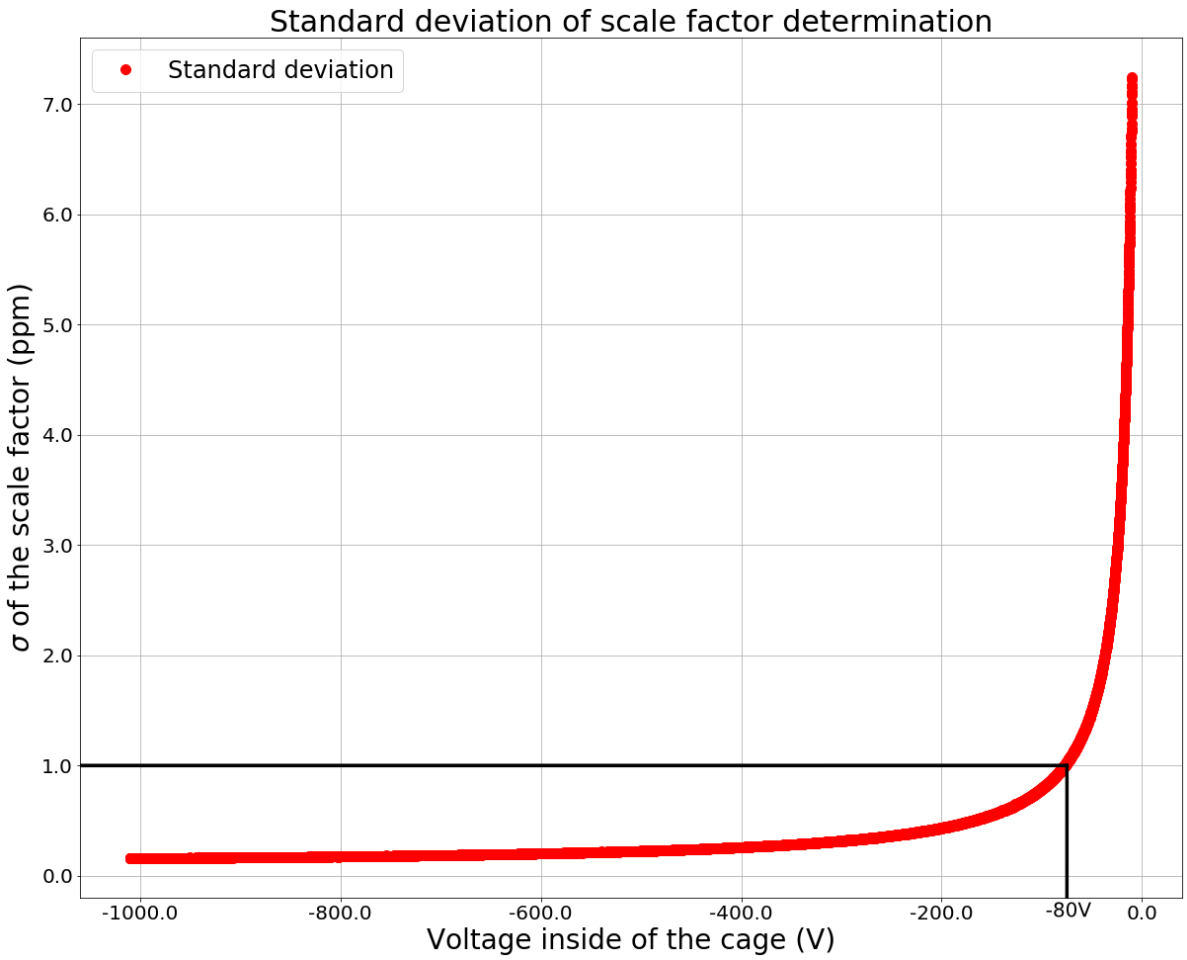

Figure 6.5.: For the simulation, each input parameter of the absolute calibration system is modulated with a Gaussian. For every measurement 3000 data points are simulated for the μ determination and for the scale factor determination, at the end for each measurement the mean scale factor and the mean standard deviation was calculated. Each voltage step has a standard deviation calculated from 10 measurements. The voltage changes with 0.1 V steps from -10 V up to -1010 V. The standard deviation decreases in this range from over 7 ppm down to below 1 ppm.

6.2. Uncertainty determination of the μ and scale factor

In this section, the uncertainties for the ratio and scale factor determination are discussed. Because every measurement needs a single uncertainty calculation, only an example with simplified values is calculated in this section. In the measurements the uncertainty of every measurement is determined and shown.

The ratio μ and scale factor M_{Signal} determinations described in sections 4.3.1 and 4.3.2 have an uncertainty due to statistical and systematical uncertainties of the digital voltmeters measured in section 5.6. At first the statistical uncertainty $\Delta\mu_{\text{stat}}$ is

calculated with a Gaussian error propagation

$$\begin{aligned}
\mu &= \frac{U_{\text{Signal}}+U_{\text{Ref}}+\frac{U_{corr-1}}{M_{\text{Signal}}}}{U_{\text{Base}}+U_{\text{Ref}}} \\
\Delta\mu_{\text{stat}} &= \Bigg[\left(\frac{\Delta U_{\text{Signal}}}{U_{\text{Base}}+U_{\text{Ref}}}\right)^2 + \left(\frac{\Delta U_{\text{Ref}}\cdot\left(U_{\text{Base}}-U_{\text{Signal}}-\frac{U_{corr-1}}{M_{\text{Signal}}}\right)}{(U_{\text{Base}}+U_{\text{Ref}})^2}\right)^2 + \left(\frac{\Delta M_{\text{Signal}}U_{corr-1}}{M_{\text{Signal}}^2(U_{\text{Base}}+U_{\text{Ref}})}\right)^2 \\
&\quad + \left(\frac{\Delta U_{corr-1}}{M_{\text{Signal}}\cdot(U_{\text{Base}}+U_{\text{Ref}})}\right)^2 + \left(\Delta U_{\text{Base}}\cdot\frac{U_{\text{Signal}}+U_{\text{Ref}}+\frac{U_{corr-1}}{M_{\text{Signal}}}}{(U_{\text{Base}}+U_{\text{Ref}})^2}\right)^2\Bigg]^{\frac{1}{2}}.
\end{aligned} \tag{6.10}$$

For the μ measurement, the statistical uncertainties can be calculated by taking an example data set:

$$\begin{aligned}
U_{\text{Signal}} &= -9.09670 \pm 0.00009 \ \text{mV} \\
U_{\text{Ref}} &= -10.00024 \pm 0.00006 \ \text{V} \\
U_{\text{cable}} &= -1.20 \pm 0.01 \ \text{mV} \\
U_{\text{Calibration}} &= 0.100 \pm 0.004 \ \text{mV} \\
M_{\text{Signal}} &= 100.00 \pm 0.01 \\
U_{\text{Base}} &= -9.0890 \pm 0.0004 \ \text{mV}.
\end{aligned} \tag{6.11}$$

The $U_{\text{Calibration}}$ and U_{cable} values are connected into the U_{corr-1} factor

$$\begin{aligned}
U_{corr-1} &= U_{\text{cable}} - U_{\text{Calibration}} = -(1.20 \pm 0.01)\,\text{mV} - (0.100 \pm 0.004)\,\text{mV} \\
U_{corr-1} &= -(1.30 \pm 0.01)\,\text{mV}.
\end{aligned} \tag{6.12}$$

The statistical uncertainties for the voltages $U_{\text{Calibration}}$, U_{Base} and U_{Signal} are calculated with the uncertainties determined in section 5.6. The uncertainty of the U_{Ref} comes from the data sheet of the 10 V reference sources [Flu83]. With these values the statistical error $\Delta\mu_{\text{stat}}$ can be calculated

$$\begin{aligned}
\Delta\mu_{\text{stat}} &= \sqrt{8.0\cdot10^{-17} + 1.5\cdot10^{-22} + 1.7\cdot10^{-20} + 1.6\cdot10^{-16} + 1.3\cdot10^{-15}} \\
\Delta\mu_{\text{stat}} &\approx 3.9\cdot10^{-8}.
\end{aligned} \tag{6.13}$$

Analogous to the statistical uncertainties a systematic uncertainty can be calculated, because the digital voltmeters are calibrated before the whole measurements. Therefore uncertainties given by the manufacturer in table 5.7 in section 5.6 are taken. The systematical uncertainties for the digital voltmeters are

$$\begin{aligned}
U_{\text{Signal}} &= -9.09670 \pm 0.00005 \ \text{mV} \\
U_{\text{Calibration}} &= 0.10 \pm 0.03 \ \text{mV} \\
U_{\text{Base}} &= -9.089 \pm 0.004 \ \text{mV}.
\end{aligned} \tag{6.14}$$

That also gives a new uncertainty for the correction term, which is calculated with Gaussian error propagation

$$U_{corr-1} = U_{\text{cable}} - U_{\text{Calibration}} = -(1.30 \pm 0.03)\,\text{mV}. \tag{6.15}$$

The systematic uncertainty $\Delta\mu_{\text{sys}}$ is then calculated

$$\begin{aligned} \Delta\mu_{\text{sys}} &= \sqrt{2.5\cdot10^{-15}+1.5\cdot10^{-22}+1.7\cdot10^{-20}+1.0\cdot10^{-15}+1.6\cdot10^{-13}} \\ \Delta\mu_{\text{sys}} &\approx 4.0\cdot10^{-7}. \end{aligned} \tag{6.16}$$

The whole μ value is therefore given as

$$\mu \pm \Delta\mu_{\text{stat}} \pm \Delta\mu_{\text{sys}} = 1.000002066 \pm 0.000000004 \pm 0.0000004. \tag{6.17}$$

For the scale factor calculation, the mean value of μ is calculated. The statistic uncertainty of the mean value $\Delta\mu_{\text{stat}}$ is given with the standard deviation σ_μ divided by the square root of the measurement point n_μ

$$\Delta\mu_{\text{stat}} = \frac{\sigma_\mu}{\sqrt{n_\mu}}. \tag{6.18}$$

For the scale factor, a data set of $n_\mu = 55$ with a standard deviation of $\sigma_\mu = 2.7\cdot10^{-8}$ was taken. The calculated ratio is $\mu = 1.000002066 \pm 0.000000004$, the other used values are

$$\begin{array}{rcrcll} U_{\text{Signal}} &=& -0.9093414 &\pm& 0.0000001 & \text{V} \\ U_{\text{Base}} &=& -0.0091630 &\pm& 0.0000004 & \text{V} \\ U_{\text{Calibration}} &=& -90.016856 &\pm& 0.000006 & \text{V} \\ U_{corr-2} &=& -0.00131 &\pm& 0.00001 & \text{V} \\ U_{\text{Ref}} &=& -10.00024 &\pm& 0.00006 & \text{V} \\ M_{\text{Base}} &=& 100 &\pm& 0.001. & \end{array} \tag{6.19}$$

The statistical uncertainty of a single scale factor $\Delta M_{\text{Signal,stat}}$ is calculated with a Gaussian error propagation

$$\begin{aligned} M_{\text{Signal}} &= \frac{M_{\text{Base}}U_{\text{Base}}+U_{\text{Calibration}}-U_{corr-2}}{U_{\text{Signal}}+(1-\mu)U_{\text{Ref}}} \\ \Delta M_{\text{Signal,stat}} &= \Bigg[\left(\frac{\Delta M_{\text{Base}}U_{\text{Base}}}{U_{\text{Signal}}+(1-\mu)U_{\text{Ref}}}\right)^2+\left(\frac{M_{\text{Base}}\Delta U_{\text{Base}}}{U_{\text{Signal}}+(1-\mu)U_{\text{Ref}}}\right)^2+\left(\frac{\Delta U_{\text{Calibration}}}{U_{\text{Signal}}+(1-\mu)U_{\text{Ref}}}\right)^2 \\ &\quad+\left(\frac{\Delta U_{corr-2}}{U_{\text{Signal}}+(1-\mu)U_{\text{Ref}}}\right)^2+\left(-\frac{M_{\text{Base}}U_{\text{Base}}+U_{\text{Calibration}}-U_{corr-2}}{\left(U_{\text{Signal}}+(1-\mu)U_{\text{Ref}}\right)^2}\cdot\Delta U_{\text{Signal}}\right)^2 \\ &\quad+\left(\frac{U_{\text{Ref}}(M_{\text{Base}}U_{\text{Base}}+U_{\text{Calibration}}-U_{corr-2})}{\left(U_{\text{Signal}}+(1-\mu)U_{\text{Ref}}\right)^2}\cdot\Delta\mu\right)^2 \\ &\quad+\left(\frac{(\mu-1)(M_{\text{Base}}U_{\text{Base}}+U_{\text{Calibration}}-U_{corr-2})}{\left(U_{\text{Signal}}+(1-\mu)U_{\text{Ref}}\right)^2}\cdot\Delta U_{\text{Ref}}\right)^2\Bigg]^{\frac{1}{2}} \\ \Delta M_{\text{Signal,stat}} &= \big[1.0\cdot^{-10}+1.6\cdot10^{-9}+3.7\cdot10^{-11}+2.0\cdot10^{-10} \\ &\quad+2.0\cdot10^{-10}+1.9\cdot10^{-11}+5.2\cdot10^{-20}\big]^{\frac{1}{2}} \\ \Delta M_{\text{Signal,stat}} &= 0.00005. \end{aligned} \tag{6.20}$$

The statistical uncertainty of the M_{Signal} is therefore 0.5 ppm. The systematic uncertainty $M_{\text{signal,sys}}$ can be calculated again with the uncertainties from table 5.7 in section 5.6

$$\begin{array}{rcrcrl} U_{\text{Signal}} & = & -0.9093414 & \pm & 0.0000009 & \text{V} \\ U_{\text{Base}} & = & -0.009163 & \pm & 0.000004 & \text{V} \\ U_{\text{Calibration}} & = & -90.0169 & \pm & 0.0003 & \text{V} \end{array} \tag{6.21}$$

$$\begin{aligned} \Delta M_{\text{Signal,sys}} &= \left[1.0 \cdot^{-10} + 1.9 \cdot 10^{-7} + 7.9 \cdot 10^{-8} + 2.0 \cdot 10^{-10}\right. \\ &\quad \left. + 1.1 \cdot 10^{-8} + 1.9 \cdot 10^{-11} + 5.2 \cdot 10^{-20}\right]^{\frac{1}{2}} \\ \Delta M_{\text{Signal,sys}} &= 0.00053. \end{aligned} \tag{6.22}$$

The systematic uncertainty for the scale factor is $M_{\text{signal,sys}} = 5.3$ ppm. The whole M_{Signal} for a single measurement is therefore given as

$$\Delta M_{\text{Signal,stat}} = \frac{\sigma_M}{\sqrt{n_M}}. \tag{6.23}$$

$$M_{\text{Signal}} \pm M_{\text{Signal,stat}} \pm M_{\text{Signal,syst}} = 99.99974 \pm 0.00005 \pm 0.00053. \tag{6.24}$$

For a data set of measurements, the statistical uncertainty is reduced

6.3. μ determination measurements

The setup for the μ determination measurement is shown in figure 6.6. The output of the outer FuG MCP 14-1250 was set to -1 kV and the relay was closed. All three voltage dividers were tested with four different calibration measurements. At first the voltage divider B was calibrated with the help of the voltage divider A. For the second measurement, divider A and divider B were swapped, so that divider A was calibrated with the help of divider B. For the third measurement, voltage divider D was self calibrated as described in section 5.1.2 and afterwards calibrated with the help of divider A. For the last measurement, divider A and D were again swapped to calibrate divider D with the help of voltage divider A. For all four measurements the μ factor and the scale factor were determined.

6.3.1. μ determination of divider A and divider B

Voltage divider B is used as the signal voltage divider and voltage divider A is used as the baseline voltage divider. The results of the first measurements are shown in figure 6.7. The indices of the μ_{AB} indicate, that the ratio is given as

$$\mu_{AB} = \frac{M_A}{M_B}. \tag{6.25}$$

The μ factor of the measurement was determined as $\mu_{\text{AB}} = 1.000002065 \pm 0.000000005 \pm 0.0000004$. The μ and the statistical uncertainty is calculated with the least square fit of the data points, done with python. The systematical error is calculated with Gaussian error propagation as shown in sec. 6.2. This is done for the following plots, if it is

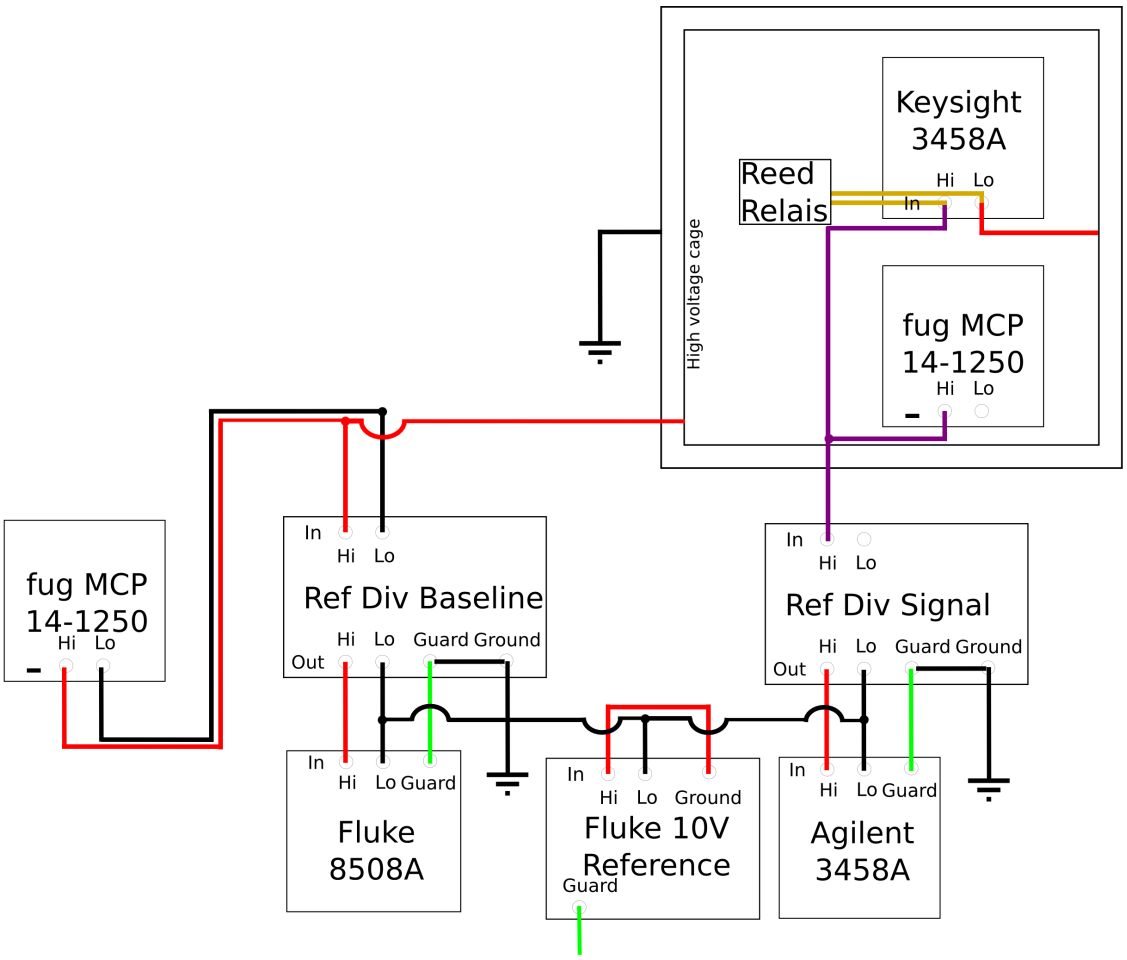

Figure 6.6.: Final measurement setup for the absolute calibration measurement. The external FuG MCP at the left produces the high voltage of about 1 kV. The voltage is guided to the first reference divider baseline and to the high voltage cage. The divided voltage after the baseline voltage divider is measured by a Fluke 8508A high precision voltmeter, against a Fluke 732A 10 V reference source. Inside the cage, the second FuG MCP is installed. In the μ measurement the MCP is short-circuited by the reed relay and the voltage is directly guided outside of the cage. In the scale factor determination, the relay is opened and the inner MCP produces an additional voltage on top of the high voltage, which is measured by the Keysight 3458A inside the cage. The voltage is guided outside of the cage directly to the signal reference divider. After the divider the voltage is measured with an Agilent 3458A high precision digital voltmeter against the same Fluke 732A 10 V reference source as the Fluke 8508A.

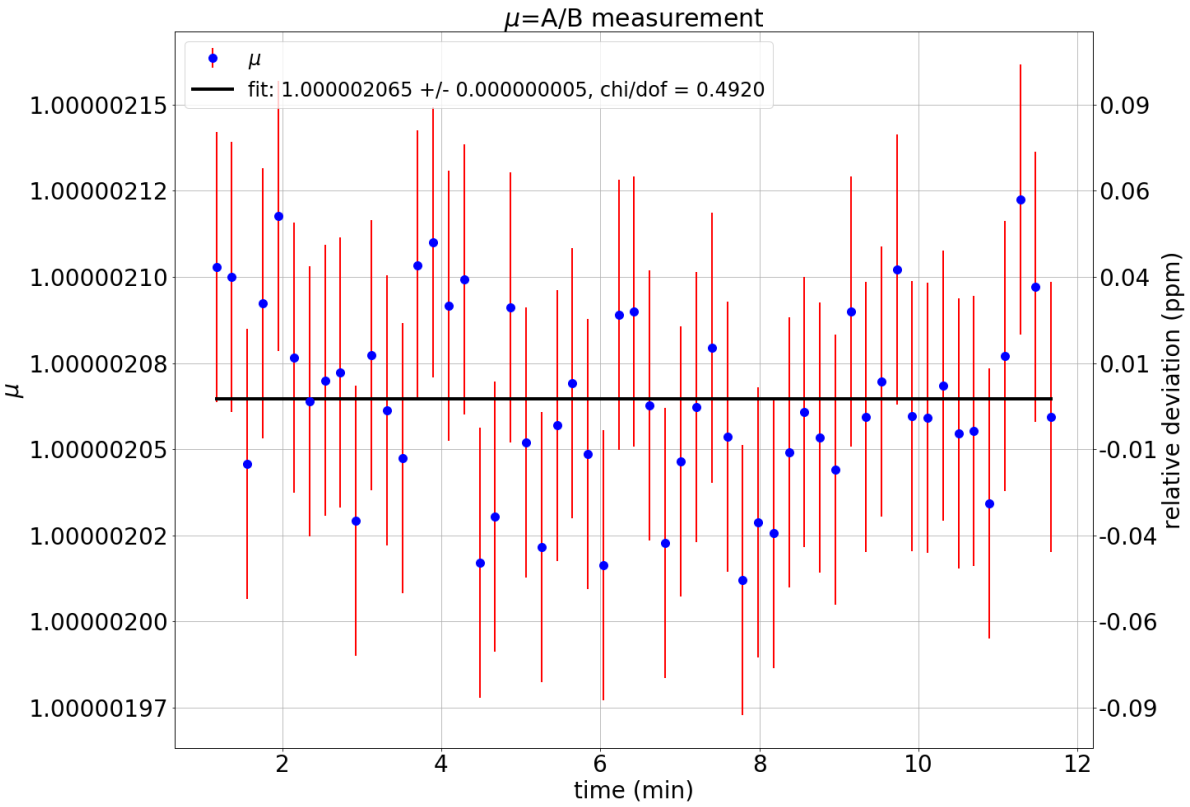

Figure 6.7.: Results of the μ determination of the absolute calibration measurement of the voltage divider B with the help of the voltage divider A. The outer FuG MCP 14-1250 was set to a voltage output of 1000.1 V with 1.0 mA current and the relay inside the high voltage cage was closed. The μ factor was determined to $\mu_{\mathrm{AB}} = 1.000002065 \pm 0.000000005 \pm 0.0000004$. In the plot only the statistical uncertainties are shown.

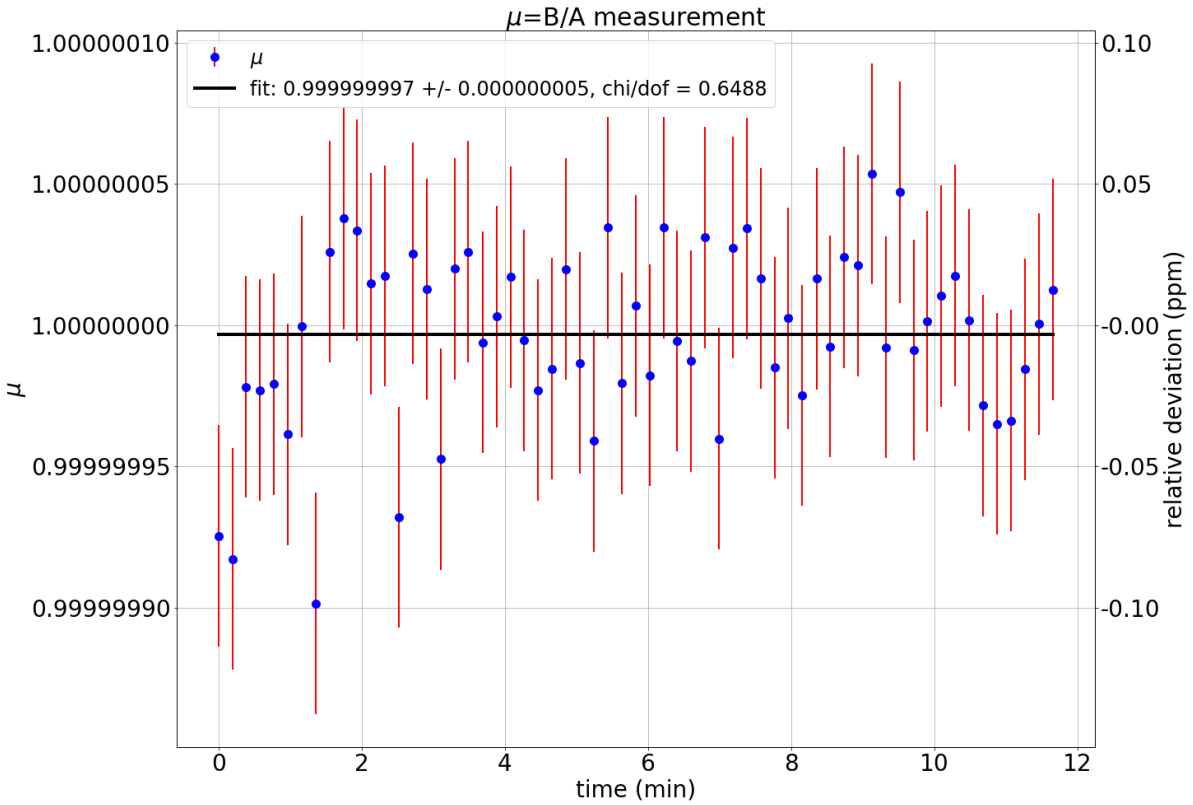

Figure 6.8.: Results of the μ determination of the absolute calibration measurement of the voltage divider A with the help of the voltage divider B. The outer FuG MCP 14-1250 was set to a voltage output of 1000.1 V with 1.0 mA current and the relay inside the high voltage cage was closed. The μ factor was determined to $\mu_{\mathrm{BA}} = 0.9999999997 \pm 0.000000005 \pm 0.0000004$. In the plot only the statistical uncertainties are shown.

not differently mentioned. The μ factor indicates, that the scale factor of the baseline divider M_{Base} should be higher than the scale factor of the signal divider M_{Signal}. The calculated μ factor is the mean value of all measured μ values. After the measurement, divider A and divider B were swapped and the μ factor was measured again (see fig. 6.8).

The μ factor of the second measurement was determined as $\mu_{\mathrm{BA}} = 0.9999999997 \pm 0.000000005 \pm 0.0000004$. That indicates both voltage dividers have the same scale factor within 0.03 ppm. That result does not fit with the first results, the μ factor should be inverse for both measurements.

Another simplified possibility to determine the μ factor is a direct measurement of the output of both reference divider. The alternative measurement setup is shown in figure 6.9. The measurements differs from the first ratio determination by loss of the high voltage cage and the used cables.

The Fluke Calibrator is connected to two reference dividers and a high precision digital voltmeter, in this case the Fluke 8508A. The digital voltmeter measures directly

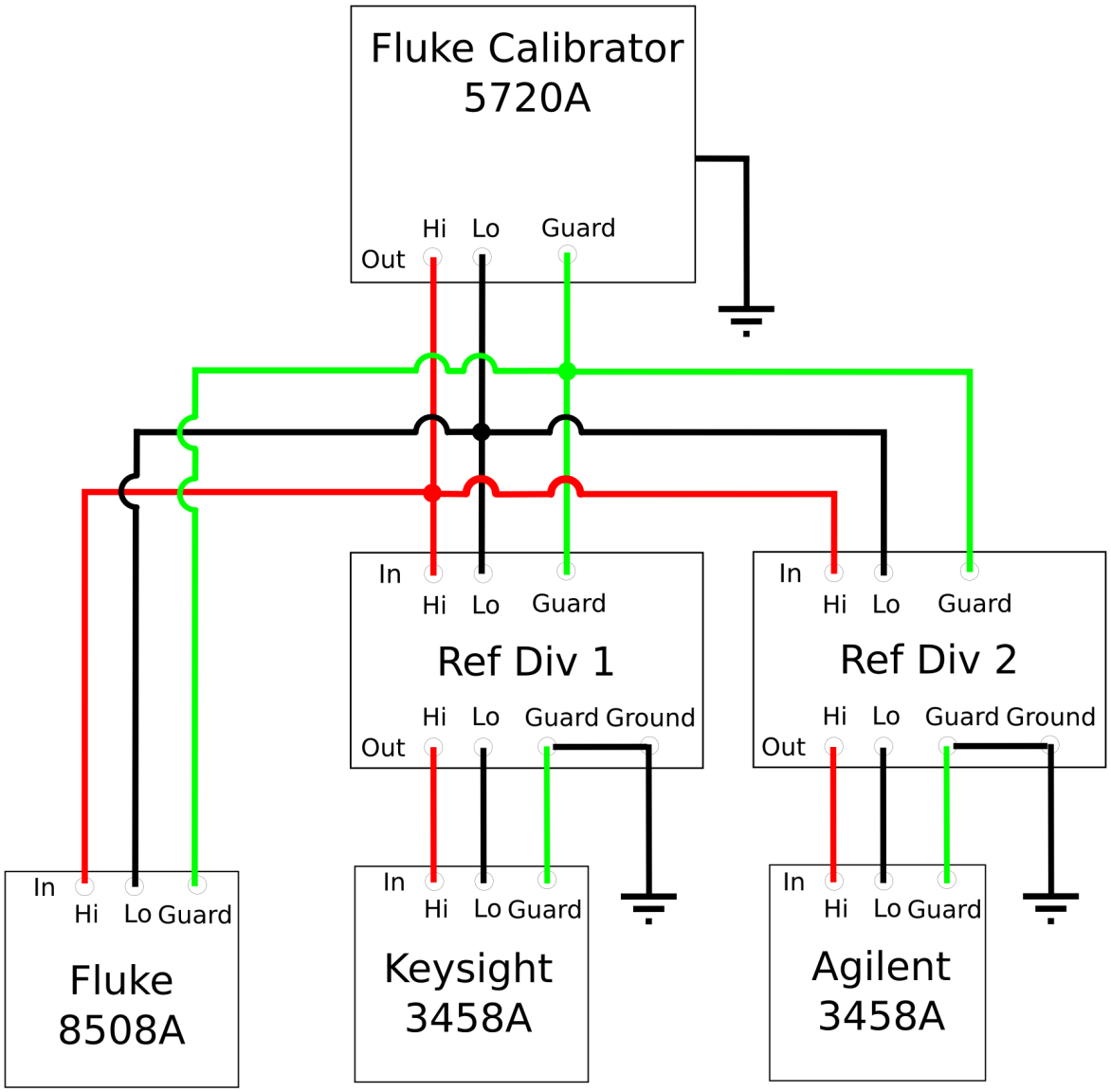

Figure 6.9.: The Fluke Calibrator provides the high voltage for this measurement. The Fluke 8508A measures directly the high voltage up to 1 kV. The Agilent and Keysight 3458a measure the downscaled voltage behind the reference voltage divider. The scale factor can be determined by the ratio of the input voltage (Fluke 8508A) and the output voltage (Agilent/Keysight 3458a). Additionally the ratio factor μ can be determined, by dividing the output voltages of the Agilent 3458a and the Keysight 3458a.

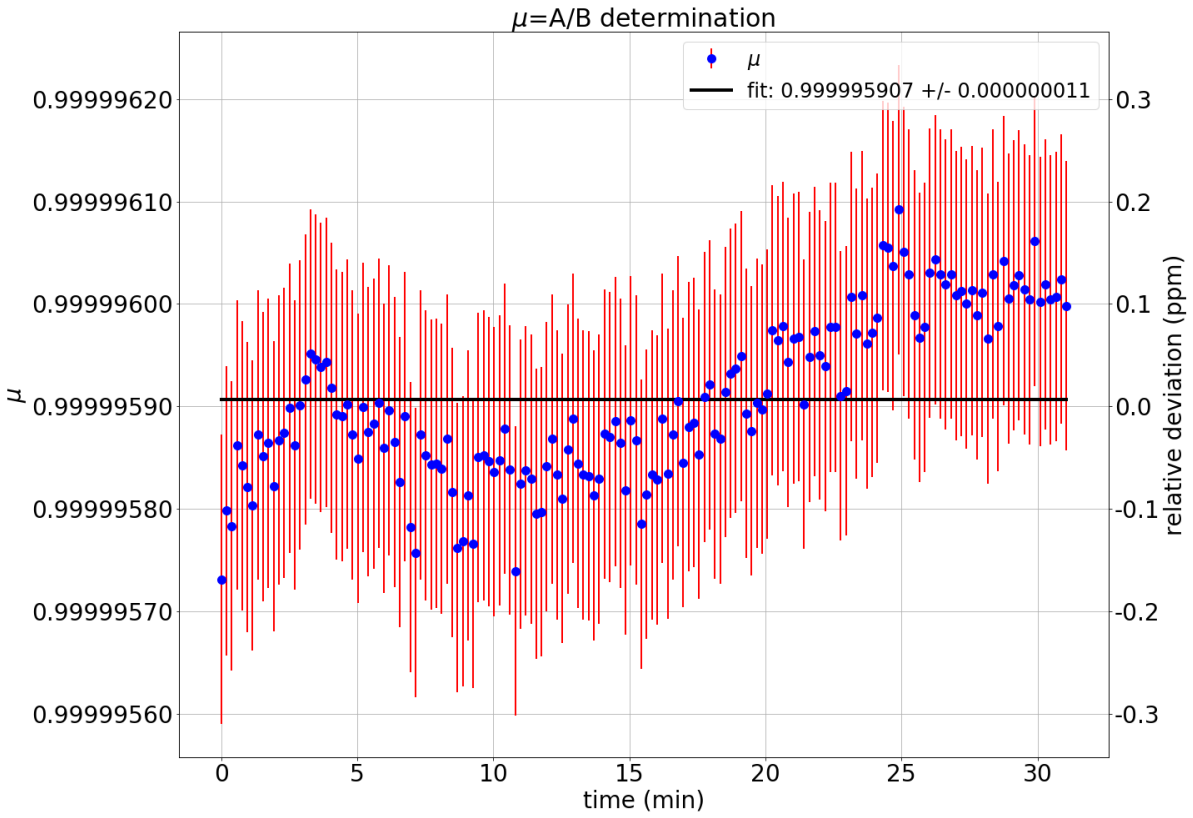

Figure 6.10.: Ratio factor μ from an independent comparison measurement of the reference divider A and B. For this measurement the Fluke Calibrator was connected to the Fluke 8508A, as a reference measurement, and with the reference divider A and reference divider B. Both dividers were read out with the Agilent 3458A and the Keysight 3458A. In this case $\mu_{BA} = \frac{M_B}{M_A}$, which is comparable with the figure 6.8. The calculated ratio factor is $\mu_{BA} = 0.99999591 \pm 0.00000001 \pm 0.0000008$. In the plot only the statistical uncertainties are shown.

the 1 kV input voltage of the Fluke 5720A calibrator. This is not suitable for high precision measurements, because the digital voltmeter has an internal voltage divider to measure this voltage. This voltage divider is not well known with its scale factor and its uncertainty. It is only used as a reference voltage measurement. After the voltage divider the voltage is measured with the Agilent and Keysight 3458A. From this measurement, the ratio μ_{AB} for both dividers can be determined. The ratio is given by the output voltages of the voltage dividers U_A and U_B

$$\mu_{BA} = \frac{U_A}{U_B}. \tag{6.26}$$

The results of this measurement are shown in figure 6.10.

The μ determination gives $\mu_{BA} = 0.99999591 \pm 0.00000001 \pm 0.0000008$. The sys-

tematic uncertainty can be calculated with the uncertainties in table 5.7:

$$\frac{\Delta\mu_{AB}}{\mu_{AB}} = \sqrt{\left(\frac{\Delta U_A}{U_A}\right)^2 + \left(\frac{\Delta U_B}{U_B}\right)^2}. \tag{6.27}$$

The voltages were measured with the Agilent 3458a and Keysight 3458a in the 10 V range, therefore the relative uncertainty in this range is $\frac{\Delta U_A}{U_A} = 0.55\,\text{ppm}$. The whole uncertainty is given by

$$\frac{\Delta\mu_{AB}}{\mu_{AB}} = 0.8\,\text{ppm}. \tag{6.28}$$

6.3.2. μ determination of divider A and divider D

After the first μ measurements the third divider was also tested. To make a crosscheck of the method, the divider D was self calibrated. That should lead to a scale factor of 100.00000 ± 0.00005 according to the manufacturer. After the self calibration the absolute calibration method was done. The first part was the calibration of the divider D with the help of divider A. The results are shown in figure B.4 in the Appendix.

In this measurement, the μ factor was calculated as $\mu_{AD} = 1.000000750 \pm 0.000000004 \pm 0.0000004$. Again, both dividers were changed, to crosscheck the μ value. Figure B.5 in the Appendix shows the results of this measurement.

This measurement gives a factor $\mu_{AD} = 1.000000271 \pm 0.000000004 \pm 0.0000004$. That result does not fit with the first results, the μ factor should be inverse for both measurements.
The second measurement to determine the μ value was also done with the reference divider D and A. In this case the result of the measurement is shown in figure B.6.

Additionally the simplified ratio measurement give $\mu_{DA} = 0.9999808 \pm 0.00000001 \pm 0.0000008$. The measurement data was also taken at the 26th of June.

Both measurements lead to different results for the μ factor, which will be discussed in the conclusion (see chapter 7)

6.4. Scale factor determination measurements

After every μ determination measurement a scale factor determination of the voltage divider was done. For these measurements the relay inside the high voltage cage was opened and a voltage of $-90\,\text{V}$ was set with the inner FuG MCP. This voltage was measured with the Keysight 3458A digital voltmeter inside the cage. The whole setup for the measurement is shown in figure 6.6.

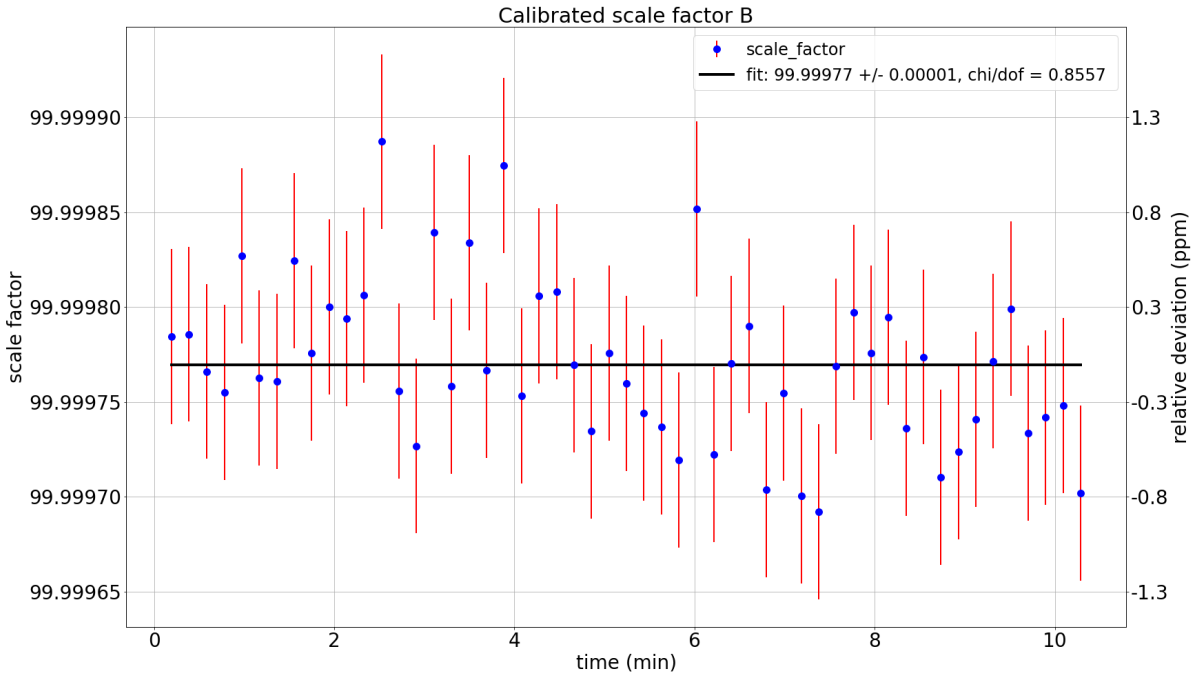

Figure 6.11.: Scale factor of the voltage divider B with the absolute calibration method and the help of the voltage divider A. The scale factor was determined as $M_{\text{Signal}} = 99.99977 \pm 0.00001 \pm 0.0005$. In the plot only the statistical uncertainties are shown.

6.4.1. Absolute calibration measurements with the voltage divider A and divider B

At first the absolute calibration measurement of the voltage divider B with the help of the divider A was done. Therefore the voltage of the inner FuG MCP was set to $-90\,\text{V}$ with a corresponding current of $0.545\,\text{mA}$. The scale factor was calculated with the help of the measured ratio factor μ in 6.3.1 and the plot is shown in figure 6.11.

The scale factor was determined to $M_{\text{Signal}} = 99.99977 \pm 0.00001 \pm 0.0005$. The scale factor is 2.3 ppm below 100. The scattering of the measurement is below 1.5 ppm, which is significantly lower than the scattering with the first used method (see fig. 6.4 30-40 ppm). The voltage divider B was not self calibrated before the measurements.

After the swap of the voltage dividers divider A was calibrated with the absolute calibration method. Therefore the same procedure was done with the relay and the FuG MCP. The results of this measurement are shown in figure B.7 in the Appendix.

The scale factor of the voltage divider A was determined to $M_{\text{Signal}} = 99.99981 \pm 0.00001 \pm 0.0005$. The scale factor is 1.9 ppm lower than 100 with a scattering below 1 ppm. The voltage divider A was also not self calibrated before the absolute calibra-

tion measurement. Both measured scale factors lead to a ratio factor

$$\mu_{AB} = \frac{M_A}{M_B} = \frac{99.99981 \pm 0.00001 \pm 0.0005}{99.99977 \pm 0.00001 \pm 0.0005} = 1.0000003 \pm 0.0000001 \pm 0.000007. \tag{6.29}$$

The measured ratio factor for both dividers was $\mu_{AB} = 1.000002065 \pm 0.000000005 \pm 0.0000004$. The calculated ratio factor from the scale factor determination is $\mu_{AB} = 1.0000003 \pm 0.0000001 \pm 0.000007$. The ratio factor determined within the ratio determination is 2.1 ppm grater than 1 and the ratio factor from the scale factor determinations is 0.3 ppm greater than one.

6.4.2. Absolute calibration measurement with the voltage divider A and divider D

The second measurements were done with the voltage divider A and D. Right before the absolute calibration, divider D was self calibrated, to make sure it has a scale factor of $M_D = 100.00000 \pm 0.00005$ according to the manufacturer. The results of the calibration measurement are shown in figure B.8 in the Appendix.

The scale factor of this measurement was determined as $M_{Signal} = 99.99981 \pm 0.00001 \pm 0.0005$. The scale factor is 1.9 ppm below 100. The divider D was self calibrated before the measurement, therefore a scale factor of 100.00000 ± 0.00005 was expected.

The second control measurement for the setup was done by swapping the voltage divider D and A, and measuring the scale factor of divider A. The results are shown in fig. B.9.

The measured scale factor is $M_{Signal} = 99.99978 \pm 0.00001 \pm 0.0005$. The scale factor is 2.2 ppm lower than 100 and the scattering is about 1 ppm. A new ratio factor can be calculated with the help of these scale factors, which is

$$\mu_{AD} = \frac{M_A}{M_D} = \frac{99.99978 \pm 0.00001 \pm 0.0005}{99.99981 \pm 0.00001 \pm 0.0005} = 0.9999997 \pm 0.0000001 \pm 0.000007. \tag{6.30}$$

The measured ratio factor for both dividers was $\mu_{AD} = 1.000000271 \pm 0.000000004 \pm 0.0000004$. The calculated ratio factor from the scale factor determination is $\mu_{AD}0.9999997 \pm 0.0000001 \pm 0.000007$.

6.5. Longterm calibration measurements

During the μ determination different ratio factors were measured. Also through other measurements a change of the ratio factor before and after a measurement was discovered. Therefore a longterm measurement was performed to investigate the behavior of the ratio factor. For the long term measurement the reference divider D was calibrated with the help of the divider A. Before the measurements the digital

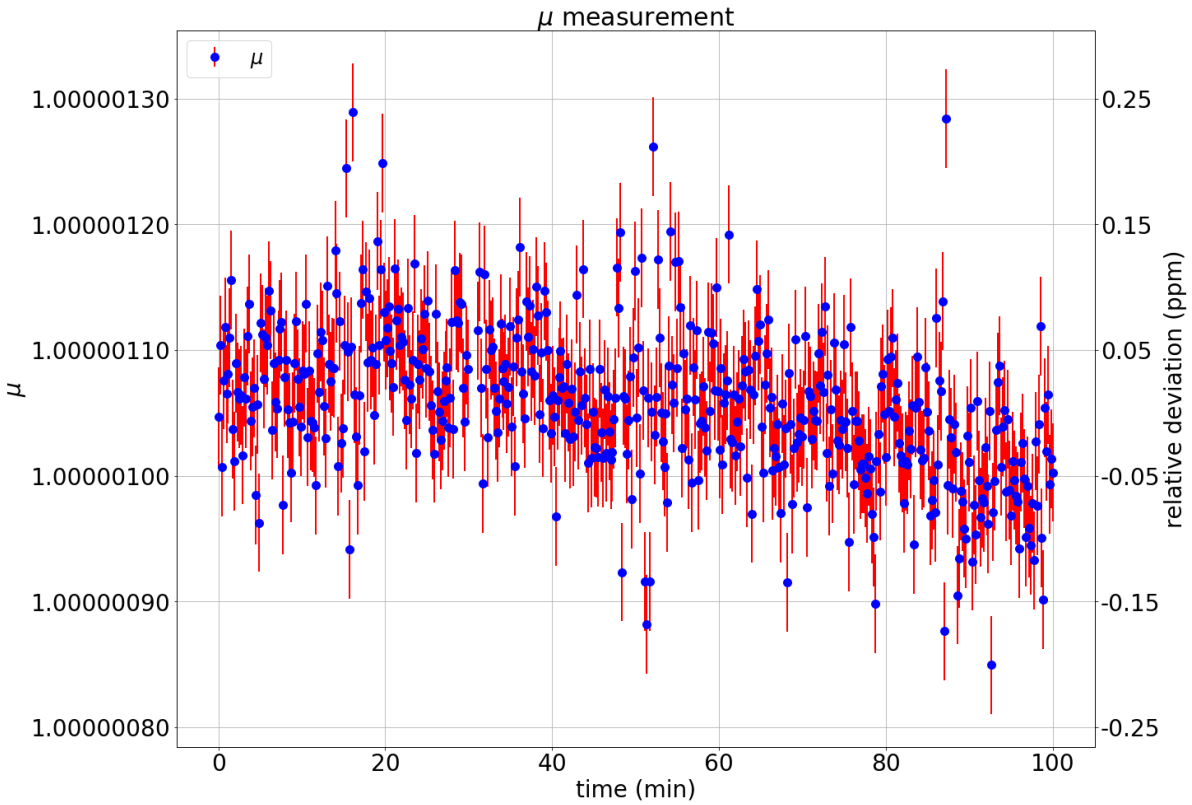

Figure 6.12.: This is the first longterm μ determination measurement with divider A and D. The ratio has a constant value of about $\mu = 1.0000011$ for the first 60 minutes. After 60 minutes the ratio factor starts to slowly decrease to a ratio of about $\mu = 1.0000010$ within 40 minutes. In the plot only the statistical uncertainties are shown.

voltmeter were calibrated with an offset and a gain measurement. The first μ determination was performed for about 100 min at a voltage of 1 kV and a current of 1 mA with the FuG MCP 14-1250. The results of the μ determination are shown in figure 6.12.

The μ factor starts with a constant value of 1.0000011 for the first 60 minutes. After 60 minutes the ratio factor slowly decreases of up to 1.0000010 within 40 minutes, which is a difference of 0.1 ppm. The statistical uncertainties for the μ determination vanish, due to the high statistics. The systematic uncertainty is calculated as $\Delta\mu_{\text{stat}} = 4 \cdot 10^{-7}$ with Gaussian error propagation. The drift of the μ value leads to the assumption, that there are systematic problems with the measurement.

After the ratio determination a scale factor determination was done for about 5.5 hours. The results are shown in figure 6.13.

The scale factor also drifts, as the μ factor. At this measurement the drift starts immediately and slows down after three to four hours. The scale factor starts with $M_{\text{Signal}} = 99.99990$ and increases up to $M_{\text{Signal}} = 100.00025$, which is a difference of 3.5 ppm. The systematical uncertainty for the scale factor is calculated with a Gaus-

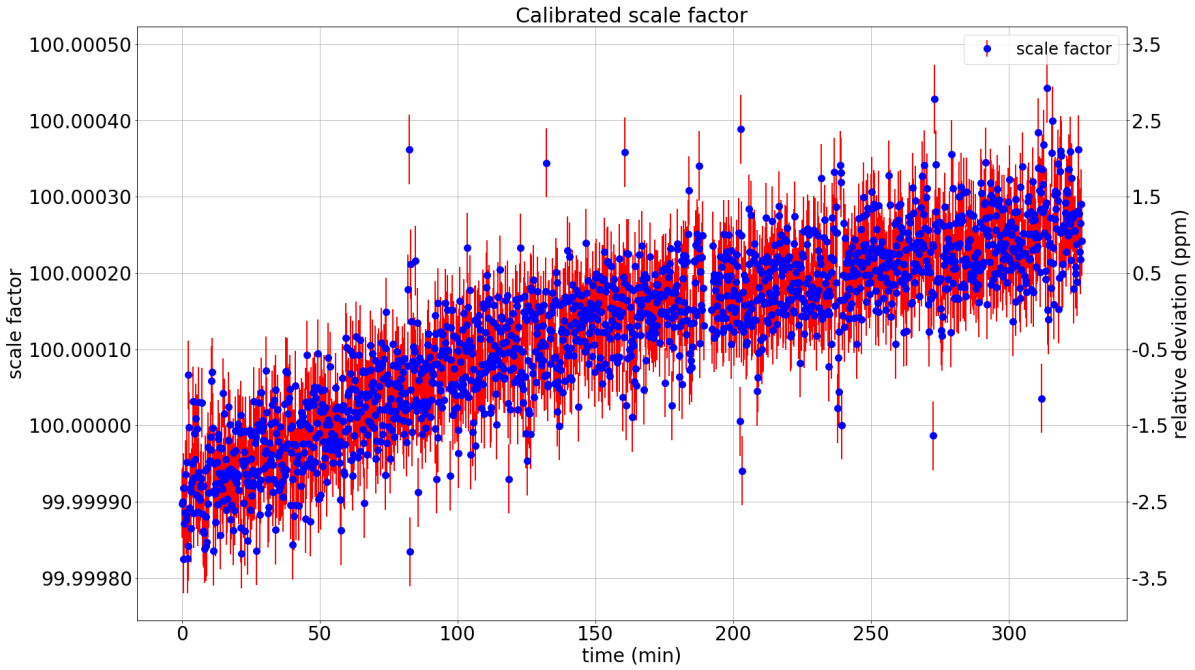

Figure 6.13.: This is the first longterm scale factor determination. Reference divider D was calibrated with the help of reference divider A. The scale factor continuous the drift of the ratio factor from the μ determination (see fig. 6.12). The scale factor starts with a value of about $M_{\text{Signal}} = 99.9999$ and drifts up to a scale factor of about $M_{\text{Signal}} = 100.00025$, where the drift slowly decreases after three to four hours. In the plot only the statistical uncertainties are shown.

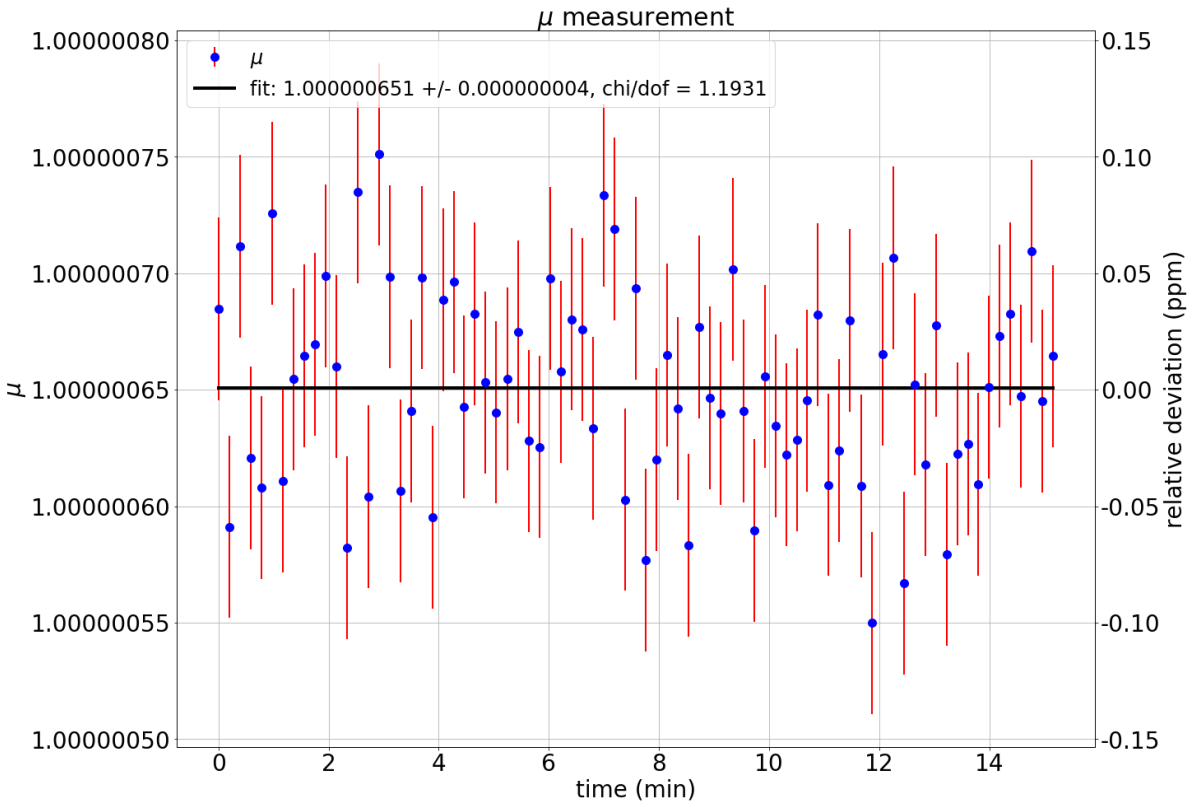

Figure 6.14.: With the second measurement the ratio was determined to $\mu_{AD} = 1.000000676 \pm 0.000000004 \pm 0.0000004$. In the plot only the statistical uncertainties are shown.

sian error propagation as $\Delta M_{signal,sys} = 0.0005$. The statistical uncertainty vanishes due to high statistics in the measurement. The drift can be estimated as $d = 0.64 \frac{ppm}{h}$. In addition to the previous μ determination measurement a second ratio determination was done after the scale factor determination. After the second μ determination another multimeter calibration was made. The results of the first and second calibration is summarized in table A.1. The results of the second μ determination are shown in 6.14.

The second μ determination gave a μ value, which is $\mu_{AD} = 1.000000676 \pm 0.000000004 \pm 0.0000004$. The ratio factor μ is 0.5 ppm lower than the first μ determination (see fig. 6.12).

In addition to the scale factor determination, a μ determination is possible with the data of the scale factor determination during the measurement with the additional -90 V inside of the cage. The equation for the ratio calculation in the scale factor determination is given by

$$\frac{M_{Base}}{M_{Signal}} := \mu = \frac{U_{Signal} + U_{Ref} + \frac{U_{corr-2} - U_{Calibration}}{M_{Signal}}}{U_{Base} + U_{Ref}}. \tag{6.31}$$

The uncertainty of this μ determination dependents on the uncertainty of the input scale factor M_{Signal}, therefore the uncertainty is not calculated for the data points. For the calculation of the data points a scale factor of $M_{\text{Base}} = 99.9990 \pm 0.001$ was chosen due to the starting value of the scale factor determination. With the given values and uncertainties from section 6.2 the statistical uncertainties $\Delta\mu_{\text{stat}}$ can be calculated as

$$\begin{aligned}
\Delta\mu_{\text{stat}} &= \left[\left(\frac{\Delta U_{\text{Signal}}}{U_{\text{Base}}+U_{\text{Ref}}} \right)^2 + \left(\frac{\Delta U_{\text{Ref}} \cdot \left(U_{\text{Base}} - U_{\text{Signal}} - \frac{U_{corr-2}-U_{\text{Calibration}}}{M_{\text{Signal}}} \right)}{(U_{\text{Base}}+U_{\text{Ref}})^2} \right)^2 + \right. \\
&\quad \left(\frac{\Delta M_{\text{Signal}}(U_{corr-2}-U_{\text{Calibration}})}{M_{\text{Signal}}^2(U_{\text{Base}}+U_{\text{Ref}})} \right)^2 + \left(\frac{\Delta U_{corr-2}}{M_{\text{Signal}} \cdot (U_{\text{Base}}+U_{\text{Ref}})} \right)^2 \\
&\quad \left. + \left(\frac{\Delta U_{\text{Calibration}}}{M_{\text{Signal}} \cdot (U_{\text{Base}}+U_{\text{Ref}})} \right)^2 + \left(\Delta U_{\text{Base}} \cdot \frac{U_{\text{Signal}}+U_{\text{Ref}}+\frac{U_{corr-1}}{M_{\text{Signal}}}}{(U_{\text{Base}}+U_{\text{Ref}})^2} \right)^2 \right]^{\frac{1}{2}} \\
\Delta\mu_{\text{stat}} &= \sqrt{1.6 \cdot 10^{-16} + 5.2 \cdot 10^{-26} + 8.0 \cdot 10^{-13} + 1.7 \cdot 10^{-16} + 3.1 \cdot 10^{-17} + 1.3 \cdot 10^{-15}} \\
\Delta\mu_{\text{stat}} &\approx 9.0 \cdot 10^{-7}.
\end{aligned} \tag{6.32}$$

All three μ factors are shown in plot 6.15.

The whole μ determination data gives a complete overview of the drift. The red data points are the μ determination before the longterm measurement, the blue data points come from the μ determination from the scale factor measurement and the black data points come from the second μ measurement after the calibration measurement. The statistical uncertainties of the μ determination are shown in green, the statistical uncertainties of the ratio determination within the scale factor measurement are not shown, because the uncertainties are in a larger range of 0.9 ppm. The drift starts after about one hour of measurement and seems to slow down after about seven hours. That is possible due to the drift of all three digital voltmeters. After about 6 hours the drift decreases, therefore the last data points from the scale factor determination can be taken to make an absolute calibration measurement with the μ determination at the end. The calibration is shown in figure 6.16.

The determined scale factor for this measurement is $M_{\text{Signal}} = 99.99982 \pm 0.00001 \pm 0.0005$. The scale factor is 1.8 ppm below 100. This scale factor measurement can be compared with a scale factor determination at the beginning of the longterm measurement. Therefore only the last 10 minutes of the ratio measurement and the first 10 minutes of the scale factor determination are taken into account. That results in the scale factor shown in figure 6.17.

For a time period of 10 minutes no drift is visible. The determined scale factor is $M_{\text{Signal}} = 99.99985 \pm 0.00001 \pm 0.0005$. The scale factor is 1.5 ppm below 100. That fits good with the result of the scale factor determination at the end of the measurement, which was shown in figure 6.16. The scale factor of the measurement was $M_{\text{Signal}} = 99.99982 \pm 0.00001 \pm 0.0005$. Both scale factors differ only with 0.3 ppm. Furthermore these measurements have shown, that a scale factor determination gives the same result for a scale factor, whether the measurement is done immediately after the beginning, or a few hours, after the system was running. The only important

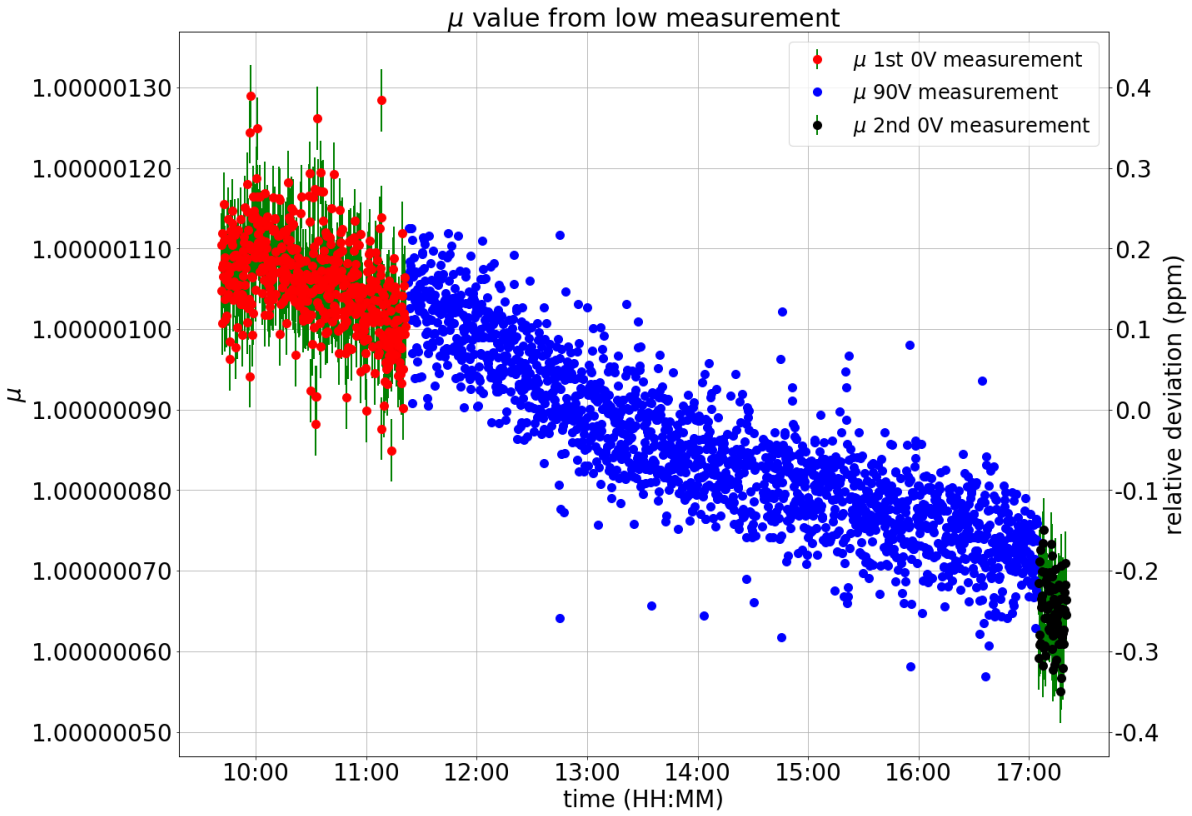

Figure 6.15.: This plot shows the μ determination for all three parts of the long term calibration measurement. The first μ measurement (red) starts with the constant μ value and begins to drift downwards. The μ factor from the scale factor determination (blue) continues with the drift, but it slowly decreases in the intensity. The uncertainty of the blue data points is not shown, due to visibility. The uncertainty is in the range of 0.9 ppm. The last μ determination (black) is again constant. All three measurements connect to each other. The uncertainties for the μ determination are shown in green. The uncertainties for the scale factor determination are not shown, because they are in range of 9 ppm.

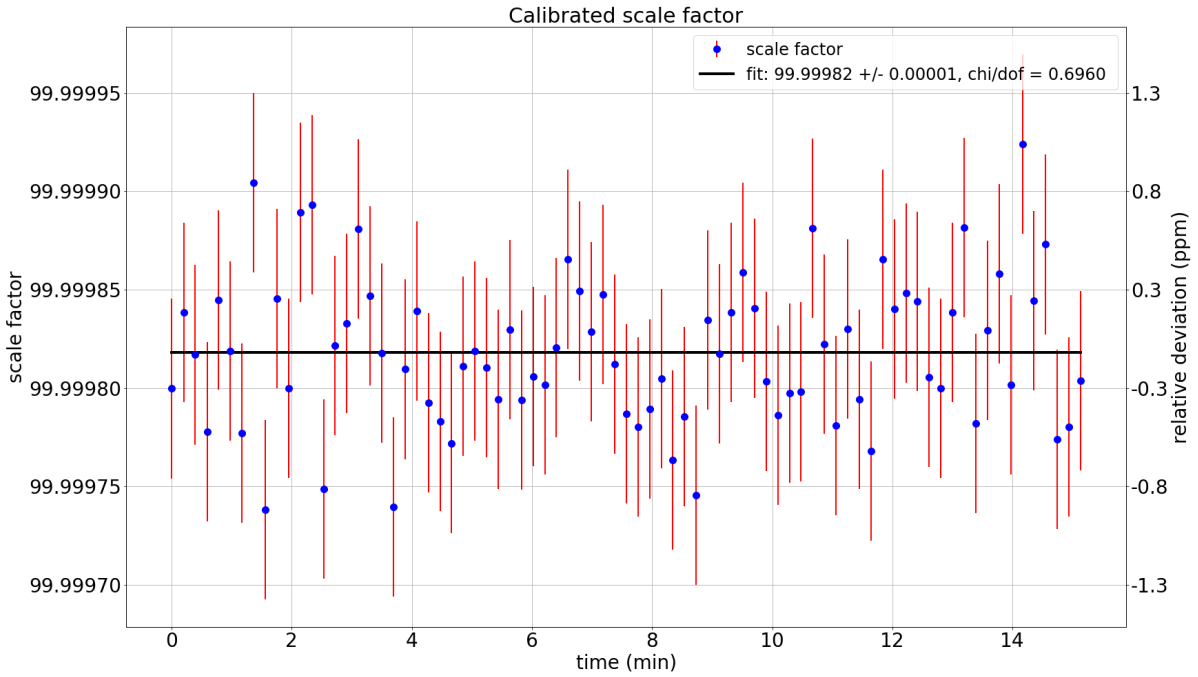

Figure 6.16.: The scale factor determination at the end of the longterm measurement gives a scale factor of $M_{\text{Signal}} = 99.99982 \pm 0.00001 \pm 0.0005$. In the plot only the statistical uncertainties are shown.

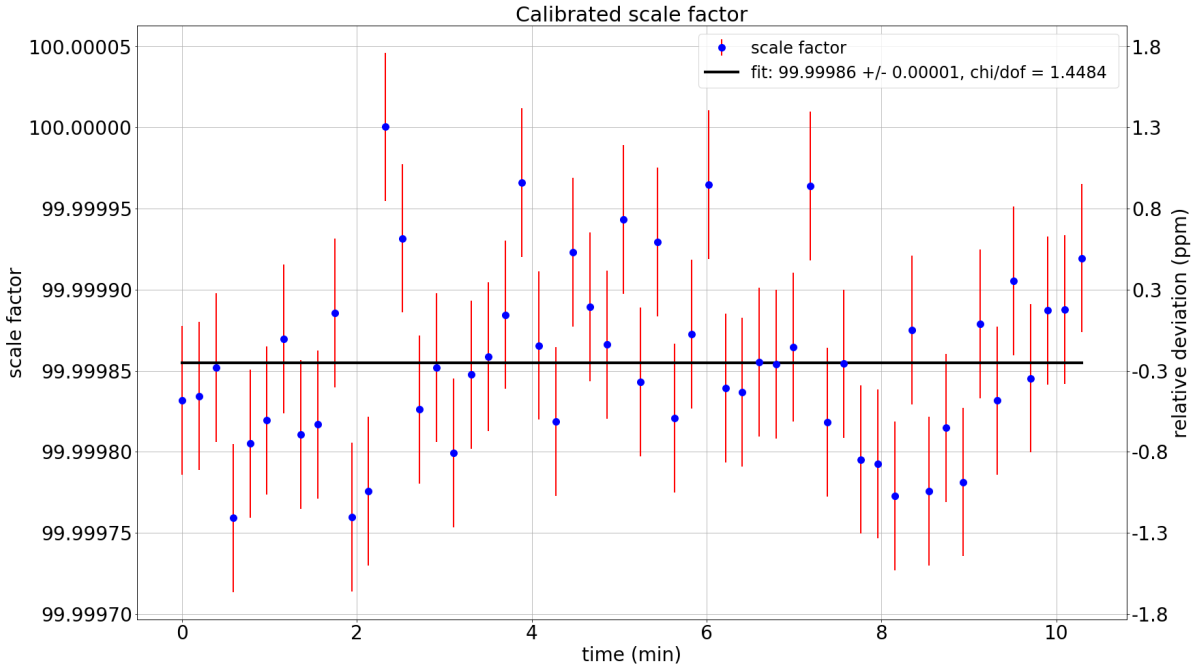

Figure 6.17.: The scale factor determination at the beginning of the longterm measurement gives a scale factor of $M_{\text{Signal}} = 99.99985 \pm 0.00001 \pm 0.0005$. In the plot only the statistical uncertainties are shown.

condition is, that the ratio determination and the scale factor determination are done immediately after each other.

7. Conclusion an outlook

The KATRIN high voltage divider K35 and K65 have to be stable in their scale factors with an uncertainty of 3 ppm. Therefore the scale factors have to be known to this uncertainty level. In the past the calibration could only be done at PTB or with low voltages. With the new absolute calibration method invented in our working group, a PTB independent possibility was created. Within this master thesis, the absolute calibration method was investigated with the help of the reference voltage dividers.

In the thesis two main corrections for the absolute calibration were detected. The first correction was a voltage drop over the reed relays inside the high voltage cage. The voltage drop of the relays was 250 mV, which was due to loose contacts of the relays. With the better contacts the voltage drop reduced to 70 μV. Nevertheless the voltage is used for the calculation of the ratio factor. The voltage drop was neglected during the original absolute calibration, but the first explorative measurements (see sec. 6.1) showed, that it is not negligible. A second correction of the calibration method is the resistance of the high voltage cables and the high voltage cage. The resistance between both connectors are $R_{\text{Cage}} = 2.4\,\Omega$. In this reduced setup the influence of the cage is about $U'_{corr-1} = (1.199 \pm 0.012)$ mV for the μ determination and $U_{corr-2} = (1.306 \pm 0.013)$ mV for the scale factor determination.

Additionally to the corrections for the analysis, the measurement setup was updated. In previous measurements, the readout of the multimeters was adjusted to have the same number of NPLCs for every multimeter. The synchronization measurements of the multimeter in section 5.5 brought the results, that the multimeters have different measurement options with different integration intervals. With the final setup of the measurement, the integration times of all three digital voltmeters are superimposed. That ensures that a drift of a high voltage supply does not affect the measurement.

In the μ determination measurements (see section 6.3) two reference dividers were measured with the new absolute calibration method. Within the measurement the dividers were swapped in the setup, to check the ratio factor. The measured ratio factors for the combination of the reference dividers A and B were

$$\begin{aligned} \mu_{\text{AB}} &= 1.000002065 \pm 0.000000005 \pm 0.0000004 \\ \mu_{\text{BA}} &= 0.999999997 \pm 0.000000005 \pm 0.0000004. \end{aligned} \tag{7.1}$$

The ratio factors should be the inverse of each other, because μ is given as the ratio of both scale factors. The inverted ratio factor $\frac{1}{\mu_{\text{AB}}} = 0.9999979 \pm 0.0000004$. The statistical uncertainty 0.000000005 can be neglected. The scale factors does not fulfill the condition. The ratio factors are not inverse, which is possible due to other systematic uncertainties. The drift of the gain and offset of one of the digital voltmeters can

cause a different scale factor, since the measurements have different start times with a time shift of $\Delta t \approx 30\,\text{min}$. Another possibility are additional resistance inside the measurement setup, which are not determined yet.

With the simplified ratio determination the ratio factor μ is dependent to the digital voltmeter. In the measurements, the ratio factor a strong drift, which indicates a dependency to a digital voltmeter. With this method, the determined ratio factor $\mu_{\text{AB}} = 0.99999591(1)$ with a systematic uncertainty of $\mu_{\text{sys}} = 0.8\,\text{ppm}$, which is about 4 ppm smaller than 1. The ratio determination done within the absolute calibration delivered a ratio factor, which is about 2 ppm greater than 1. That difference can come from the drift of a digital voltmeter. At the absolute calibration measurement, the voltmeters are calibrated 4.5 hours after the first measurement. For the other ratio determination, the calibration was made 1 hour after the first measurement began.
In the measurement in figure 6.10 the influence of the voltmeter is visible. The ratio factor starts with a value of about 0.99999580 and after the 30 minutes measurement the ratio factor increased to about 0.99999600, which is about 0.2 ppm larger. Additionally the scattering of the data points in smaller sections is about 0.1 ppm. In the ratio determination within the absolute calibration (see figure 6.7), the scale factor is stable for measurement times smaller than 1 hour and the scattering of the points in the whole measurement range is also about 0.1 ppm. That shows, that the influence of the voltmeters is smaller in this measurements.

In the absolute calibration measurements (see section 6.4) the scale factors for the three used reference divider were determined. The scale factor were in a range of 2.3-2 ppm lower than 1. That leads to the assumption, that the scale factors are stable in the ppm range, even for larger time scales, because only the reference divider D was self calibrated before a measurement. In the first part the dividers A and B were calibrated with

$$\begin{aligned} M_{\text{A}} &= 99.99981 \pm 0.00001 \pm 0.0005 \\ M_{\text{B}} &= 99.99977 \pm 0.00001 \pm 0.0005. \end{aligned} \tag{7.2}$$

The scale factor determination is only possible with an accuracy of 5 ppm given by the systematic uncertainties. The determined ratio of the scale factors is $\mu_{\text{AB}} = 1.000000 \pm 0.000007$, where the uncertainty is calculated with Gaussian a error propagation of the systematic uncertainties. The ratio factor is, to the given limit, equal to 1. With the systematic uncertainties, the ratio factor is within the range of the estimated ratio factors, but the uncertainty is very large.

The scale factor of divider A was determined with the divider B and with the divider D, that lead to the scale factors

$$\begin{aligned} M_{\text{AB}} &= 99.99981 \pm 0.00001 \pm 0.0005 \\ M_{\text{AD}} &= 99.99978 \pm 0.00001 \pm 0.0005. \end{aligned} \tag{7.3}$$

The scale factor only differ with 0.3 ppm. The systematic uncertainties are in the order of 5 ppm, which are larger than the difference of the scale factor. The slightly

shift of the data points can result due to the time interval of $\Delta t \approx 3.5\,\mathrm{h}$ between both measurements.

The longterm measurement (see section 6.5) showed the biggest problem of the current setup for the absolute calibration. The ratio determination and the scale factor determination is not possible with the used digital voltmeters in a time interval larger than 1 hour. The ratio factor drifted in the long term measurement from 1.00000110 down to 1.00000065, which is 0.45 ppm in about 8 hours. In this measurement, the impact of the Agilent 3458a drift is visible.

Nevertheless an absolute calibration can be made at any time. That was proven with the two absolute calibrations at the beginning of the long term measurement and at the end. The scale factor at the beginning of the measurement was

$$\begin{aligned} M_{\text{beginning}} &= 99.99985 \pm 0.00001 \pm 0.0005 \\ M_{\text{end}} &= 99.99982 \pm 0.00001 \pm 0.0005. \end{aligned} \tag{7.4}$$

The scale factor reduced by 0.3 ppm with a time difference of about 6 hours. The reduction of the scale factor can be due to the different time differences for the calibration of the digital voltmeters. The only condition for the calibration is, that larger measurement times as $t = 30\,\mathrm{min}$ can be a problem, due to a drifting behavior within the longterm measurement.

The manufacturer gives an accuracy for the calibration of 100.00000 ± 0.00005, which could not be proven within the measurements, because the systematic uncertainties calculated for the measurements are one order of magnitude larger than the given accuracy from the manufacturer. Therefore the measurement conditions have to be improven. The high precision Agilent 3458a digital voltmeter showed a strange behavior with different voltage measurements. This voltmeter could be exchanged by a new voltmeter. Additionally the voltmeters could be exchanged among themselves, to check, whether the influence of the voltmeter can be reduced.

A. Tables

Table A.1.: These are the gain and offset values for all three digital volt meters before the long term measurement and afterwards.

		Offset (V)		Gain	
Voltmeter	Range (V)	before	after	before	after
Keysight 3458a	100	$-3.39 \cdot 10^{-5}$	$-2.56 \cdot 10^{-5}$	0.9999949	0.9999947
Agilent 3458a	10	$-9.01 \cdot 10^{-7}$	$-9.19 \cdot 10^{-7}$	1.0000063	1.0000067
Fluke 8508A	20	$-8.88 \cdot 10^{-6}$	$-1.05 \cdot 10^{-5}$	0.9999994	0.9999989

Table A.2.: Every absolute calibration measurement has a single μ determination for the calculation. Here are all absolute calibration measurements listed, which are used in this thesis, with their date.

Measurement	date	Calibration reference	μ reference
First measurement	21.02.2017	6.2	6.1
Corrected first measurement	21.02.2017	6.4	6.3
B calibration with A	20.06.2017	6.11	6.7
A calibration with B	20.06.2017	B.7	6.8
D calibration with A	20.06.2017	B.8	B.4
A calibration with D	20.06.2017	B.9	B.5
long term measurement total	06.07.2017	6.13	6.12
calibration after long term	06.07.2017	6.16	6.14
calibration at beginning of long term	06.07.2017	6.17	B.10

B. Plots

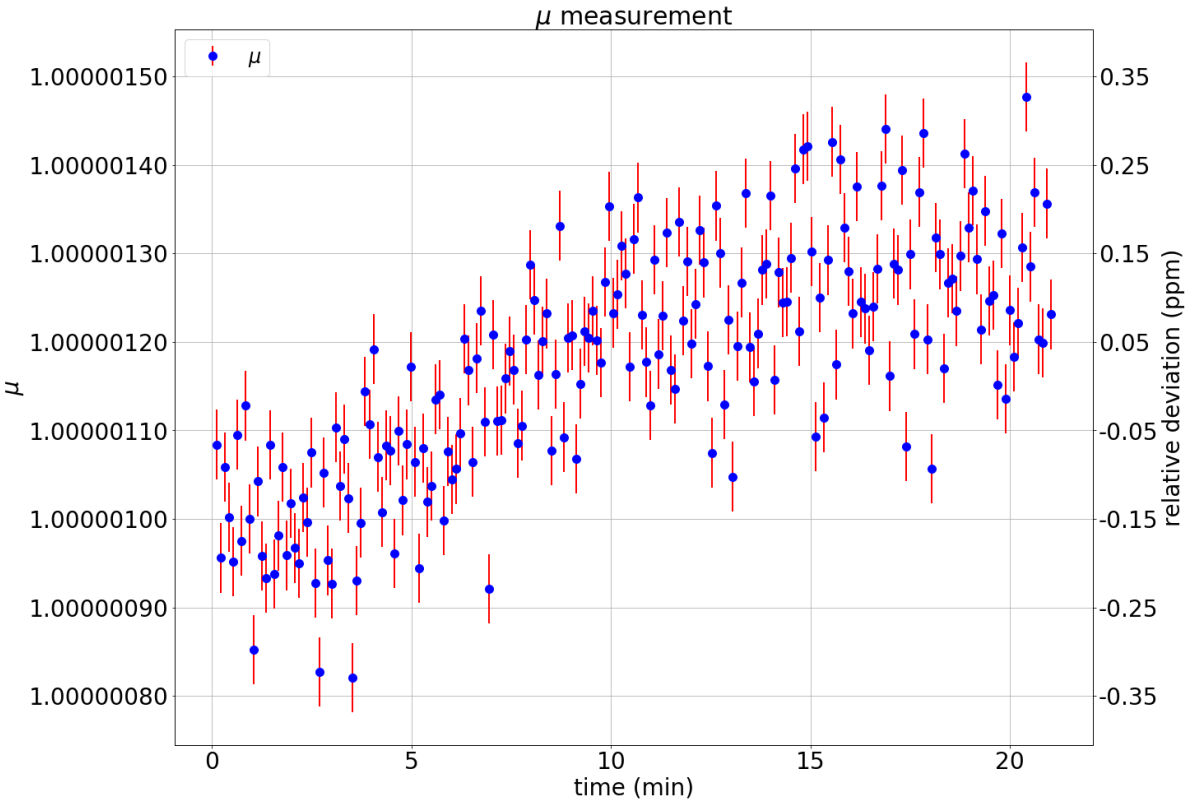

Figure B.1.: The μ determination showed a strong drift of about $\mu_{\text{drift}} = 0.1\,\text{ppm}\frac{1}{10\,\text{min}}$. The cause of the drift was a desynchronization of two digital voltmeters shown in figure B.2.

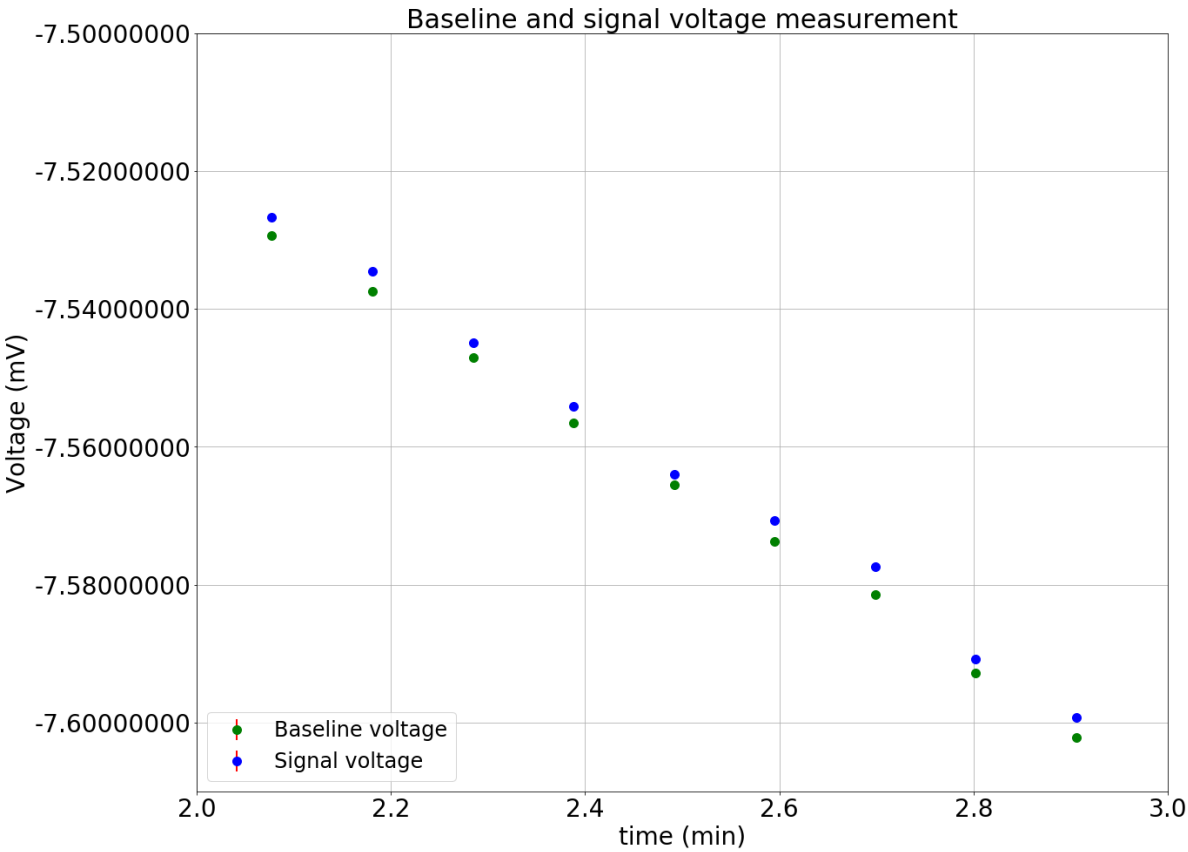

Figure B.2.: Offset between two digital voltmeters withtin the μ determination in figure B.1.

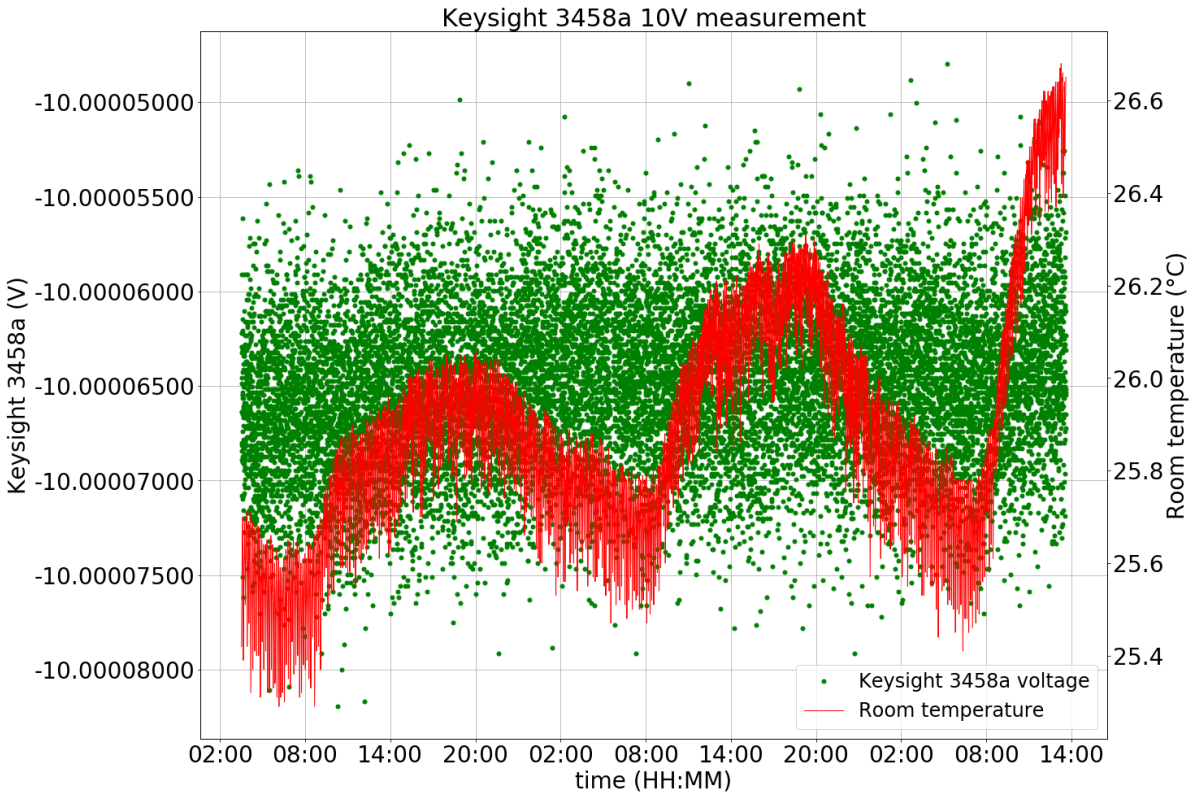

Figure B.3.: The Keysight 3458a measured $-10\,\mathrm{V}$ of the Fluke 7520A calibrator for 70 h (green). The high precision digital volt meter shows a shows a temperature depending drift of $D_{\mathrm{Keysight}} = 7\,\frac{\mu\mathrm{V}}{\mathrm{K}}$. Additionally the temperature read out from the Keysight 3458a is shown (blue).

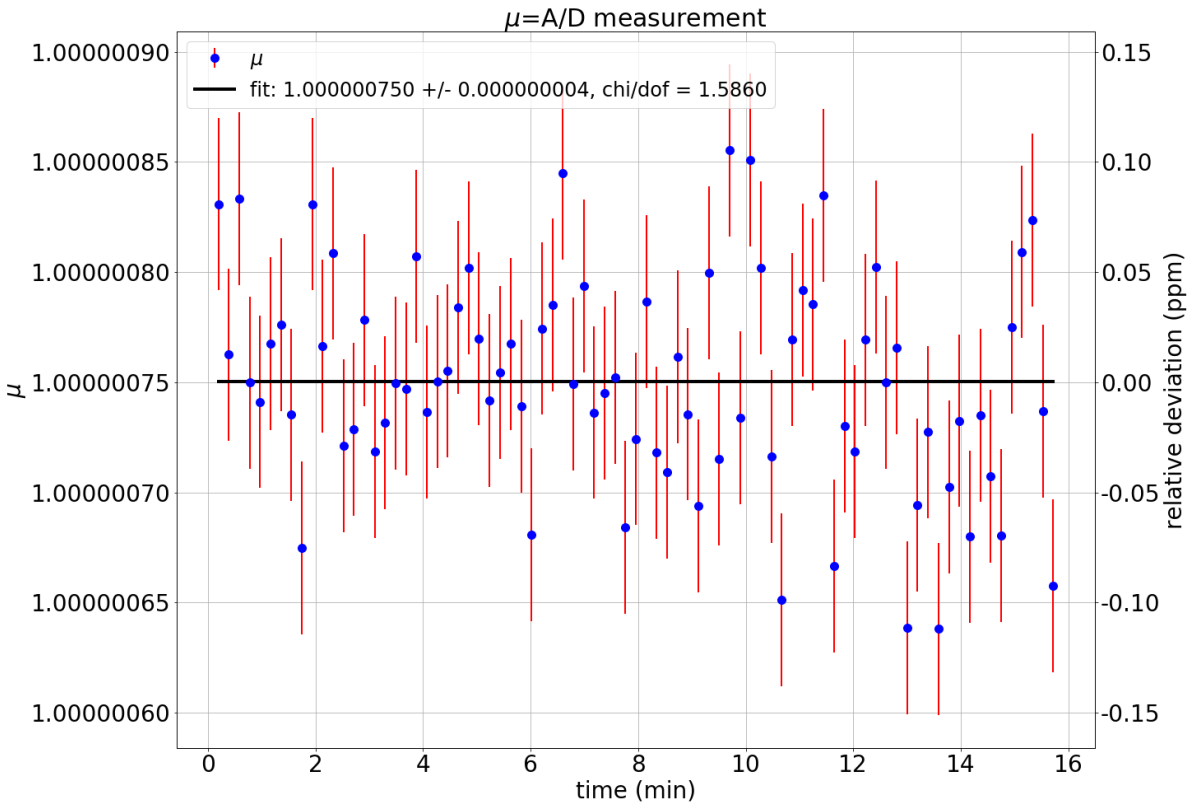

Figure B.4.: Results of the μ determination of the absolute calibration measurement of the voltage divider D with the help of the voltage divider A. The outer FuG MCP 14-1250 was set to a voltage output of 999.3 V with 1.0 mA current and the relay inside the high voltage cage was closed. The μ factor was determined to $\mu_{\mathrm{AB}} = 1.000000750 \pm 0.000000004 \pm 0.0000004$. In the plot only the statistical uncertainties are shown.

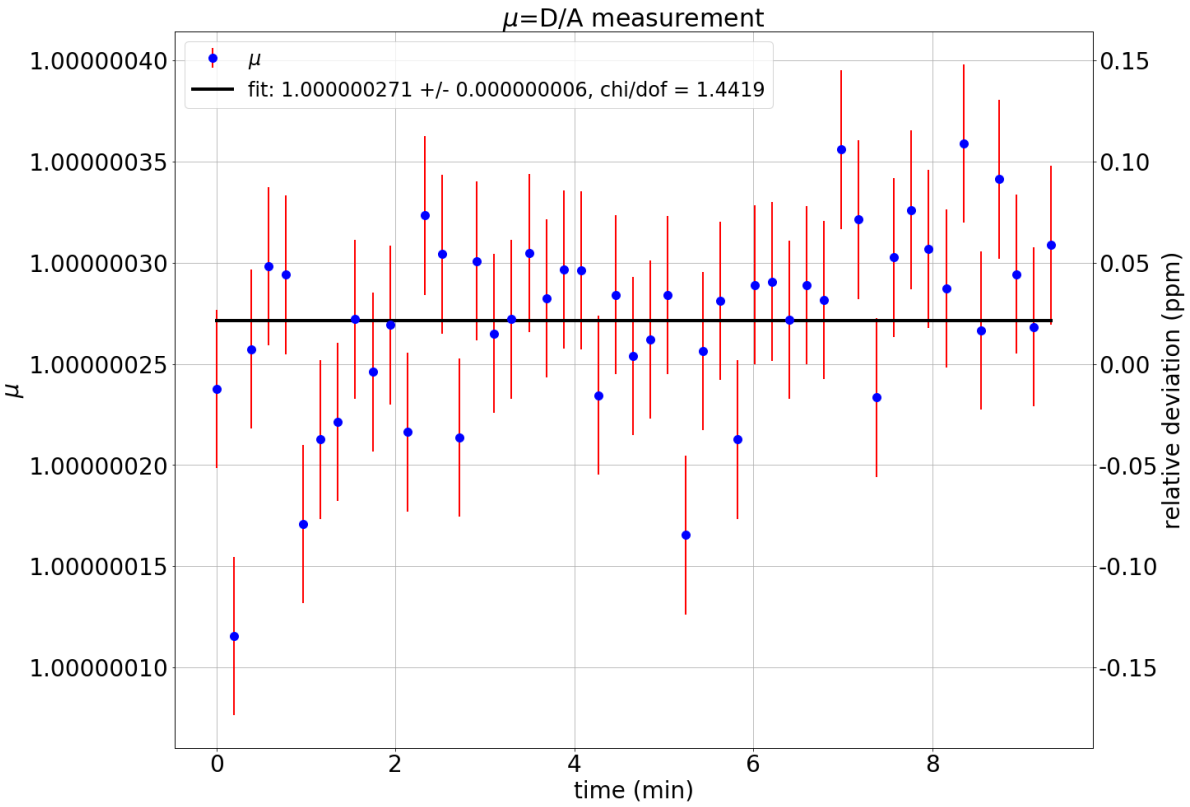

Figure B.5.: Results of the μ determination of the absolute calibration measurement of the voltage divider A with the help of the voltage divider D. The outer FuG MCP 14-1250 was set to a voltage output of 999.2 V with 0.999 mA current and the relay inside the high voltage cage was closed. The μ factor was determined to $\mu_{\mathrm{AB}} = 1.000000271 \pm 0.000000006 \pm 0.0000004$. In the plot only the statistical uncertainties are shown.

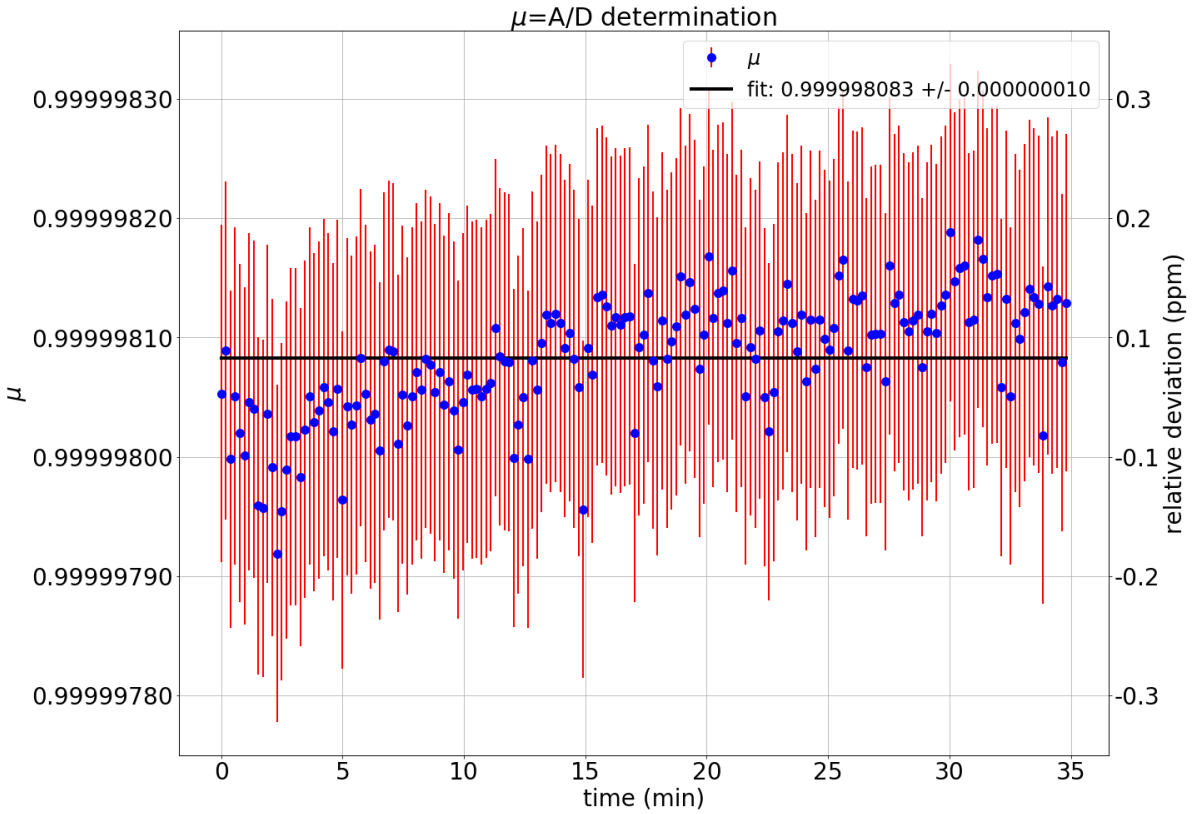

Figure B.6.: Ratio factor μ from an independent comparison measurement of the reference divider A and D. For this measurement the Fluke Calibrator was connected to the Fluke 8508A, as a reference measurement, and with the reference divider A and reference divider D. Both dividers were read out with the Agilent 3458A and the Keysight 3458A. In this case $\mu_{\mathrm{DA}} = \frac{M_{\mathrm{D}}}{M_{\mathrm{A}}}$, which is comparable with the figure B.5. The calculated ratio factor is $\mu_{\mathrm{BA}} = 0.99999808 \pm 0.00000001 \pm 0.0000008$. In the plot only the statistical uncertainties are shown.

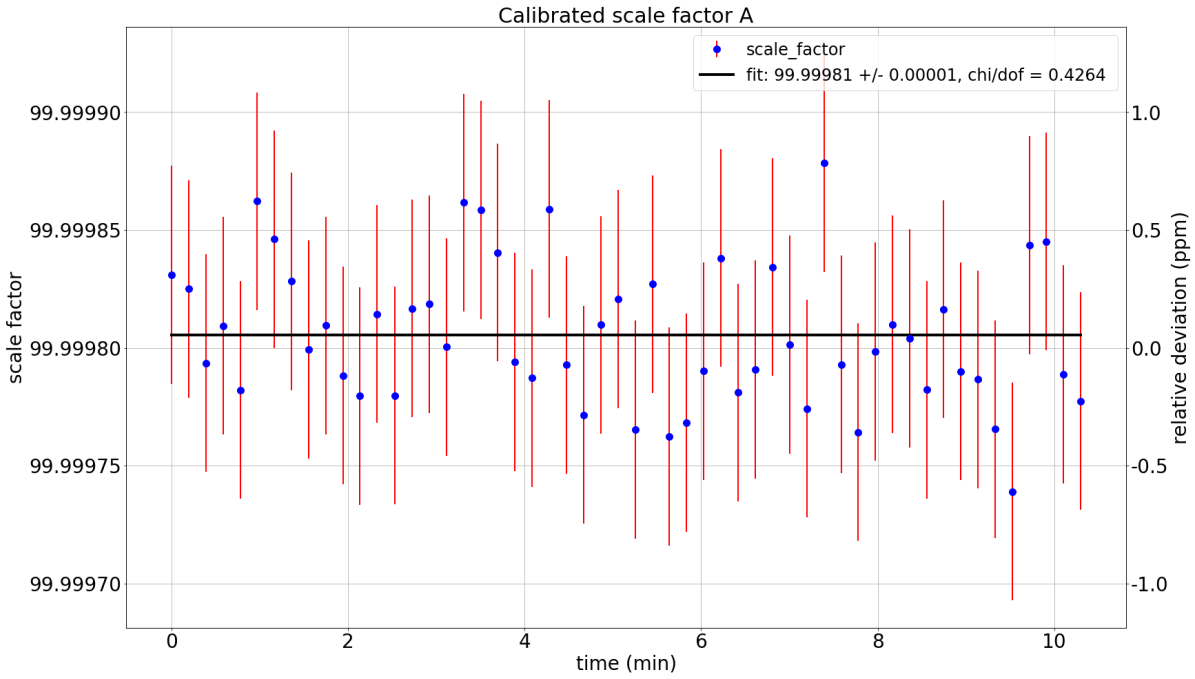

Figure B.7.: Scale factor of the voltage divider A with the absolute calibration method and the help of the voltage divider B. The scale factor was determined as $M_{\text{Signal}} = 99.99981 \pm 0.00001 \pm 0.0005$. In the plot only the statistical uncertainties are shown.

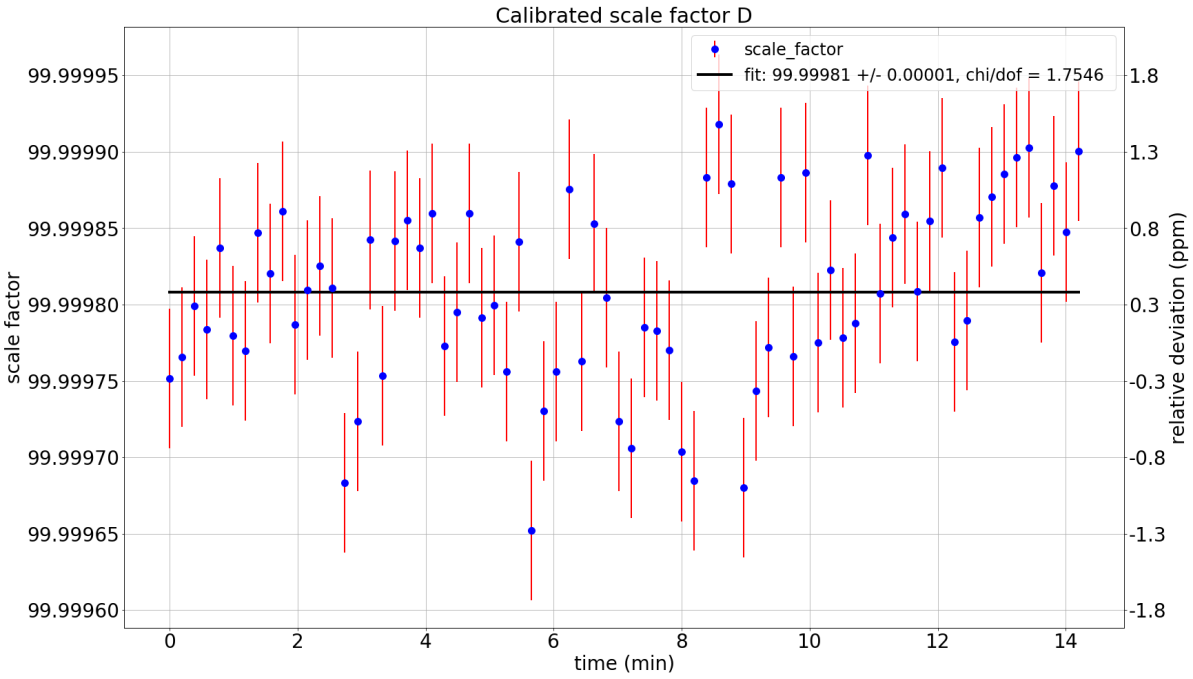

Figure B.8.: Scale factor of the voltage divider D with the absolute calibration method and the help of the voltage divider A. The scale factor was determined as $M_{\text{Signal}} = 99.99981 \pm 0.00001 \pm 0.0005$. In the plot only the statistical uncertainties are shown.

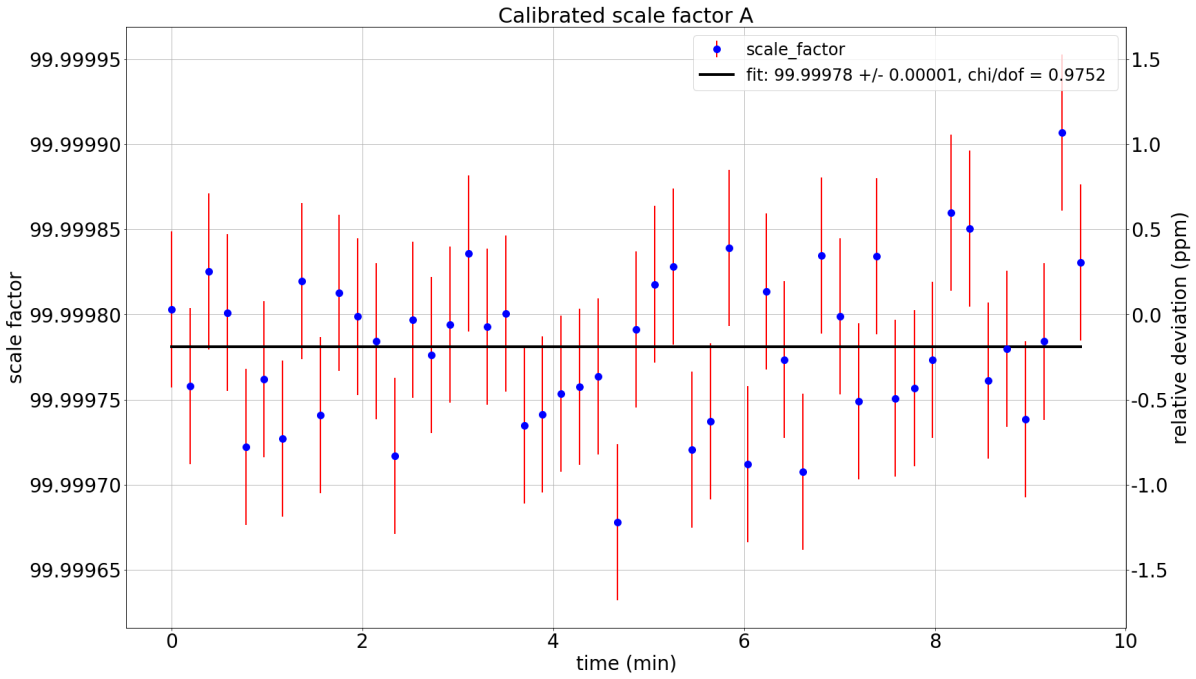

Figure B.9.: Scale factor of the voltage divider A with the absolute calibration method and the help of the voltage divider D. The scale factor was determined as $M_{\text{Signal}} = 99.99978 \pm 0.00001 \pm 0.0005$. In the plot only the statistical uncertainties are shown.

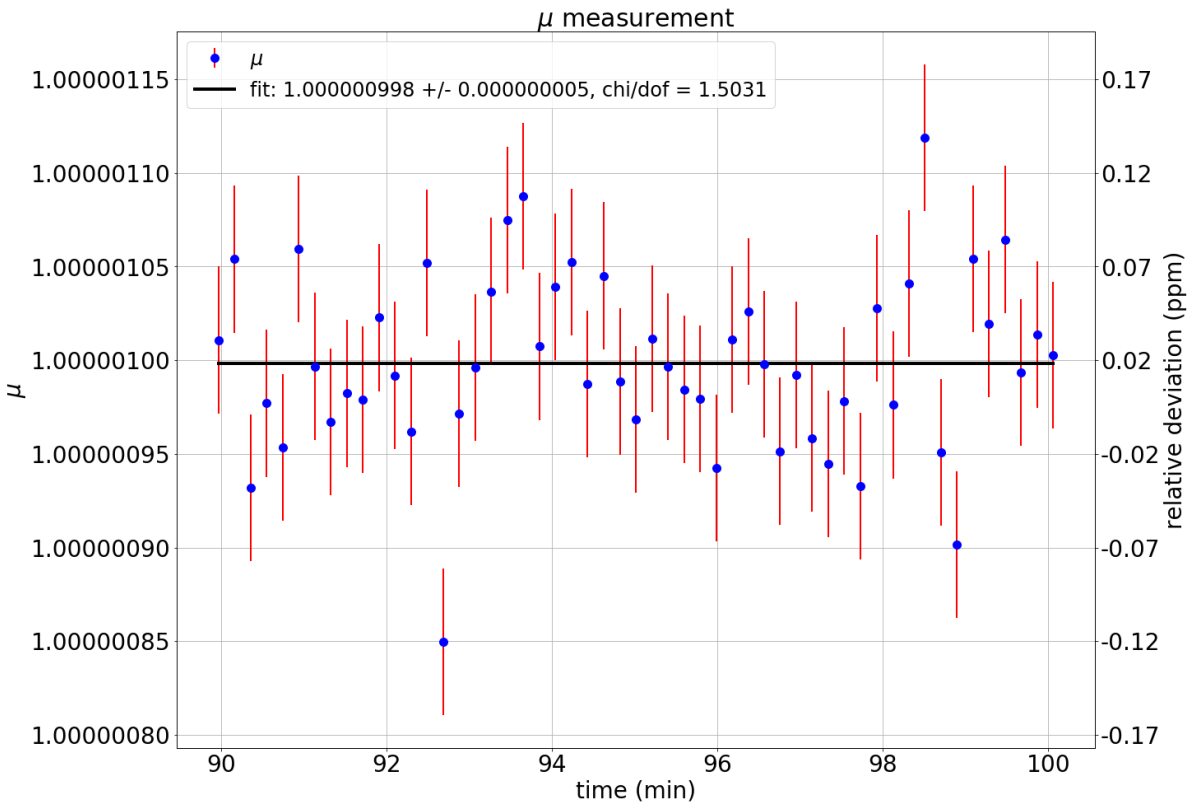

Figure B.10.: With the second measurement the ratio was determined to $\mu_{\mathrm{AD}} = 1.000000998 \pm 0.000000005 \pm 0.0000004$. In the plot only the statistical uncertainties are shown.

Bibliography

[Agi12] Agilent Technologies, *Agilent Technologies 3458A Multimeter Users Guide*, 2012 5.4, 5.3, 5.4, 5.7

[Ams15] J.F. Amsbaugh et al, *Nuclear Instruments and Methods in Physics Research Section A: Accelerators, Spectrometers, Detectors and Associated Equipment*, Nucl. Inst. Meth. A **778**, 2015 3.1

[Ase11] V. N. Aseev, et al, *Upper limit on the electron antineutrino mass from the Troitsk experiment*, Phys. Rev. D **84**, 112003, 2011

[ATL12] The ATLAS Collaboration, *Observation of a new particle in the search for the Standard Model Higgs boson with the ATLAS detector at the LHC*, Phys. Lett. B **716** 1-29, 2012

[Bab12] M. Babutzka et al, *Monitoring of the operating parameters of the KATRIN Windowless Gaseous Tritium Source*, New Journal of Physics, **14** (2012), URL `http://iopscience.iop.org/article/10.1088/1367-2630/14/10/103046` 3.2

[Bau10] S. Bauer, *Aufbau und Inbetriebnahme des zweiten Präzisions-Hochspannungsteilers bis 65 kV fr das KATRIN-Experiment*, thesis, 2010 1, 3.6, 3.12, 3.13

[Bau13] S. Bauer, *Energy calibration and stability monitoring of the KATRIN experiment*, dissertation, 2013 3.14, 4.1.2

[Bea80] G. Beamson, H. Q. Porter and D. W. Turner, *The collimating and magnifying properties of a supercunducting fiel photoelectron spectrometer*, J. Phys. E **13**.1 (1980), URL `http://iopscience.iop.org/article/10.1088/0022-3735/13/1/018/pdf` 3.4.1

[Bec14] M. Beck et al, *An angular-selective electron source for the KATRIN experiment*, Journal of Instrumentation **9** (2014), URL `http://iopscience.iop.org/article/10.1088/1748-0221/9/11/P11020/meta` 3.5

[CR56] C. L. Cowan Jr., F. Reines, *Detection of the Free Neutrino: a Confirmation*, Science **124** 103-104, 1956 2.1

[Dyb18] S. Dyba, *A condensed krypton source for the KATRIN experiment*, dissertation, work still in progress 1, 3.6.1

[DON01] The DONUT Collaboration, *Observation of Tau Neutrino Interactions*, Phys. Lett. B **504** 218-224, 2001
2.1

[Ele17] Elektronik Kompendium, *Homepage of Elektronik Kompendium*, **retrieved:** 10.08.2017, URL: `https://www.elektronik-kompendium.de/sites/slt/0201111.htm` 3.10

[Erh14] M. Erhard et al, *High-voltage monitoring with a solenoid retarding spectrometer at the KATRIN experiment*, Journal of Instr. **9**, 2014 1, 3.6.1

[Flu83] Fluke Corporation, *Fluke 732A DC Reference Standard Instruction manual*, 1983 6.2

[Flu93] Fluke Corporation, *Fluke 752A Reference Divider Instruction Manual*, 1993 5.2, 5.3, 5.4, 6.1

[Flu06] Fluke Corporation, *Fluke 8508A Digital reference multimeter users manual*, 2006 4, 5.3, 5.1, 5.2, 5.4, 5.7

[Fri15] M. Friedrich, *Charakterisierung von Komponenten und Geräten für die Präzisionshochspannungsmessung beim KATRIN-Experiment und beim CRYRING-Speicherring*, bachelor thesis, 2015 5.5, 5.6, 5.7

[FuG14] FuG, *MCP Datenblatt*, URL: `http://www.fug-elektronik.de/de/files/133000/MCP_Datenblatt.pdf` 4.3.1, 6.1

[Jos62] B. D. Josephson, *Possible new effects in superconductive tunnelling*, Phys. Lett. **1** 251-253, 1962 4

[Kat04] The KATRIN Collaboration, *KATRIN Design Report 2004*, 2005, URL `http://primo.bibliothek.kit.edu/primo_library/libweb/action/dlDisplay.do?vid=KIT&docId=KITSRCE0270060419&tab=kit_evastar&srt=date` 1, 2.3, 3, 3.1, 3.6

[Kat17] The KATRIN Collaboration, *Homepage of the KATRIN experiment*, **retrived** 17.07.2017 3.3, 3.4, 3.7, 3.8

[Kra05] Ch. Kraus et al, *Final results from phase II of the Mainz neutrino mass searchin tritium β decay*, Eur. Phys. J. C **40** 447-468, 2005
2.10, 3

[Led62] L. M. Lederman et al, *Observation of High-Energy Neutrino Reactions and the Existence of Two Kinds of Neutrinos*, Phys. Rev. Lett. **9**, 36, 1962
2.1

[Lob03] V. M. Lobashev, *The search for the neutrino mass by direct method in the tritium beta-decay and perspectives of study it in the project KATRIN*, Nuclear Physics A, **719** 153-160, 2003 2.10, 3

[Mar01] R. Marx, *New concept of PTBs standard divider for direct voltages of up to 100 kV*, Instrumentation and Measurement, IEEE Transactions on **5**, 426 - 429
4.1.1

[Med11] Meder electronic, *Data sheet reed relay H12-1A69*, 2011 6.1

[MS86] S. P. Mikheyev, A. Yu. Smirnov, *Resonant amplification of ν oscillations in matter and solar-neutrino spectroscopy*, Il Nuovo Cimento C **9** 17-26, 1986
2.3

[Nob15] Class of Physics of the Royal Swedish Academy of Science, *Scientific Background on the Nobel Prize in Physics 2015, Neutrino Oscillations*, 2015 2.2

[OW08] E. W. Otten, C. Weinheimer, *Neutrino mass limit from tritium beta decay*, Rept. Prog. Phys. **71**, 2008
2.2, 2.4

[Rem10] REMO-HSE, *HV-Voltmeter 20P, Datenblatt*, 2010 4

[Res14] O. Rest, *Inbetriebnahme der Präzisionshochspannung am Hauptspektrometer des KATRIN-Experiments*, master thesis, 2014
4.1.1, 4.1.2, 4.1, 4.2

[Res18] O. Rest, *Absolute calibration of high voltage dividers K35/K65 for the KATRIN-Experiment*, dissertation, work still in progress 1

[Sup17] The Super-Kamiokande Collaboration, *Homepage of the Super-Kamiokande experiment*, **retrived** 27.07.2017
`http://www-sk.icrr.u-tokyo.ac.jp/sk/physics/atmnu-e.html`
2.2.1, 2.1

[Tec05] Tectronix, *Tectronix AFG 3102 data sheet*, 2005, URL: `http://www.testequipmenthq.com/datasheets/TEKTRONIX-AFG3102-Datasheet.pdf` 5.5

[Tec16] Tectronix, *Low Level Measurements Handbook*, 2016, 7^th Edition
5.6

[Thu07] T. Thümmler, *Präzisionsüberwachung und Kalibration der Hochspannung für das KATRIN-Experiment*, dissertation, 2007
1, 3.6, 3.6.1

[Pau30] W. Pauli, *Offener Brief an die Gruppe der Radioaktiven bei der Gauvereins-Tagung zu Tübingen*, 1930
2.1

[Wol78] L. Wolfenstein, *Neutrino oscillations in matter*, Phys. Rev. D **17**, 2369, 1978 2.3